TUDelft

Delft University of Technology

Ambient-Energy Powered Multi-Hop Internet of Things

Rao, Vijay

Important note
To cite this publication, please use the final published version (if applicable).
Please check the document version above.

AMBIENT-ENERGY POWERED

MULTI-HOP INTERNET OF THINGS

AMBIENT-ENERGY POWERED

MULTI-HOP INTERNET OF THINGS

Proefschrift

ter verkrijging van de graad van doctor
aan de Technische Universiteit Delft,
op gezag van de Rector Magnificus prof. ir. K.C.A.M. Luyben,
voorzitter van het College voor Promoties,
in het openbaar te verdedigen op maandag 16 oktober 2017 om 12:30 uur

door

Vijay Sathyanarayana RAO

elektrotechnisch ingenieur, Technische Universiteit Delft
geboren te Bangalore, India.

This dissertation has been approved by the

promotor: prof. dr. ir. I.G.M.M. Niemegeers
copromotor: dr. R. Venkatesha Prasad

Composition of the doctoral committee:

Rector Magnificus,	Chairman
Prof. dr. ir. I.G.M.M. Niemegeers	Delft University of Technology, The Netherlands
Dr. R. Venkatesha Prasad	Delft University of Technology, The Netherlands

Independent Members:

Prof. dr. C. Douligeris	University of Piraeus, Greece
Prof. dr. K. U. Römer	Graz University of Technology, Austria
Prof. dr. ir. I. Moerman	Ghent University of Technology, Belgium
Prof. dr. ir. S. Heemstra de Groot	Eindhoven University of Technology, The Netherlands
Prof. dr. ir. D. Epema	Delft University of Technology, The Netherlands

Reserve Member:

Prof. dr. K. Blok	Delft University of Technology, The Netherlands

An electronic version of this dissertation is available at
`http://repository.tudelft.nl/`.

CONTENTS

1

INTRODUCTION

The Internet of Things (IoT) is one of the most disruptive technologies in today's connected world. IoT enables the interconnection between every *thing* via the Internet regardless of whether it is a computing device or not. For example, while it is fairly common to see people having an Internet presence (e.g., through social networks), it is also possible to connect inanimate objects, such as a crate of apples, to the Internet. The idea behind this is to either monitor and/or control the IoT *things* (also referred to as IoT objects), or the physical environment around it without any human intervention. Currently, an estimate of 6.4 billion IoT devices exist (without accounting for smartphones and laptops), with a projection that this number doubles in five years [1].

Embedded systems in the form of sensors and actuators have been well-known and long-used for monitoring applications [2]. However, with the proliferating number of sensors and actuators being used, these embedded devices are intrinsically tied to their monitor and control task of the IoT applications in the context of a larger system [3]. Examples of the larger system are smart homes, smart healthcare systems, smart grids, smart transportation, smart industry (Industry 4.0), and the IoT applications could be smart lighting in a smart home, monitoring and maintaining a controlled environment for degradable freight in smart transportation and so on. These technologies and applications are envisioned to enable a better quality of life and sustainable lifestyle[1]. An overview of several smart applications is shown in Figure 1.1, where both information and communications technology (ICT) objects such as sensors and non-ICT objects such as appliances can be monitored and controlled.

One of the earliest visions on smart lifestyle by Mark Weiser is becoming a reality. In his momentous work [4], he envisioned "ubiquitous computing", that is, personal computers integrate seamlessly into a person's environment and enrich his/her everyday life by automating many routine tasks. The personal computers he refers to could be a large number of embedded devices (sensors and actuators) that will gather and process information to both control the physical processes and to interact with human users. Since he envisioned these devices to seamlessly integrate or even *disappear*, wired technologies are not an option due to the lack of flexibility and the associated costs.

---

[1]Here, sustainability refers to the ability to maintain the human-ecosystem equilibrium.
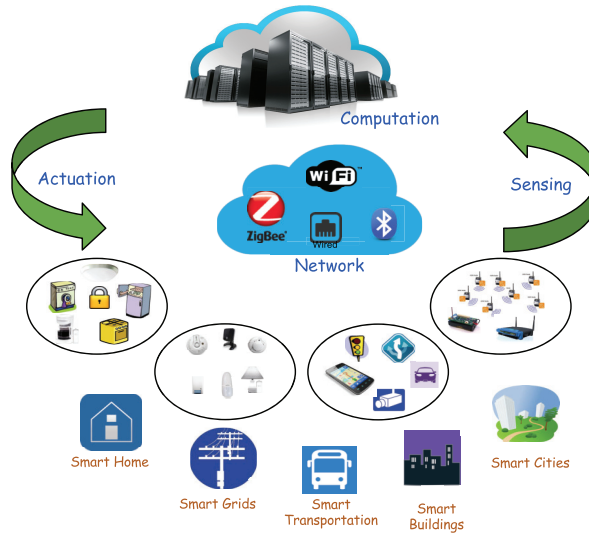
Figure 1.1: An overview of several smart applications with IoT.

One of the most commonly used technologies for IoT is Wireless Sensor Networks (WSNs). Earlier, WSNs were seen as a distributed system of wireless sensors that could monitor an area for events and report them to a base station or sink. In fact, WSNs were referred to as a *macroscope*, contrasting to a microscope, that enables us to gather fine-grained information over large areas, which hitherto was difficult to obtain [5]. WSNs can also have actuation capabilities. Advances in low-power circuit design and networking techniques have reduced the overall power consumption of wireless sensor nodes drastically. Thus, WSN nodes offer computation, communication and control capabilities allowing them to be molded to support a variety of IoT applications. Due to the varied application requirements, it is not possible to have definitive requirements of the nodes and the networks. However, we can enumerate a few typical characteristics of these nodes[2] [2] as follows:

1. Small in size and weight as they often must be hidden from view of the users. This implies low computational resources due to the form factor;

2. Wireless connectivity, for enabling communications and physical portability;

3. Low power consumption, thus, in turn the range of the wireless connectivity is restricted; and

4. Operate perpetually, or at least for long periods, without manual intervention.

The embedded devices used for WSNs are typically battery-powered for portability. In WSNs, a sensor node's operating time is a crucial design parameter as this has a direct implication on the longevity of the network. As electronic systems continue to shrink, the amount of energy stored also reduces due to the reduced battery size as

---

[2]The words 'devices' and 'nodes' are used interchangeably.
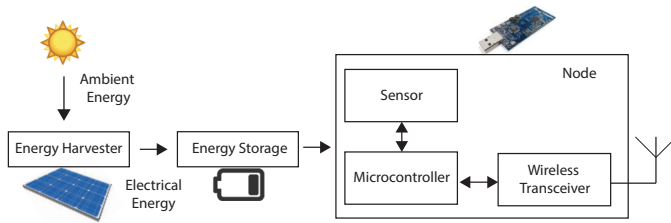
Figure 1.2: Block diagram of a typical energy-harvesting wireless sensor node.

smaller form factors are desired. The research to develop higher energy-density batteries is on-going, but with the current state-of-the-art batteries, lifetime of the node, and hence the network's lifetime are limited ranging from a few months to a few years. Frequent battery replacement is labor intensive in many cases, and in other situations battery replacement is impractical due to physical or deployment conditions. Thus, the grand idea of ubiquitous computing comes with the nightmare of limited lifetime or the burden of battery replacement. Furthermore, the processes of producing and recycling batteries is also harmful to the environment [6].

A promising approach for perpetual and sustainable network operations is to harvest energy from ambient sources, such as light, radio waves, temperature differences, vibrations, motion, salinity gradients, wind and water flows [7]. By tapping into the harvesting opportunities in the ambiance, the nodes gain autonomy with respect to energy. The motivation for this work is to completely replace the batteries in order to realize virtually immortal and sustainable IoT applications by powering the devices through ambient energy-harvesting techniques. This dissertation proposes to achieve this by means of energy-aware power management across the communication stack in the energy-harvesting devices.

In this chapter, we introduce the different energy harvesting technologies and their applications. Following this, we describe the research challenges in networking the energy-harvesting powered sensor nodes. Lastly, we present the contributions made by this work.

1.1. Energy-harvesting Nodes and Networks

An energy-harvesting node, in this work, refers to a low-power wireless sensor node that derives its power from ambient energy sources such as light, linear motion, vibrations, temperature differences, radio frequency transmissions, wind and water flows. A network of these nodes is known as energy-harvesting WSNs (EH-WSNs).

The block diagram of a typical energy-harvesting wireless sensor node is depicted in Figure 1.2. The wireless sensor node consists of a microcontroller, a transceiver chip and a set of sensors, and the node is powered by an energy storage buffer such as rechargeable batteries or supercapacitors. To recharge the storage buffer, the node consists of a harvesting device (e.g., a solar panel, thermo-electric generator, flow harvester etc.). We shall present an overview of the harvesting and storage technologies in Section 1.2.

1.1.1. BENEFITS

There are several benefits of ambient-energy powered wireless sensor networks due to which there has been an enormous interest in this field, not just in academia [8, 9, 10, 7, 11] but also in industry through startups [12, 13, 14, 15, 16]. Some of the benefits are listed below:

1. The first one is the promise of perpetual operations without the need for frequent replacement of batteries. Due to the nodes being self-powered, they can now be used in applications that require them to be in harsh and/or inaccessible locations. One such example is the Permasense project in which self-powered sensors are deployed in the high mountains of the Alps to quantify the connection between climate, cryosphere (permafrost, glaciers, snow) and geomorphodynamics over several years [17].

2. The sensor nodes are more sustainable, i.e., the number of batteries used can be significantly reduced thereby reducing the carbon-footprint as compared to the battery-powered counterparts.

3. Batteries take the bulk of the volume of a sensor node. Due to energy-harvesting, the size and the cost of the nodes reduce. This has led to creating thinner wearables and smart fabrics [18].

1.1.2. NEW APPLICATIONS

In order to understand the importance and relevance of an energy-harvesting network, we must understand the various applications it enables or enhances over battery-powered WSNs. As mentioned in the previous section, the energy-harvesting WSNs can be deployed in inaccessible locations for monitoring and control, which was not previously possible with their battery-powered counterparts. Apart from Permasense, other similar applications include structural health monitoring [19], and monitoring the health, habitat and habits of animals [20]. Energy-harvesting also benefits the IoT applications in order to realize smart and sustainable lifestyle through applications such as smart homes, smart cities, smart healthcare and smart agriculture [21]. Making the nodes self-powered not only allows for traditional wireless sensor networks and IoT applications being perpetually operational but also enables new applications and enhancements. We list only a few categories here though there are many more such possibilities.

1. Modern cars have a lot of sensors that are wired around the vehicle since the central power source is either placed in the front or the back of the car [22]. These can be replaced with energy-harvesting wireless sensors to make the vehicle lighter. Typical sources for energy here are the vibrations in the car. Similarly, energy-harvested sensors can be used for aircraft health monitoring without using cables or batteries that carry the danger of being explosive [23] and save weight.

2. Smart wearables, such as smart textiles, will be usable if they are self-powered [24]. The energy sources here are the kinetic energy from human motion and thermal energy from the human body.

Table 1.1: Comparison of power density from various energy-harvesting sources [27].

Energy Source	Power Density
Ambient Light	$100\,\text{mW/cm}^2$ (direct sunlight)
	$100\,\mu\text{W/cm}^2$ (indoor lighting)
Thermal difference	$60\,\mu\text{W/cm}^2$ (@ 40°C)
Vibration (piezoelectric)	$116\,\mu\text{W/cm}^3$ (@ 120Hz)
Airflow	$1\,\text{mW/cm}^2$
Push buttons	$50\,\mu\text{J/N}$
Shoe Inserts	$330\,\mu\text{W/cm}^3$

3. Nano-sensor networks that enable the manipulation of matter on atomic and molecular scales are envisioned to be used for healthcare applications [25]. They are extremely small [26], so the best way to power them is through energy-harvesting. Typical energy sources envisioned here are the flow of fluids and salinity gradients in the human body.

1.2. Overview of Energy-harvesting and Storage Technologies

1.2.1. Energy-harvesting Technologies

Energy-harvesting technologies are broadly classified based on the type of the energy source. Examples include incident light, heat, mechanical movement, fluid flow and ambient radiation. Each of these sources is unique leading to different harvesting technologies for the extraction of energy from them. The nature of the sources and their corresponding harvesting technologies must be thoroughly studied and characterized in order to design systems that rely on them. A comparison of the power density from various energy-harvesting sources is given in Table 1.1. To guarantee a sustained operation, it is imperative to choose the best energy-harvesting technology based on the application and where it is to be deployed.

Yildiz [27] consolidates the working principles of the devices used for harvesting energy from sources such as electromagnetic sources, piezoelectric, electrostatic, thermoelectric, and solar energy harvesting devices. This is effectively summarized in Figure 1.3, where, the first of the rows marked with dotted lines classifies the various energy sources in terms of the broad type of technology used, the second row indicates the type of device that is used to harvest energy, and the third row explains the physical principles used for harvesting. In the following paragraphs, we describe the commonly used energy-harvesting technologies.

1.2.1.1. Solar energy-harvesting

Energy-harvesting from photovoltaic cells has been well-known and well-studied [28, 29, 30]. This is mainly due to the readily available and abundant solar irradiation. When light is incident on a solar cell, a voltage is created due to the photovoltaic effect. Due to the small amounts of power required by the wireless sensor nodes, sufficient power can also be generated from indoor lighting systems. A Texas Instrument's
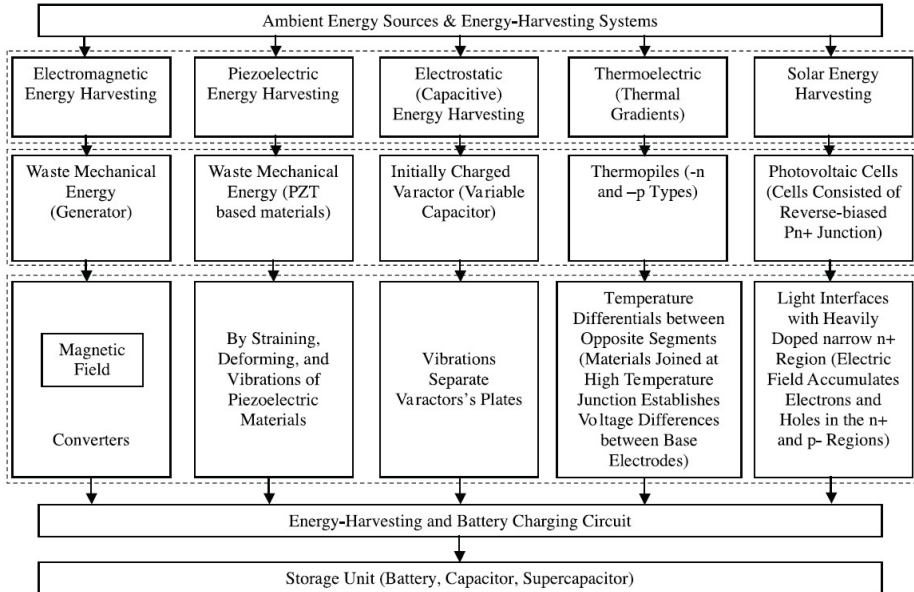
Figure 1.3: Summary of energy extraction principles from energy-harvesting sources [27].

CC2530 based sensor node powered by a solar panel, which was designed in ZENLAB, Indian Institute of Science is shown in Figure 1.4.

While photovoltaic cells are the most popular for energy-harvesting systems because of the readily available solar irradiation and low cost solar panels, the efficiency of the solar cells is poor with a maximum of 34%. In order to improve the efficiency, methods such as maximum power point tracking (MPPT) are employed [31]. MPPT circuits operate on the basis of the maximum power transfer theorem to extract as much power as possible by impedance matching, in order to compensate for the varying characteristic resistance of solar panels (due to varying levels of irradiation), thus providing higher power outputs.

1.2.1.2. VIBRATION ENERGY-HARVESTING

There are three mechanisms to convert vibrational motion to electrical energy - electromagnetic, electrostatic and piezoelectric [27]. Electromagnetic harvesters work on Faraday's law of induction, exploiting the current that flows due to the relative motion between a coil and a magnet. In electrostatic harvesting, the relative motion between two conductors that form a capacitor is used to generate energy. Piezoelectric harvesters are made of materials that develop a charge when mechanical strain acts on them. Table 1.2 compares these conversion mechanisms. Piezoelectric harvesters are widely available from companies such as Mide Volture [32] and AdaptivEnergy [27]. Most of these devices promise approximately 10 mW at 50Hz vibrations. One such device from Mide Volture [32] is seen in Figure 1.6(a). It is also possible to harvest energy from a button-press action through harvesters such as the linear motion har-

Figure 1.4: A CC2530 node powered by a solar panel and supercapacitor.
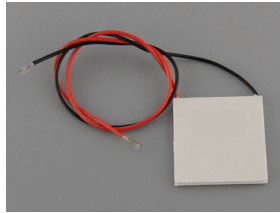
Figure 1.5: A commercial thermoelectric generator [33].

vester (ECO100) from Enocean [14] (see Figure 1.6(b)).

1.2.1.3. THERMAL GRADIENT ENERGY-HARVESTING
Thermal gradients can be converted to electrical energy through the Seebeck (thermoelectric) effect. Charges flow from a high concentration region to a low concentration region when there is a difference in temperature between the opposite segments of a conducting material. Thermopiles consisting of n- and p-type materials electrically joined at the high-temperature junction are therefore constructed, allowing the heat flow to carry the dominant charge carriers of each material to the low temperature end. This process establishes a voltage difference across the base electrodes. The generated voltage is proportional to the difference in temperature and the Seebeck coefficient of the thermoelectric materials. A commercial thermoelectric generator is shown in Figure 1.5.

1.2.1.4. WIND FLOW ENERGY-HARVESTING
Advances have been made in wind energy harvesting that eliminate the need for rotating air-foils. Figure 1.7 shows such a compact system from Humdinger [34] that makes use of a phenomenon known as aero-elastic flutter. The device consists of a flexible polymer ribbon stretched between supports transverse to the wind direction, with magnets glued to it. When the wind blows across it, the ribbon vibrates due to flutter, inducing current by the magnets through electromagnetic induction. Energy generated from this movement is of the order of 1 kWh per month for wind speeds of 2 to 12 m/s. Novel methods such as extraction of energy from other fluidic motion such as water from a tap are also being considered [21].

Table 1.2: Comparison of mechanisms for harvesting from vibrations.

Mechanism	Advantages	Disadvantages
Piezoelectric	No voltage source needed	More difficult to integrate
Electrostatic	Easier to integrate	Separate voltage source needed
Electromagnetic	No voltage source needed	Output voltage is 0.1 - 0.2V
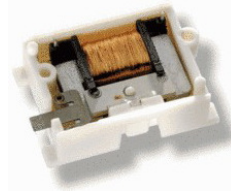
(a) Piezoelectric Harvester   (b) Linear Motion Harvester ECO100

Figure 1.6: Commercial vibration energy harvesters from Mide [32] and Enocean [14].

1.2.2. STORAGE TECHNOLOGIES

Energy storage plays an important role in energy-harvesting WSNs. The storage elements act as buffers to reduce the nodes from dying when energy is being harvested intermittently. In order to support the application requirements, a suitable storage element must be chosen. The choice depends on the node power requirements, and the expected power from the harvesting source. Energy storage technologies have been improving vastly. While there are several technologies, we discuss the suitability of the two most important ones - supercapacitors and rechargeable batteries.

1.2.2.1. SUPERCAPACITORS

The Ragone plot graphs the energy density of the energy storage devices against their power densities [35]. From the position of an energy storage device on this plot, it is possible to assess the ability of the device to store energy for long durations of time (high energy density) against their ability to provide a large amount of power in a short duration when required (high power density). Figure 1.8 shows the Ragone plot comparing the supercapacitors and the batteries for micro-devices [36]. Supercapacitors are placed between capacitors and batteries, indicating that they have the advantage of higher power density than batteries as well as higher energy density than the ordinary capacitors. Furthermore, supercapacitors do not undergo irreversible chemical reactions, thus they have charge-discharge cycles in the order of millions.

Compared to the batteries, the supercapacitors have a less complex charging cir-

Figure 1.7: Wind energy harvester from Humdinger.
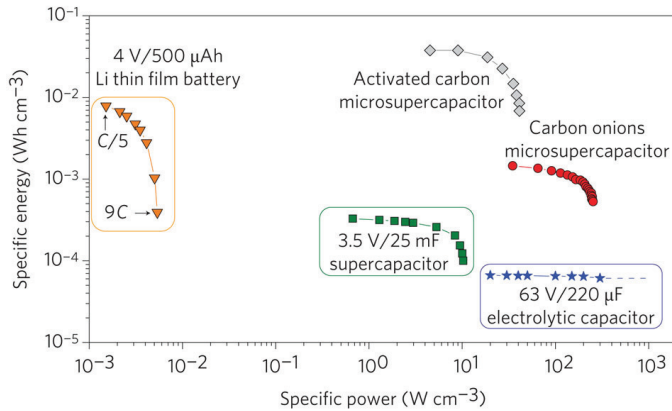
Figure 1.8: Ragone plot comparing the specific energy and power density of typical electrolytic capacitors, supercapacitors and batteries with the micro-devices [36].

cuitry [37], though they do need some smart solutions such as voltage threshold turn-on switch due to the "zero energy bootstrap problem" [21]. This happens when the system starts from a total lack of energy; the harvester must generate enough energy and must also have a large enough voltage for the system to operate stably.

Residual energy in a supercapacitor is easily calculated using $E = CV^2/2$, E being the energy, C the capacitance and V the terminal voltage. Energy consumption for every operation or over a period of time can be simply calculated as $E = C(V_2^2 - V_1^2)/2$, V_1 and V_2 being the initial and the final voltages. This allows for ease of energy measurements in sensor nodes leading to an increased accuracy of energy awareness which forms the basis of energy-aware solutions in energy-harvesting wireless sensor nodes.

The capacitance of a supercapacitor is an important parameter as the amount of energy that can be accumulated depends on the capacitance. The larger the capacitance, the higher the amount of energy that can be stored in the supercapacitor. However, it has been found that supercapacitors with a larger capacitance undergo larger losses of the stored energy due to leakages. Thus a large capacitance supercapacitor not only takes longer to charge, but it also discharges faster. Another drawback of these devices is the phenomenon known as internal charge redistribution, which causes self-discharge of up to 10% of the stored energy every day [38]. Apart from this disadvantage, the supercapacitors seem ideal for energy-harvesting WSNs.

1.2.2.2. BATTERIES

In the Ragone plot, rechargeable batteries are towards the top-left, indicating that they have higher energy densities but lower power densities. This means that the batteries can act as a stable source of energy, and with rechargeability from the ambient energy sources, the lifetime of the nodes should increase.

The batteries undergo reactions after each charge-discharge cycle leading to a limited lifetime. There have been studies on how much useful energy can be extracted from a battery after charging to a given level [39]. The lifetime of (NiMH and NiCd) batteries appears to be more stable with an increasing charging current when

they are charged to 60% of the battery capacities as compared to the case when they are charged to 30% of the capacities. This indicates that it is beneficial to charge a battery to a larger percentage of its rated capacity. Their results also indicate that there is a small decrease in battery lifetime as the charging current increases. Another work [40] suggests that by separating the charging and discharging phases of a battery, the partial charge or discharge cycles that are detrimental to battery lifetimes would be prevented.

Charging the batteries would generally need higher voltage from the ambient energy sources. This would mean that batteries are not well-suited when the energy source is weak. On the other hand, the leakage from a battery is negligible, leading to better usability. Thus, when an application requires high power density as well as high energy density, it is possible to employ a hybrid of both the devices.

Another disadvantage of the batteries is the measurement of residual energy: estimating their charge in real-time is an issue. Several techniques such as load voltage technique, coulomb counting technique, and internal resistance technique are adopted commercially [41]. The load voltage technique is suitable for applications with constant load. The coulomb counting technique accumulates the dissipated coulombs from the beginning of the discharge cycle and estimates the remaining capacity based on the difference between the accumulated value and a prerecorded full-charge capacity. The internal resistance method needs to measure the frequency response of the battery to determine its battery state. The internal resistance technique is the best of the three but this method normally requires extra function generators and separate testing period. This method is expensive and difficult to implement as part of the battery pack itself.

Comparing the supercapacitors and batteries, batteries are not preferred over supercapacitors due to their limited lifetimes, low power densities, and tendencies to leak with increasing energy density.

1.3. NETWORKING WITH ENERGY-HARVESTING WIRELESS SENSOR NODES

The main benefit of energy-harvesting wireless sensor networks is the autonomy of power they gain over battery-powered networks. Unfortunately, merely replacing the batteries with energy harvesters is not enough to reap the benefits. In this section, we shall look at various challenges in networking them.

Table 1.3 shows the power requirements of two low-power WSN motes, namely TMote Sky [42] and TI CC2530 [43], that are compliant with the IEEE 802.15.4 standard. TMote Sky has Texas Instrument's (TI) MSP430 microcontroller (MCU) along with TI CC2420 radio, while CC2530 is a system-on-chip solution with 8051 microcontroller and TI CC2530 radio. Comparing the numbers from the table to the amount of energy that can be harvested, it is apparent that the power harvested is not enough to keep the nodes operating without a storage buffer.

Figure 1.9 displays the recordings of solar light intensity on four different days in Elizabeth City, New Jersey [44]. The figure exemplifies the temporal variations of the available solar energy in an outdoor environment. It indicates that a solar energy-harvesting node will not be continuously powered, and when harvesting, it may not harvest the same amount on different days. Statistics show that the difference among

Table 1.3: Power requirements for various operations in TMote Sky [42] and CC2530 [43] nodes.

Operation	TMote Sky	CC2530
MCU on, Radio TX (@ 0 dBm)	58.5 mW	84 mW
MCU on, Radio RX	65.4 mW	81 mW
MCU on, Radio off	6.3 mW	21 mW
MCU standby	15.4 μW	3.4 μW

the available solar power in shadowy, cloudy and sunny environments can be up to three orders of magnitude [45].

Apart from the temporal variations, the nodes can also experience spatial variations. Figure 1.10 shows an example of this spatial variations, wherein different nodes receive different amounts of energy depending on their location. Although the solar source is an infinite energy source, the harvested power can only be regarded as constant on average in a long-term perspective. On a short-term perspective, however, the harvested power is highly unstable. We can summarize these observations as follows:

1. Power availability varies with time and location.

2. Instantaneous power is limited, but not energy.

3. Excess energy availability is a possibility.

Energy is a precious resource. Hence, carefully designed power management algorithms must be applied in order to avoid wasting the precious energy. Consequently, energy-harvesting in these devices necessitates a redesign of algorithms, communication techniques, and network protocols to achieve perpetual operations without hindering the application requirements. This thesis, therefore, focuses on the design of *energy-adaptive solutions* to use the energy efficiently.

From a networking perspective, classical sensor network protocols cannot harness the full potential provided by the harvesting technology. Some attempts [46] were made to make harvesting-aware routing or clustering decisions, they did not pay off well. Some constraints due to harvesting that make it more challenging for networking the energy-harvesting devices are as follows:

1. Nodes may have different energy-levels and different energy-harvesting opportunities.

2. No node has complete knowledge of the entire network's energy status.

3. Nodes even in a static network may leave and re-enter the network, making the set of immediate neighbors different at different instants.

The energy required for sophisticated control algorithms may introduce a high control overhead for low-power applications. Thus, distributed networking protocols

1
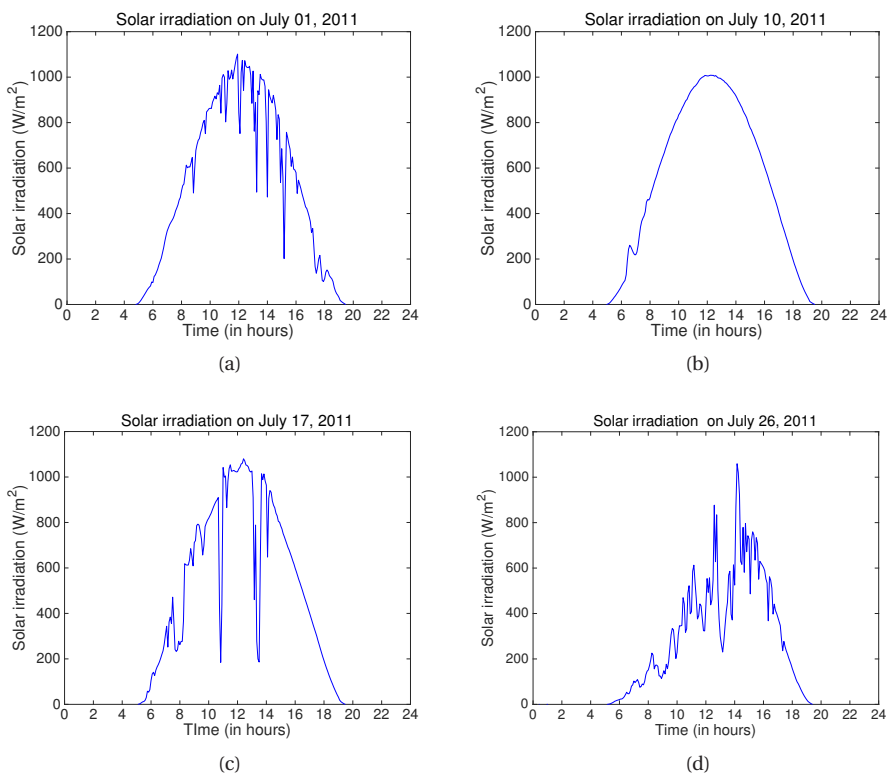
Figure 1.9: Solar irradiation on different days of July 2011 in New Jersey [44].
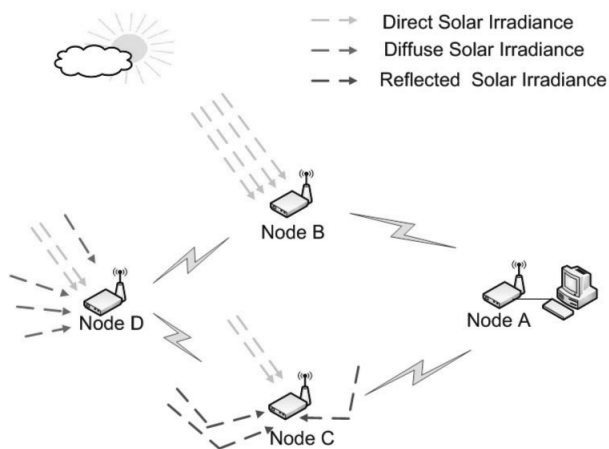
Figure 1.10: Spatial variations of solar energy experienced by energy-harvesting nodes.

must be designed with low-overheads. Moreover, based on the knowledge of the currently available and the harvested power at the nodes, the network connectivity, lifetime and performance must be optimized by shifting the communication and computation loads. That is, the nodes having higher energy levels must unburden the nodes with lower energy levels.

1.3.1. Challenges in Networking Energy-harvesting WSNs

As mentioned before, the variation of energy across nodes introduces several constraints necessitating that the nodes adopt distributed solutions to networking. These protocols must be energy efficient in order to utilize the precious energy optimally. In this section, we present several important challenges in networking beginning with a single node discovering its neighbors to a context-aware application for IoT with energy-harvesting WSNs.

In this work, we are interested in a battery-less system that operates on harvested energy and uses supercapacitors as energy buffers. While each harvesting technology can pose a different dimension to the same networking challenge, we generalize the problems and their solutions. Therefore, we model the energy harvested as a stochastic process. Such models have been used in predicting the amount of energy harvested for a long time. For example, Poggi et al. [28] provide a Markov chain model to predict the solar irradiation in France with high accuracy. Similar models exist for wind energy [47] and vibration harvesting [48]. Therefore, in addition to performing classical power saving techniques, the sensor node has to adapt to the stochastic nature of the energy source and has to decide how and when to use this energy. Goal of this adaptation is to maximize the utility of the application in a long-term perspective.

In this thesis, we address several challenges that arise in order to realize an energy-harvesting WSN, and the IoT applications thereof. We concisely introduce some of the challenges below.

1. Consider a single node's perspective of discovering its neighbors. In an energy-harvesting wireless sensor network where nodes die and come alive often, what factors affect the discovery of neighbors? Should neighbor discovery be a continuous process? If so, how do we achieve that efficiently?

2. Utilization of the available energy and the link efficiently: given that two neighboring nodes have different amounts of energy and an unreliable wireless channel connecting them, how can the two nodes exchange large amounts of data energy efficiently?

3. Connectivity of the whole network: although an energy-harvesting node may see many neighbors, only a subset of nodes must be chosen in order to create a connected network. How to choose the right subset of nodes being energy-aware so that connectivity is maintained as well as higher energy nodes?

4. Routing algorithms in order to utilize a connected network: how to collect and disseminate data reliably an energy-harvesting network? Two main constraints that need to be considered here are that the nodes wake-up asynchronously and the routing protocol must be light-weight.

5. Reliability and latency guarantees of data delivery. This scenario is more challenging as there can be unavailability of nodes due to low energy and unreliability of the data delivery due to the wireless channel effects. The question, therefore, is how to collect and disseminate data reliably an energy-harvesting network with guaranteed latencies?

6. WSNs are used to build ambient intelligence applications such as smart homes. In this scenario, how can we make use of energy-harvesting WSNs to gather contextual data reliably? While one part is routing which is already challenging as mentioned above, the other part is gathering the contextual data reliably when the nodes may run out of energy by spending it on sensing even before routing due to low energy levels?

We mainly approach some of the issues listed above through analytical, simulation and experimental methods. Implementation and measurement studies are also conducted when deemed appropriate.

1.4. CONTRIBUTIONS AND OUTLINE OF THE THESIS

In this thesis, we propose energy-aware power management schemes at the medium access and the network layers of the communication stack. Through these methods, we focus on achieving a completely ambient-energy harvesting WSNs. While we listed several challenges, we solved a few important ones through the course of this dissertation. The contributions of the individual chapters are as follows.

Neighbor discovery - Chapter 2. Several factors affect the neighbor discovery (ND) process making it non-trivial in energy-harvesting WSNs. Nodes may have different energy levels and different energy-harvesting opportunities. Furthermore, nodes even in a static network may leave and re-enter the network, making the set of available neighbors different at different instants. Therefore, ND should be seen as a continuous process throughout the deployment phase of the network. Moreover, nodes may have no knowledge of the number of neighbors a priori in practical settings, which makes it difficult to know when to begin and end the process. In order to identify the various parameters that affect ND we first describe a generic analytical model of an energy harvesting device. Next, we study a network of these devices through exhaustive simulation study considering these various parameters. We analyze a scheme that nodes could use to discover their neighbors during initial deployment and another scheme that could be used for subsequent discovery on re-entry into the network. We present few important tradeoffs in ND for energy-harvesting WSNs.

Topology control - Chapter 3. The most energy consuming operation on a wireless sensor node is the wireless communication – the current consumption by the radio is high and is further aggravated by idle-listening and retransmission of packets. One popular method to increase the energy-efficiency is by restricting the number of communication links through topology control. Topology control is a technique that conserves energy by reducing the transmission powers and improves the network capacity by reducing interference. Most of the topology control algorithms in the literature cannot handle the situation when the nodes have different energy levels, and when the number of active nodes varies with time in an energy-harvesting

WSN. Since the number of nodes alive in the network varies, there is no possibility of having a centralized solution. To address this issue, we present two localized energy-based topology control algorithms, viz., E-ACT-s and E-ACT-d. E-ACT-s is for convergecast applications of WSNs and E-ACT-d is for a generic scenario where all the nodes are required to be strictly connected. A distinguishing feature of both these algorithms is that they select neighbors based on energy levels, and render the global topology well-connected.

A study of constructive interference - Chapter 4. Constructive Interference (CI) occurs when two or more nodes transmit the same data concurrently, which makes the signals superpose. Hence, receivers can decode the packet successfully with high probability due to, supposedly, the increased signal power at the receivers. CI based protocols have been shown to reduce the latency for flooding an entire network considerably and these protocols supposedly deliver packets with high reliability. Before leveraging CI in energy-harvesting WSNs, we deviate to first study the working of CI. CI has generated huge interest in the research community, however, from the previous studies, there appears to be an inconsistent and often contradicting picture about the working of CI. In this chapter, we aim to provide comprehensive insights by taking a receiver's perspective in CI. We derive the resultant signal obtained from the superposition of several concurrent transmissions in order to study CI from a receiver's perspective. Based on the resultant signal, we show the influence of various parameters from the expressions of the resultant signal. Then we conduct an exhaustive experimental study considering minute details in real-life settings. We present comprehensive insights into the impact of the factors through these experimental results. Since CI based protocols cannot have an explicit acknowledgment packet, we make use of *destructive* interference on a designated byte to provide feedback. We leverage this feedback to adapt transmission powers in order to make CI based protocols more reliable.

Understanding synchronous transmission techniques - Chapter 5. Concurrent transmission techniques have been successfully used in wireless sensor networks (WSNs) to design energy-efficient networking protocols. While CI is a recent entrant into this category, packet capture, or simply capture effect (CE), is the more well-known concurrent transmission phenomenon. Due to the significant similarities between the two phenomena, CI has often drawn speculation if the underlying physical phenomenon is just CE. That is, the receiver receives only one of transmitted signals with the other signals not interfering destructively. If CI does not exist, then protocols can be redesigned for higher energy efficiency. Thus, this chapter is dedicated to understanding the two phenomena. We gain deeper understanding on the working of CI and CE phenomena through experimentation in almost ideal conditions. We explain the differences and what exactly *locking* to one of the many transmitted signals means in packet capture.

Low latency and high reliability routing in energy-harvesting WSNs - Chapter 6. With the understanding of CI phenomenon, we aim to leverage its benefits in an energy-harvesting WSN setting. A large number of IoT applications require closed loop control. End-to-end latency, data yield and lifetime of the network are the critical parameters that determine the usability and success of the deployment. Recently, many CI based protocols, such as Low power Wireless Bus (LWB), have been proposed to offer reliable data delivery with low delay and high energy efficiency. They

invariably assume the availability of battery, while we wish to eliminate them through energy-harvesting. We target to gain the benefits of CI based protocols, particularly LWB, by handling the variations in harvested energy through distributed, energy-aware policies. To this end, we propose a distributed, energy-management module called *GLEAM*, for LWB that optimally utilizes the available energy in order to achieve low latency and high reliability. Specifically, we propose a Markov decision model to maximize the energy utility in the infinite horizon by allocating energy optimally. To this end, we also propose a policy and prove its optimality. We also employ protocol optimization to achieve better node availability and CI performance in GLEAM. We find that better usage of redundant nodes deployed in the network contributes significantly. We also outline briefly a method to calculate the required node redundancy in the network to achieve performance similar to battery-powered WSNs.

Context-event triggering with energy-harvesting WSNs - Chapter 7. A large number of sensors are envisioned to be deployed in indoor smart spaces with IoT. The data generated from these nodes can, therefore, be huge. However, only part of the data may be significant that represents the context. Several techniques are proposed to reduce the data sent by each node including event based reporting. Furthermore, these techniques may not be energy efficient. In the chapter on context-event triggering, we propose a technique driven by energy-harvesting to address both the problems together. We propose to exploit the energy harvesters as transducers and to detect change in context. We give examples wherein we can make use of the harvesters. Furthermore, we propose an adaptation to context-aware framework to utilize the proposed mechanism. Finally, we show the benefits of this approach with a use-case. Here, the proposed approach marks only the beginning of a research direction.

Before we end this chapter, we wish to mention here that although there are many challenges in realizing a battery-less ambient-energy powered multi-hop IoT, we chose the important challenges and addressed them in depth. Many others are yet to be addressed. The contributions of this work are shared with the research community through the following publications.

1. **Vijay S. Rao**, R Venkatesha Prasad, T Venkata Prabhakar, Chayan Sarkar, Madhusuhan Koppal and Ignas Niemegeers, *Understanding and Improving the Performance of Constructive Interference in WSNs*, ACM/IEEE Transactions on Networking.

2. **Vijay S. Rao**, Madhusuhan Koppal, R Venkatesha Prasad, T Venkata Prabhakar, Chayan Sarkar, and Ignas Niemegeers, *Murphy loves CI: Unfolding and Improving Constructive Interference in WSNs*, The 35th Annual IEEE International Conference on Computer Communications (INFOCOM 2016). San Francisco, USA, Apr. 2016

3. Xin Wang, **Vijay S. Rao**, Venkatesha Prasad, and Ignas Niemegeers, *Choose Wisely: Topology Control in Energy-Harvesting Wireless Sensor Networks*, 2016 13th Annual IEEE Consumer Communications and Networking Conference (CCNC 2016). Las Vegas, USA, Jan. 2016

4. **Vijay S. Rao**, R Venkatesha Prasad, and I Niemegeers, *Optimal Task Scheduling Policy in Energy Harvesting Wireless Sensor Networks*, IEEE Wireless Communications and Networking Conference (WCNC), pp. 1-6, 2015

5. **Vijay S. Rao**, SN Akshay Uttama Nambi, R Venkatesha Prasad, and I Niemegeers, *On Systems Generating Context Triggers Through Energy Harvesting*, IEEE Communications Magazine, vol. 52, no. 6, pp. 70-77, 2014

6. R Venkatesha Prasad, Shruti Devasenapathy, **Vijay S. Rao**, and Javad Vazifehdan, *Reincarnation in the Ambiance: Devices and Networks with Energy Harvesting*, IEEE Communications Surveys and Tutorials, vol. 16 no.1, pp. 195-213, 2014

7. Shruti Devasenapathy, **Vijay S. Rao**, R Venkatesha Prasad, Ignas Niemegeers, and Abdur Rahim, *Between Neighbors: Neighbor Discovery Analysis in EH-IoTs*, 10th International Conference on Autonomic Computing -Self-IoT Track - ICAC '13. pp. 193-200. Usenix. 2013

8. Shruti Devasenapathy, R Venkatesha Prasad, **Vijay S. Rao**, and Ignas Niemegeers, *Impact of antenna directionality and energy harvesting rate on Neighbor Discovery in EH-IoTs*, IEEE Consumer Communications and Networking Conference (CCNC), pp. 302-307, 2013

9. R Venkatesha Prasad, **Vijay S. Rao**, Ignas Niemegeers and Sonia Heemstra de Groot, *Wireless Sensor Networks for a Zero-Energy Home*, Mobile Lightweight Wireless Systems, pp. 338-346, Springer, 2012

1

2

NEIGHBOR DISCOVERY

2.1. INTRODUCTION

Most WSNs are required to build the network themselves upon deployment, in order to establish an energy-efficient communication infrastructure. The knowledge of *active* one-hop neighboring nodes is essential to create and maintain paths in these multi-hop networks. Knowledge of the one-hop neighbors is essential for many networking protocols, such as the collection-tree protocol [49]. Thus, neighbor discovery (ND) is one of the first steps after deployment of the network.

Typically, a node builds its neighbor table either by sending beacons, called 'HELLO' messages, periodically or by listening to the on-going communications in the channel. Thus, ND is not only performed at the deployment stage of the network but continuously until the deployment lasts. One of the characteristics of energy-harvesting WSNs is that every node may see different energy availability, e.g., a device with a photovoltaic (PV) panel facing south and north. Such heterogeneity implies that ND is no longer a trivial task in such networks. Furthermore, the burden of ND could be handed over to a node that harvests more frequently or larger quantities of energy, or is powered by the electricity grid.

In Chapter 1, we have seen that in energy-harvesting WSNs, although energy availability in theory is perennial, power availability is not guaranteed at every instant. Due to this, energy-harvesting nodes can leave and re-enter the network. Therefore, the network even in a static deployment behaves as a dynamic network. Following are the challenges of ND in energy-harvesting WSNs that make the discovery process non-trivial:

1. Nodes may have different energy-levels and different energy harvesting opportunities. While it is easy to discover the neighbors when a node has excess energy, it becomes highly challenging when the energy is limited.

2. Nodes even in a static network may leave and re-enter the network, making the set of available neighbors different at different instants. Therefore, ND should be seen as a continuous process throughout the deployment phase of the network.

3. Nodes may have no knowledge of the number of neighbors a priori, which makes it difficult to know when to begin and end the process.

4. Since the energy-levels are inherently different on the nodes, they operate asynchronously. That is, each node wakes up at a different instants. It is possible to get the nodes synchronized, but this may cause a huge overhead in the context of the deployment. Therefore, the discovery process should be able to discover neighbors efficiently despite the asynchrony.

In this chapter, we investigate the two most commonly used ND protocols: two-way (active) neighbor discovery and one-way (passive) neighbor discovery protocols. We adapt them to energy-harvesting WSNs and study the influence of various parameters such as energy availability, duty cycle, and beamwidth on the ND process through analysis, numerical evaluation and simulations. We focus on understanding the tradeoffs in energy-harvesting WSNs. The contributions of this chapter are listed below.

1. We adapt two most commonly used ND protocols for energy-harvesting WSN. Further, we propose to use directional antennas for ND, since nodes can transmit at lower transmit powers, reducing their instantaneous power requirement. We shall see a major improvement over omni-directional transmissions also because of reduced interference.

2. We propose an analytical method to evaluate the performance of these protocols in energy-harvesting WSNs wherein the nodes die and re-enter the network.

3. We perform a numerical evaluation as well as simulations to study the performance of the ND protocols with respect to the time taken and the energy consumed. The outcome of these evaluation gives insights into the tradeoffs between parameters such as harvesting rate, storage capacity, node duty cycle, beamwidth and node density.

The chapter is organized as follows. Section 2.2 describes the related work. Section 2.3 describes the the phases of a network deployment when neighbor discovery protocols are necessary, and describe the system model followed by the two protocols that we investigate. In Section 2.4, we develop the analytical models for the protocols. In Section 2.5, we evaluate the protocols with the models using simulations, and discuss the results. The chapter concludes in Section 2.6.

2.2. RELATED WORK

Although ND in WSNs is not executed as a process by itself, it has been studied separately due to its importance and the challenges involved in the process [50]. ND is not a trivial problem in dynamic networks where it is not easy or practical to predict if and when a node will find a neighbor nearby. These networks include mobile networks in which energy is a constraint – e.g., battery-operated ad hoc networks.

Dutta et al. [50] address the problem of neighbor discovery in a network where nodes wake up asynchronously. Their solution, Disco, is based on the birthday protocol method [51] for networks of mobile nodes that sleep and wake up at regular intervals. Their recommendation is that nodes choose their duty cycles as the sum of the reciprocals of two prime numbers that are distinct for each node. This duty

cycle setting is performed based on the worst case discovery latency required by the applications. Similarly Iyer et al., suggest that the beaconing rate must be based on the estimate of the neighborhood size [52]. Such an estimate of neighborhood size is calculated using the *NetDetect* algorithm that uses a maximum likelihood estimator which is fed with the number of errors occurring on the wireless channel. However, in case of energy-harvesting networks, a popular technique adopted for energy management is to adapt the duty cycle to the rate of energy harvesting [8]. Such a rate adaptation causes additional complexity in the ND process.

Cohen and Kapchits describe a cooperative scheme for continuous ND which is performed by nodes in collaboration with known neighbors to find a node that may have recently entered the network [53]. Such a discovery process is different from the initial discovery process when no node is aware of the other. Again, the application of this scheme to energy-harvesting networks is not straightforward as the nodes that have already been discovered by their neighbors would attempt to perform an initial ND again. Thus, there would be a heavy overhead caused by nodes trying to discover neighbors who are already aware of them. A node that suffers heavy fluctuation between on and off state due to very low energy availability could potentially cause congestion by re-initiating the ND process in its vicinity repeatedly.

Discovery in wireless networks using directional antennas has been studied by Vasudevan et al. [54] where the authors describe direct and gossip based algorithms. ND protocols in ad hoc wireless networks using directional antennas have been described by An and Hekmat [55]. They describe handshake based directional ND scheme and study its performance. An et al. describe the various protocols that can be used for ND and the impact of beamwidth and link models on these protocols [56]. Each of these studies describes the benefits of directional antennas in discovery and provides an analytical model for the same. However, they do not expand on a network in which nodes duty cycle due to the non-availability of a continuous source of power.

There is only one important work on neighbor discovery in energy-harvesting WSNs. Panda [57] is a protocol that performs continuous ND by beaconing at a frequency proportional to the energy left in a node's storage buffer. Furthermore, instead of ALOHA-like discovery beacons, it adopts the listen-before-talk principle. While the algorithm is shown to work well, the finding node is assumed to always have power since the application scenario is tracking energy-harvesting powered RFID tags. Furthermore, they do not present the multiple tradeoffs that exist in the ND process, which can be used as the basis for designing optimal discovery algorithms. Thus we study the effects of infrequent energy arrival and variable beamwidth on the neighbor discovery process in energy-harvesting WSN nodes. In the next section, we describe the scenario under consideration and the protocols that are analyzed.

2.3. NEIGHBOR DISCOVERY PROTOCOLS

We consider a deployment of wireless sensor nodes that are placed randomly in an area of interest. Figure 2.1 shows a part of an example deployment. Every node in the network is powered by an energy harvester. All nodes may or may not be powered by the same type of harvester. Thus, the energy opportunities of each node in the network could be different from the other.

We focus our study on the neighbor discovery process of a single node in the
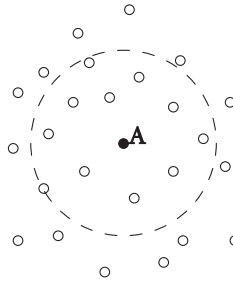
Figure 2.1: Network model with nodes indicated by circles. Node A is the finding node. The dotted circle indicates the communication range of node A.

energy-harvesting network. We label this node as the 'finding node' or 'A', which is represented as the black node in Figure 2.1. Two scenarios can occur with respect to the ND process on A - when the network or node A is in the bootstrapping phase, and when the neighbors around A were discovered but are switching on or off due to their energy-harvesting process.

Bootstrapping phase: In the bootstrapping phase, the network is newly deployed. All the nodes in the network must discover each other. Since we focus on one node, node A, it must find all or at least a predefined number of its neighbors, so that it can build a network thereon. The bootstrapping phase could also occur on node A when it becomes alive after being completely dead wherein its memory or the neighbors list is considered invalid. Furthermore, the bootstrapping phase begins when the network is deployed until the instant when all the nodes have acquired a pre-defined number of neighbors.

Networking phase: This phase occurs when node A is aware of many of its neighbors, but they may be changing their states due to the variation in harvesting energy. In this case, node A must know which neighbors are alive at any instant in order to create a multi-hop network successfully.

Two commonly used protocols corresponding to each of these two phases are active or two-way neighbor discovery and passive or one-way neighbor discovery protocols [58]. Before describing them, we describe the network and energy models, and the assumptions made in order to develop the analytical model in the following section.

2.3.1. System Model
As mentioned earlier, we focus our study on the ND process of the 'finding node'. In this subsection, we shall describe the system, the assumptions made in this work and validation of these assumptions.

The system setup is shown in Figure 2.1. The 'finding node' or 'A' has a number of nodes within its communication range. While a circle is used to indicate the communication range of node A in the figure, our analysis does not depend on the perfect circular communication range.

We do not consider any physical phenomena of the wireless channel (i.e., attenuation, fading, etc.) apart from collisions. In practice, these phenomena affect the ND process. However, we are interested to analyze the effects caused by the energy-
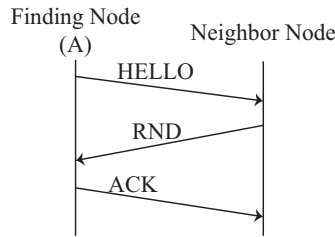
Figure 2.2: Sequence diagram for two-way ND.

harvesting process on the ND in ideal conditions.

Omni-directional antennas are the most commonly used type of antenna for WSNs. At the same time, there has been some development for using directional antennas in these networks, for example SPIDA [59]. Therefore, we consider both type of antennas in this work. In this chapter, we assume that the node can choose a certain beamwidth with a maximum of 360°, at which the transmitter becomes an ideal omni-directional antenna.

As getting the nodes synchronized can be difficult, especially in the bootstrapping phase, we do not assume any synchronization between the nodes. That is, the nodes wakeup asynchronously. However, the nodes try to maintain a fixed duty cycle whenever they have sufficient energy. The wakeup period is uniformly distributed, maintaining the duty cycle. Each transmission takes τ ms. For the sake of simplicity, we do not account for time required for the microcontroller to switch from sleep to active mode, active to sleep mode and the radio turnaround times. All nodes other than the finding node sleep for T_{OFF} ms and are awake for T_{ON} ms as in Figure 2.3(c). In all the protocols, the nodes use ALOHA medium access, i.e., the nodes broadcast as soon as they have a message to transmit and do not use listen-before-transmit techniques. The nodes do not participate in any other communication apart from the neighbor discovery process. Such a mechanism has been considered since the nodes at times may not harvest enough energy to perform CSMA/CA before transmission.

We assume that the harvesting sources are modeled by a stochastic process, mentioned in Chapter 1 (Section 1.3.1). For the analytical model, we further assume that there is no storage element. Hence, the node participates in the ND process only when it is harvesting energy at the moment. Lastly, we assume that the node A has a priori information about its maximum number of neighbors, i.e., k.

2.3.2. TWO-WAY NEIGHBOR DISCOVERY

The two-way ND protocol is used in the bootstrap phase. In this two-way ND process, the finding node actively performs the discovery by sending 'HELLO' message. A neighbor node that receives this message responds with a reply, Reply to ND (RND), message. If node A receives this message, then it retransmits this RND message, which serves as as acknowledgment. This process is shown in Figure 2.2.

Due to the ALOHA-like discovery process, collisions between messages can occur. Collisions can be easily detected by the neighbors who responded with RND if they do not receive the ACK. Furthermore, we do not adopt any explicit collision resolution technique. The nodes have a fixed duty cycle, however each time the node
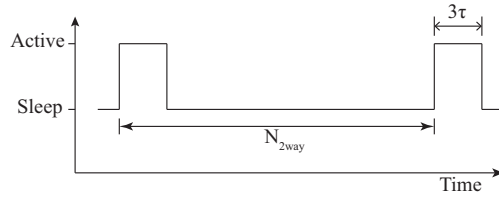
(a) Omni-directional finding node's timing diagram for two-way ND
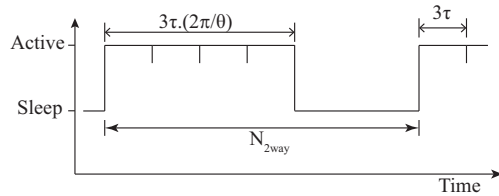
(b) Directional finding node's timing diagram for two-way ND
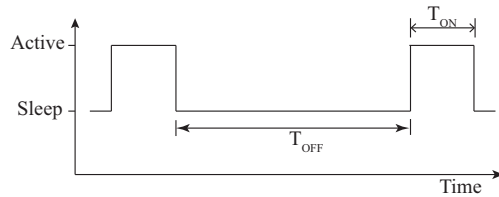
(c) Neighbor node's timing diagram for two-way ND

Figure 2.3: Timing diagrams for Two-way ND.

has to wakeup, it chooses the wakeup time randomly. Therefore, the same two nodes colliding are less likely. Once discovered, the nodes do not randomize their wakeup intervals so that they are synchronized with the finding node. If the received and transmitted packets match, the discovered node marks itself as found and does not respond to any subsequent ND packets. Thus, as nodes are found, the rate at which collisions are experienced is reduced.

OMNI-DIRECTIONAL TWO-WAY ND
In the omni-directional ND case, we assume that every node has an omni-directional antenna. The finding node, node A, attempts to find its neighbors actively. The finding node transmits a HELLO message, whose duration is τ and waits for a RND for a duration τ. The finding node transmits a HELLO message every N_{2way} ms. The timing diagrams for the two-way neighbor discovery is shown in Figure 2.3. The procedure followed during the ND process is listed in Algorithm 1.

DIRECTIONAL TWO-WAY ND
In the directional two-way ND process, the finding node has a directional antenna with a beamwidth θ and thus the search area is divided into $\frac{2\pi}{\theta}$ sectors. An example timing diagram when the area is divided into four sectors of 90° beamwidth is seen in

---

Algorithm 1 Omni-directional Two-way ND algorithm.

1: At the scanning node A when having sufficient energy:
2: **while** k neighbors are not found **do**
3:     Advertise a neighbor discovery (HELLO) packet using omni-directional antenna
4:     Wait for a Reply ND (RND) packet in the next τ ms
5:     **if** RND for a neighbor node B is successfully received **then**
6:         Mark B as found
7:         Transmit ACK indicating that B has been found
8:     **end if**
9:     Sleep for (N_{2way} - 3τ) ms
10: **end while**

11: At a neighbor node C with sufficient energy:
12: **if** HELLO packet is received successfully **then**
13:     Send a Reply ND (RND) packet
14:     Wait for A to confirm if C is found
15:     **if** C is not found by A **then**
16:         Pick a random wakeup time with a mean of T_{OFF} ms
17:     **end if**
18: **end if**

Figure 2.3(b). The finding node transmits a HELLO packet of duration τ and listens for τ milliseconds for an RND packet every N_{2way} milliseconds. The finding node transmits HELLO packets in a fashion similar to the wheeled-iteration method [58], i.e., the finding node transmits a HELLO packet and awaits an RND in each of the sectors 1 through $\frac{2\pi}{\theta}$ in sequence. Thus the total transmit time for the finding node is $3\tau.\frac{2\pi}{\theta}$. The assumptions for the neighbor nodes remain the same as before. The algorithmic steps followed are listed in Algorithm 2.

A new scenario arises with the use of directional antennas. Since the node would have to use lower energy to transmit over a smaller sector area, it can reach the same range as an omni-directional transmitter at lower transmit powers. Thus, for a directional transmission, if the node increases its transmit power, it could reach farther. This would cause the node to discover nodes that were not reachable by the omni-directional antenna. While this is beneficial since it improves the connectivity of the network, the advantage is lost because nodes may no longer discover each other mutually. That is, unless the neighbor node found in the extended range also has a directional antenna and chooses to transmit using the same power, two-way discovery is not possible. However, the purpose of a directional antenna in neighbor discovery for energy-harvesting WSNs is not increased transmission range but reduced instantaneous power consumption and lower interference among neighbors. For this reason, we limit the directional antenna's range to the same range as of an omni-directional antenna by controlling the transmit power. In practice, such transmit power control for a directional antenna could be achieved using topology control schemes described in the next chapter.

Algorithm 2 Directional Two-way ND algorithm.

 1: At the scanning node A when having sufficient energy:
 2: **while** k neighbors are not found **do**
 3:     **for all** $s \in \{1, 2, \dots \frac{2\pi}{\theta}\}$ sectors **do**
 4:         Advertise a neighbor discovery (HELLO) packet using an directional antenna with beamwidth θ
 5:         Wait for Reply ND (RND) packet in the next τ ms
 6:         **if** RND for a neighbor node B is successfully received **then**
 7:             Mark B as found
 8:             Transmit ACK indicating B has been found
 9:         **end if**
10:     **end for**
11:     Sleep for ($N_{2\text{way}}$ - $3\tau.\frac{2\pi}{\theta}$) ms
12: **end while**

13: At a neighbor node C with sufficient energy:
14: **if** HELLO packet is received successfully **then**
15:     Send a Reply ND (RND) packet
16:     Wait for A to confirm if C is found
17:     **if** C is not found by A **then**
18:         Pick a random wakeup time with a mean of T_{OFF} ms
19:     **end if**
20: **end if**

2.3.3. One-way Neighbor Discovery

Apart from the two-way ND algorithm, another popular neighbor discovery method is to passively listen to the on-going transmissions and update the neighbors list. This technique is more useful to keep track of the changes in an already discovered neighborhood, particularly, in an energy-harvesting network where the nodes constantly leave and re-enter the network. Moreover, storing a neighbor table in non-volatile flash memory of a node is often too expensive in terms of energy, especially if the node density is high. In such a case, it is economical and practical for a node to attempt to discover its neighbor nodes every time it re-enters the network. This necessitates a continuous ND process in this dynamic network. However, a two-way neighbor discovery process could be avoided in this case as most nodes are already aware of their neighbor nodes.

It is apparent that the one-way ND method is more suited to perform the continuous ND process. In this method, all nodes send out 'HELLO' messages when they wakeup. These messages can then be heard by the newly "reborn" sensor node and can be used to discover its neighbors. Such a beaconing could be useful not just for neighbor discovery but also to convey important information such as energy-level of the node or other parameters. Since through this process, only the node that is listening for beacons discovers nodes, we call it a "one-way" scheme.

A sequence diagram of the one-way ND method is shown in Figure 2.4. In the one-way discovery process, as there is no feedback from the passive finding node, each neighbor node simply randomizes the time slot at which it transmits the next
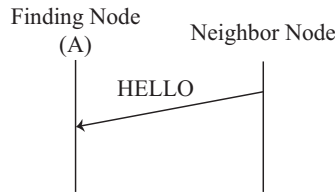
Figure 2.4: Sequence diagram for one-way ND.
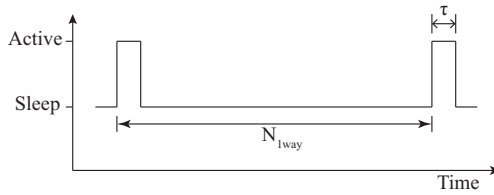
(a) Omni-directional finding node's timing diagram for one-way ND
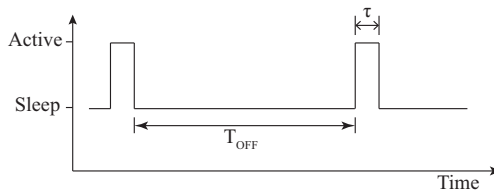
(b) Neighbor node's timing diagram for one-way ND

Figure 2.5: Timing diagrams for One-way ND.

ND packet.

OMNI-DIRECTIONAL ONE-WAY ND

In the omni-directional case, the finding node as well as every other node is assumed to have omni-directional antennas. The finding node listens for a 'HELLO' message every N_{1way} ms for τ ms as shown in Figure 2.5(a). Every neighbor node transmits a HELLO message of duration τ ms every T_{OFF} ms on an average as shown in Figure 2.5(b). The algorithmic steps involved in ND for the omni-directional case are listed in Algorithm 3.

DIRECTIONAL ONE-WAY ND

The only difference from the omni-directional one-way discovery is that the finding node listens for τ ms in each of sectors 1 through $\frac{2\pi}{\theta}$ sectors in sequence every N_{1way} ms. Neighbor nodes transmit omni-directionally as before. The steps followed in this method are listed in Algorithm 4.

Algorithm 3 Omni-directional One-way ND algorithm.

1: At the scanning node A when having sufficient energy:
2: **At** every N_{1way} ms **do**
3: Wait for beacon in the next τ ms
4: **if** beacon for a neighbor B is successfully received **then**
5:     Mark B as found
6: **end if**
7: Sleep for (N_{1way} - τ) ms
8: **end**

9: At a neighbor node C with sufficient energy:
10: Transmit a beacon at time t
11: Pick a random wakeup with a mean of T_{OFF} ms

2.4. ANALYTICAL MODELS

In this section, we present the analytical models to analyze the all the ND algorithms described in the previous section.

2.4.1. TWO-WAY OMNI-DIRECTIONAL FINDING NODE

Here we describe the model for a finding node with omni-directional antenna that attempts to discover k of its neighbors using the two-way ND process. Let node A act as the finding node and it must discover k nodes labeled B_1 to B_k. A neighbor node is denoted by B.

Algorithm 4 Directional One-way ND algorithm.

1: At the scanning node **A** when having sufficient energy:
2: **At** every N_{1way} ms **do**
3: **for all** $s \in \{1, 2, \dots \frac{2\pi}{\theta}\}$ sectors **do**
4:     Wait for beacon in the next τ ms
5:     **if** beacon for a neighbor B is successfully received **then**
6:         Mark B as found
7:     **end if**
8: **end for**
9: Sleep for (N_{1way} - $\tau.\frac{2\pi}{\theta}$) ms
10: **end**

11: At a neighbor node C with sufficient energy in storage:
12: Transmit a beacon at time t
13: Pick a random wakeup with a mean of T_{OFF} ms

In order to discover these nodes, A transmits HELLO message with a probability P_{t_A} given as

$$P_{t_A} = \frac{1}{N_{2way}} P_{e_A},\tag{2.1}$$

where N_{2way} is the period with which A attempts ND and P_{e_A} is the probability that

A has the energy required to initiate and complete the ND process at that instant of time. This probability in a real system would be equal to the probability of the energy storage buffer having the required amount of energy.

Every node B listens for an ND message from A with a probability P_{l_B} which is given as:

$$P_{l_B} = \frac{T_{\text{ON}}}{(T_{\text{ON}} + T_{\text{OFF}})} P_{e_B},$$ (2.2)

where P_{e_B} is the probability that B has the energy to respond to the ND message.

Thus, the probability that an ND packet transmitted by A reaches B successfully is given as:

$$P_{A \to B} = P_{t_A} P_{l_B}.$$ (2.3)

This also gives the probability P_{t_B} that node B that receives this ND packet responds to it by sending an RND. In order for the discovery process to be completed, B_k nodes must respond to A without their RNDs colliding with each other. The probability that of n nodes that have not been discovered by A, only 1 responds is given as $(1-P_{t_B})^{n-1}$. Thus the probability that only a single node reaches the finding node successfully (without collisions) is given as:

$$P_{B \to A} = \binom{n}{1} P_{t_B} (1 - P_{t_B})^{n-1}.$$ (2.4)

From this expression it is possible to calculate the time required to find a given node B_i as:

$$T_{ND}(i) = \frac{1}{P_{B_i \to A}},$$ (2.5)

where T_{ND} is the time to discover the neighbor B_i. The total time that is required to find all k nodes is given as:

$$T_{ND} = \sum_{i=1}^{k} \frac{1}{P_{B_i \to A}},$$ (2.6)

where i denotes the number of nodes out of k that have been found by A.

2.4.2. TWO-WAY DIRECTIONAL FINDING NODE

In the case where the finding node employs a directional transmitting antenna to discover its neighbors brings changes to the analysis, which will be described in this section. As in the omni-directional case, the probability of transmission at directional finding node A_d is given as:

$$P_{t_{A_d}} = \frac{1}{N_{2\text{way}}} P_{e_{A_d}},$$ (2.7)

and the probability that a neighbor node B is listening is given as:

$$P_{l_B} = \frac{T_{\text{ON}}}{(T_{\text{ON}} + T_{\text{OFF}})} P_{e_B}$$ (2.8)

as before in the omni-directional case.

The probability that node B is in the same sector as the finding node is given as $\frac{\theta}{2\pi} = \frac{1}{N_s}$, where θ gives the beamwidth of the directional beam and N_s is the resultant

number of sectors. Thus the probability that node B responds to the ND packet from A_d is given as $P_{t_B}(1/N_s)$ where P_{t_B} is defined as before in the omni-directional case. The probability that no other node responds to A depends on the number of nodes that fall within the beam of A_d. We define the probability that out of k number of neighbor nodes there are j nodes in the same beam sector as the considered node, B. This is given by,

$$P_j = \binom{N_s}{1}\binom{k-1}{j-1}\left(1 - \frac{1}{N_s}\right)^{k-j}\left(\frac{1}{N_s}\right)^j. \tag{2.9}$$

Finally, the probability that node B is successfully discovered by node A_d is given as,

$$P_{B \to A_d} = \sum_{j=1}^{k} P_j \binom{j}{1}\frac{P_{t_B}}{N_s}\left(1 - \frac{P_{t_B}}{N_s}\right)^{j-1} \tag{2.10}$$

and this reduces to Equation 2.4 for $N_s = 1$, which is the case for an omni-directional finding node.

Again, the number of time slots required to discover a single node is given as $1/P_{B \to A_d}$ and the ND time, T_{ND}, for all k nodes is the summation for all nodes,

$$T_{ND} = \sum_{i=1}^{k} \frac{1}{P_{B_i \to A_d}}, \tag{2.11}$$

where $i = 1, 2, \dots k$ denotes the number of nodes found by node A_d.

2.4.3. ONE-WAY OMNI-DIRECTIONAL FINDING NODE
In this case, the finding node passively listens to the transmissions from its neighbors. All nodes have omni-directional antennas as described in Section 2.3.3. This case can easily be derived from the two-way omni-directional analysis.

A neighbor node B transmits with a probability P_{t_B} given by

$$P_{t_B} = \frac{T_{ON}}{(T_{ON} + T_{OFF})}P_{e_B},$$

where the denominator is the period with which B sends a HELLO message and P_{e_B} is the probability that B has the energy required to send the message at that instant.

The finding node A listens for the message with a probability P_{l_A}, which is given by,

$$P_{l_A} = \frac{1}{N_{1way}}P_{e_A},$$

where N_{1way} is the period with which node A listens for transmissions and P_{e_A} is the probability with which node has the energy to listen to the message. Thus, the probability that the message reaches A is $P_{t_B}P_{l_A}$. Since there are $n \le k$ nodes that may send a beacon, the probability with which a HELLO message successfully reaches A is given by

$$P_{B \to A} = \binom{n}{1}(P_{t_B}P_{l_A})(1 - P_{t_B}P_{l_A})^{n-1}. \tag{2.12}$$

The total time required to receive at least one beacon from all the nodes can be calculated as,

$$T_{ND} = \sum_{i=1}^{k} \frac{1}{P_{B_i \to A}}. \tag{2.13}$$

2.4.4. ONE-WAY DIRECTIONAL FINDING NODE

Similar to the omni-directional case, the probability with which a HELLO message reaches the finding node A is $P_{t_B} P_{l_A}$, where P_{t_B} is the probability with which a neighboring node B sends a message and P_{l_A} is the probability with which node A listens to the transmissions. The latter value, P_{l_A}, will be divided by the number of sectors, N_S since the antenna is directional. The probability that there is more than one neighbor node in the same sector, P_j, is given by Equation 2.9. Thus, the probability that the HELLO message from node B successfully reaches node A is given by,

$$P_{B \to A_d} = \sum_{j=1}^{k} P_j \binom{j}{1} \left(\frac{P_{t_B} P_{l_A}}{N_S} \right) \left(1 - \frac{P_{t_B} P_{l_A}}{N_S} \right)^{j-1}. \tag{2.14}$$

Again, the ND time is the inverse of the probability given by,

$$T_{ND} = \sum_{i=1}^{k} \frac{1}{P_{B_i \to A_d}}. \tag{2.15}$$

2.5. EVALUATION

In this section, we seek to evaluate the performance of ND to study the influence of energy-harvesting as well as other parameters other than the harvesting process. The performance of ND is mainly quantified by the time required, T_{ND}, to discover the neighbors. T_{ND} depends on several factors which are as follows:

- energy availability,

- number of nodes or node density,

- node duty cycle, and

- beamwidth.

In this section, we will analyze the dependencies of these factors on the neighbor discovery process by two methods: numerical evaluation and through simulations. For the purpose of evaluation, we define the time slot as the basic time unit required for one transmission. For instance, if the ND process uses a 32 B packet with IEEE 802.15.4, then the time slot is approximately equal to 1 ms. We assume that all time related parameters, such as τ, T_{ON}, T_{OFF}, N_{2way}, and N_{1way}, are all multiples of the time slot. Furthermore, we consider the number of nodes k around the finding node to be 40 unless mentioned explicitly. These k nodes are randomly placed according to a uniform distribution. Let us first present the results followed by the insights we gained.
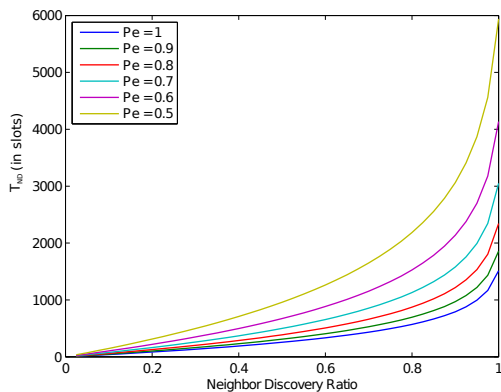
(a) Omni-directional case
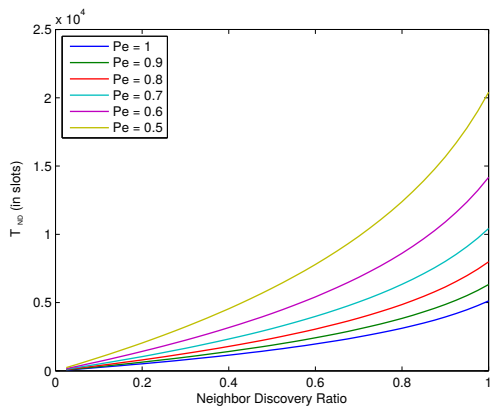
(b) Directional case

Figure 2.6: Two-way ND for various energy probabilities.

2.5.1. NUMERICAL RESULTS

All the numerical results were computed using MATLAB. Since the one-way discovery process can be visualized as one part of the two-way discovery, the results presented here are for the two-way ND process only.

2.5.1.1. ENERGY

Figure 2.6 shows numerical results from the analysis for T_{ND} for the case under several energy availability probabilities $P_e = P_{e_A} = P_{e_B}$ for both omni-directional and directional finding nodes. The beamwidth for the directional case is set to $\theta = 45°$. As expected, with lower energy probabilities, the performance of ND deteriorates, and the time required with directional case is more than the omni-directional case.

2.5.1.2. NODE DUTY CYCLE

The duty cycle of the nodes gives the probability that a responding node B is awake. The higher the duty cycle, the better are the chances that neighbor nodes respond
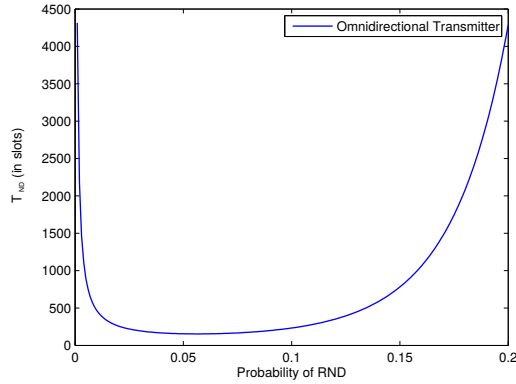
(a) Omni-directional case
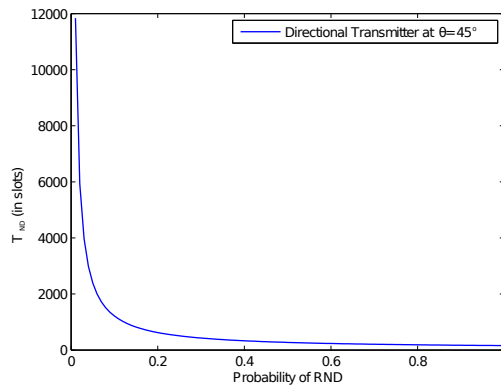
(b) Directional case

Figure 2.7: ND Time versus probability that node *B* responds to the HELLO message.

to the HELLO messages. Thus, the parameter of interest here is the probability with which a neighbor node can respond to the HELLO message. This is given by Equation 2.4 for the omni-directional case and by Equation 2.10 for the directional case. Plotting the ND time against this parameter gives us insight into the possible advantage that directional transmission may provide to the ND process.

On the one hand, we see in Figure 2.7(a) that the ND time, T_{ND} increases dramatically, starting at an extremely low RND probability of 0.12. On the other hand, since there is a low probability that several of the *k* nodes occupying the same sector, the ND time is relatively unaffected by the probability of responding with an RND as shown in Figure 2.7(b).

2.5.1.3. NODE DENSITY
The ND time for various values of *k*, or node density, for both omni-directional and directional transmitters can be observed in Figure 2.8. The monotonously increasing curves seem to saturate for higher values of *k*. This behavior is because, once a node
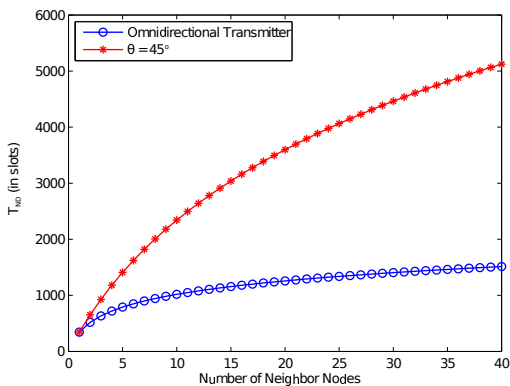
Figure 2.8: Performance of two-Way ND for various node densities.
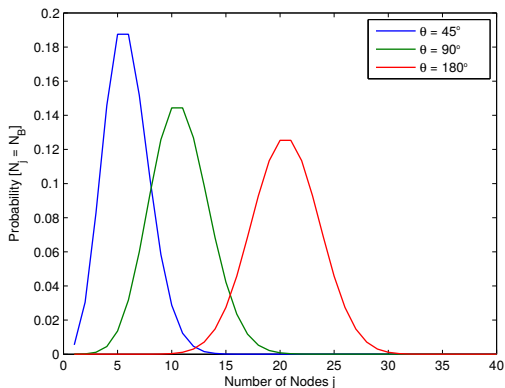
Figure 2.9: Effect of beamwidth on the probability of nodes occupying the same sector.

has been found, it does not respond to subsequent HELLO packets from the finding node.

The beamwidth of the directional finding node has an effect on the probability P_j, which is the probability of having j nodes in the same beam sector as the considered neighbor node B that should respond to the HELLO message from the finding node. The effect of beamwidth is shown in Figure 2.9. The probability density function is a bell-shaped one that gets shorter and wider with an increasing θ value.

The implication of a shorter and wider curve is that the probability of a given number of nodes occupying the same sector and thus contributing to interference becomes more distributed. However, since the PDF curve also moves to the right while becoming shorter and wider, the probability that a larger number of nodes would be present is higher.
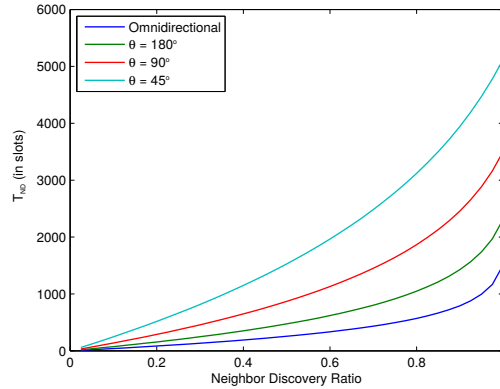
Figure 2.10: Two-way ND for various beamwidths.

2.5.1.4. BEAMWIDTH

We can see in Figure 2.10 that the performance gets progressively worse with a decreasing beamwidth. The major cause for this is the lower probability that at a given time, any neighboring node is listening in the same sector as the one in which A is transmitting. This is also evident in Figure 2.6, where the performance of the directional finding node is worse than the omni-directional case.

2.5.1.5. DISCUSSIONS

From the results presented until now, we have observed that

1. directional finding takes more time than the omni-directional case, and

2. node duty cycle impacts the omni-directional discovery but not the directional finding case.

However, there are two main factors missing in these results: collisions of packets and the impact of the stored energy that will allow more nodes to respond. While these theoretical numbers are a good indication of the impact of the parameters considered (i.e., beamwidth, duty cycle, and energy), they are not presenting the picture completely. In order to study the process in detail, we perform simulations which is presented in the next section.

2.5.2. SIMULATION MODELING

We assume the energy arrival follows a stochastic process (see Section 1.3.1), specifically a Poisson process for all the simulations. That is, the time between the arrival of two discrete packets of energy is exponentially distributed. We use the term energy interarrival time (T_E) to indicate the time between two consecutive arrivals of energy packets. Thus, an energy regime that sees an interarrival time of 15 time slots is injected with a random quantity of energy every 15 time slots on average. The quantity of arriving energy is randomized to emulate a varying energy availability level similar to the varying power levels available from a solar panel at noon versus at sunset.

Table 2.1: Energy consumed by a node for various operations.

Event	Energy Consumption
Transmission of one message	0.075 mJ
Transmission of one message ($\theta = 45°$)	0.054 mJ
Transmission of one message ($\theta = 90°$)	0.063 mJ
Transmission of one message ($\theta = 180°$)	0.069 mJ
Transmission in $\frac{2\pi}{\theta}$ sectors	Cost for a message $\times \frac{2\pi}{\theta}$
Receive mode for 1 time slot	0.072 mJ
Staying on (asleep) for 1 time slot	0.006 mJ

We consider a supercapacitor as the energy storage buffer. We use a simple linear relationship between stored energy and leakage, but Weddell et al. describe a complex model for accurate supercapacitor modeling [60] which could improve the study. Since almost every ambient source is quite random, an energy buffer is recommended. With the presence of a storage element, the variations in energy availability are smoothened. We shall see in the results of our simulation and analytical models, how this impacts system performance. For all our simulations, unless indicated otherwise, we consider that every node is equipped with a supercapacitor with a capacitance of 0.7 F which translates to an energy capacity of 3 mJ. As mentioned in Chapter 1, supercapacitors undergo leakage of charge. For simulations here, we assume the supercapacitors undergo a leakage that is around 5% of the available energy.

Each node can measure the amount of available energy in its storage buffer. A node initiates or responds to an ND process only if it has energy required for the entire process. For example, the directional finding node in the two-way discovery process would start transmission only if it has energy to transmit to and receive from all sectors.

The energy consumed for various operations that we consider in our study is listed in the Table 2.1. The values assumed are taken for an Iris mote from Crossbow [61]. The energy consumption of one directional message is less than one omni-directional message as we assume that the directional transmitter can transmit at a lower transmit power than the omni-directional transmitter and cover approximately the same range. However, the cost for a series of transmissions to each sector for the directional transmitter would prove costlier as this cost for a single transmission would be multiplied by the number of sectors. We begin with the study of the two-way discovery process.

2.5.3. Simulation Results of Two-way ND

In order to understand the effect of various relevant parameters on the process of neighbor discovery in energy-harvesting WSNs, we perform simulations and present the results in this section. Again, the main metric used here is ND time along with number of collisions and energy with which the parameters are evaluated.
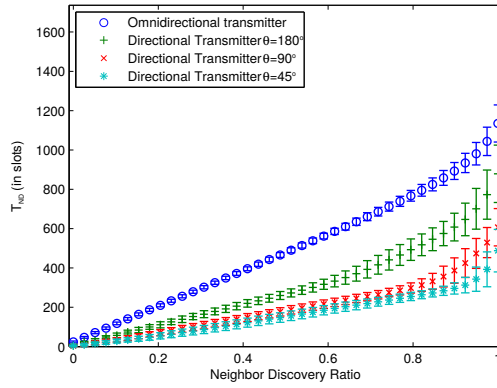
Figure 2.11: Effect of beamwidth on ND time.
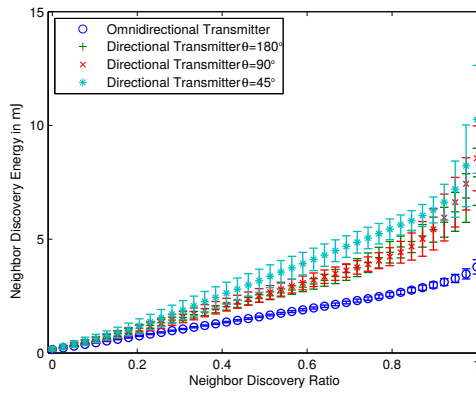
Figure 2.12: Effect of beamwidth on ND energy.
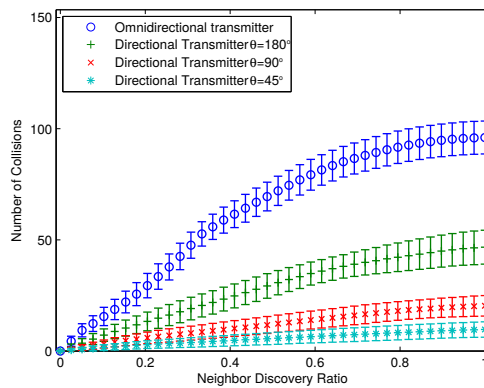
Figure 2.13: Effect of beamwidth on ND collisions.
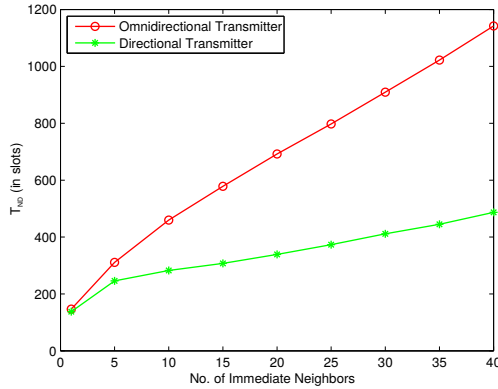
Figure 2.14: Effect of node density on ND time.
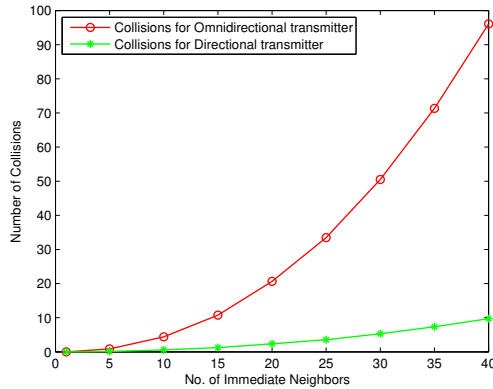
Figure 2.15: Effect of node density on ND collisions.

2.5.3.1. BEAMWIDTH

In this study, all nodes including the finding node have excess energy availability i.e., T_E is 0. Neighbor nodes operate at 20% duty cycle. Contrary to the numerical results, we see the advantage of using a directional finding node in Figure 2.11, which shows the mean and standard deviation of the ND time, T_{ND}, required to find each neighbor node, taken from 1000 samples. The node with the lowest beamwidth at 45° provides the best performance in terms of the ND time.

The energy required for finding all 40 nodes can be seen in Figure 2.12. We assume that the finding node transmits with less power for covering the same range. Yet, the advantage that the finding node has in lower ND time for low beamwidth is offset by the higher energy consumption due to the increased number of transmissions. Thus, at $\theta = 45°$ the energy spent by the finding node is the highest and decreases when the beam becomes wider.

As the beamwidth of the finding node decreases, the number of collisions that
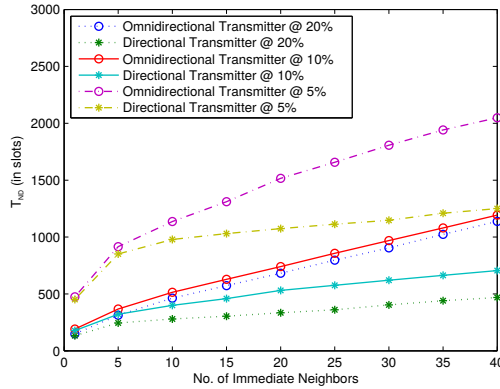
Figure 2.16: Effect of node duty cycle on ND time.
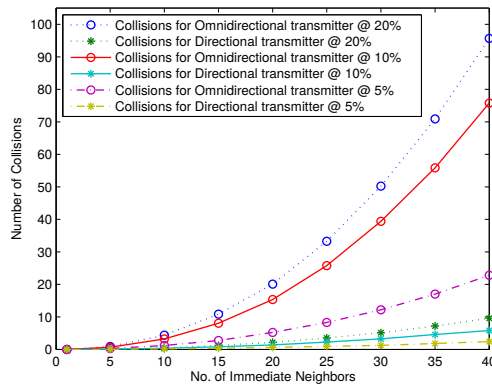
Figure 2.17: Effect of node duty cycle on ND collisions.

occur among responding nodes goes down. Thus, the required neighbor discovery time decreases. As the percentage of nodes discovered goes up, the deviation of the various samples from the mean value increases. Such an increase is the result of the randomized wakeup time of the nodes. In Figure 2.13, we see the cumulative number of collisions that occurred before discovery of each of the 40 nodes. For the omni-directional finding node, a sharp rise can be seen in the number of collisions till about 40% of the nodes are found. Beyond this point, the number of collisions saturates visibly. The reason is that as each node is found, the probability of a collision keeps reducing as the found node no longer responds to the subsequent ND packets.

We can now conclude that the directional transmitter performs better in terms of the ND time, T_{ND}, due to two reasons, both relating to interference: (i) fewer collisions allow nodes to be found faster; (ii) nodes suffer lower energy wastage due to collisions, and thus do not deplete their energy storage buffer quickly. Thus, they are likely to be able to respond more often.

2.5.3.2. NODE DENSITY

In investigating the effect of the number of neighbor nodes on the neighbor discovery time, from Figure 2.14 it can be observed that it takes the same time for the finding node to discover a single neighbor node (i.e., $k = 1$) in both omni-directional and directional cases. Here $\theta = 45°$, but the number of sectors scanned does not have an impact on the neighbor discovery time, since the rate at which all sectors are scanned is equal to the rate at which the omni-directional transmitter transmits.

However, as the number of nodes to be discovered increases, the number of collisions between responses to the HELLO messages increases (Figure 2.15). The effect of these collisions is less in the case of directional discovery since fewer nodes listen and respond to the DND messages and hence there are fewer RND messages. As before, the study was conducted for the case when excess energy is available ($T_E = 0$), neighbor nodes operate at 20% duty cycle and the shown result is the mean of 1000 samples.

2.5.3.3. NODE DUTY CYCLE

As discussed previously, neighbor nodes operate at a fixed duty cycle. For ease of study, we assume that all nodes choose to operate at the same duty cycle. This works since we assume that none of the neighbor nodes interact among each other. In order to understand what duty cycle suits our setting best, we plotted the neighbor discovery time for various node densities at different duty cycle settings. The time for which the node is awake is set and only the T_{OFF} changes.

The duty cycle at which neighbor nodes operate has a bearing on the time taken for neighbor discovery as seen in Figure 2.16. The study is conducted with the excess energy condition and results are computed with the mean of 1000 samples. We consider cases in which nodes duty cycle at 20%, 10% and 5% and as expected it takes longest to discover nodes at 5%.

However for a 5% duty cycle, the number of collisions that are observed is the least. This lower collision count is simply because the neighbor nodes listen to and therefore respond to fewer HELLO packets. We do not study the effect of changing the rate at which the finding node sends HELLO packets as this would result in longer time to discover nodes and it does not provide any new insights.

2.5.3.4. ENERGY INTERARRIVAL TIMES

Here we consider that energy arrives at each of the nodes including the finding node as a Poisson arrival process with an interarrival time of 15, 10 and 5 time slots. The effect of energy interarrival times on the neighbor discovery time can be seen in Figure 2.18. The time or number of slots required in each case to find neighbor nodes is recorded for both an omni-directional and a directional finding node ($\theta = 45°$) in Figure 2.18. As intuition suggests, the performance of the finding node in terms of neighbor discovery times is worse at low energy arrival rates. But it is interesting to see the behavior of the directional finding node versus the omni-directional one.

When $T_E = 15$, the omni-directional finding node outperforms the directional node. This is caused by the excess energy that the directional node must spend in comparison with the omni-directional node as seen in Figure 2.19 and the lower availability that the $T_E = 15$ case offers. Since the nodes in the vicinity of the finding node in the $T_E = 15$ case suffer from a shortage of energy, they respond less frequently to
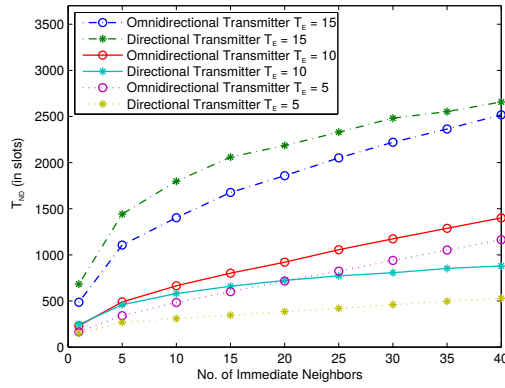
Figure 2.18: Effect of energy interarrival times on ND time.
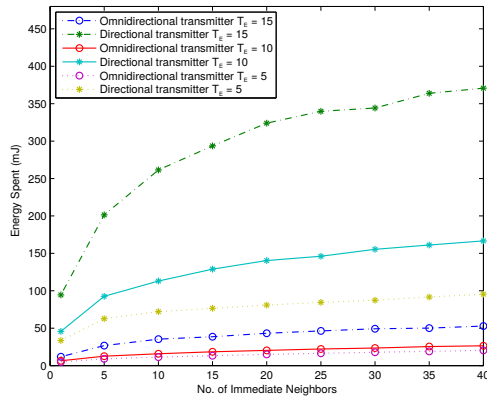
Figure 2.19: Effect of energy interarrival times on ND energy.
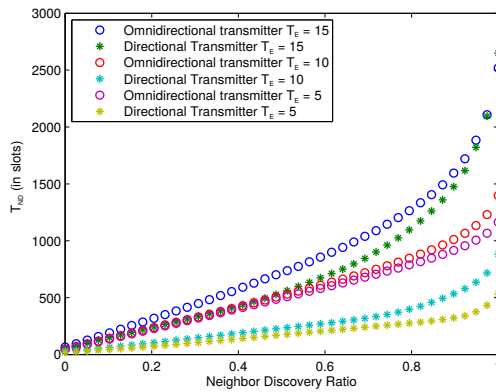
Figure 2.20: Effect of energy interarrival times for $k = 40$ on ND time.
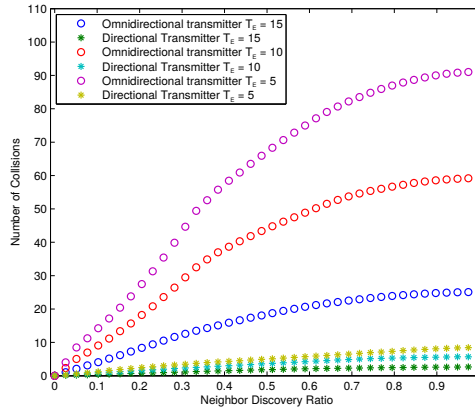
Figure 2.21: Effect of energy interarrival times for $k = 40$ on ND collisions.

the ND packets of the finding node. As a result, the finding node bears the brunt and has to spend a longer time and more energy for the discovery process. Furthermore, as the directional node defers the ND process to a time when it has sufficient energy to carry out discovery in all sectors, there is a further increase in its ND time.

However, the directional node still finds 90% of its neighbors faster in the $k = 40$ case, as can be observed in Figure 2.20. Furthermore, as the energy interarrival time decreases, the directional transmitter performs better. It can be seen that the directional transmitter with $T_E = 10$ performs even better than the omni-directional transmitter that sees more frequent energy arrivals with $T_E = 5$.

Again, this better performance of the directional transmitter can be explained by the higher number of collisions in the omni-directional case. It can be seen from Figure 2.21 that as the T_E increases, the number of collisions decreases. This can be explained by the fact that nodes respond less often to the finding node's ND packets due to lower frequency of energy arrival.

2.5.3.5. Storage Capacity

As discussed earlier, we consider that the harvested energy is stored in a supercapacitor. In the previous discussions, we consider a supercapacitor whose C is approximately 0.7 F such that the maximum amount of energy it can store is $E = 0.5CV^2 = 3$ mJ. To understand if the C of the supercapacitor has an effect on the ND time, we studied the performance for various values of C. The study was conducted entirely for the $T_E = 15$ case to understand how the system behaves in the most adverse condition. For all cases that we study here, we vary C for all nodes in the network. As before, neighbor nodes operate at 20% duty cycle and the results are an average of 1000 simulation runs.

As can be seen in Figure 2.22, as C increases, the ND time reduces as expected. Since the storage buffer can store larger amounts of energy, the effects of constantly changing input energy conditions is reduced as the supercapacitor now has a smoothing effect on these variations. Another interesting consequence of an increased C is that the difference in the ND time between the directional and omni-directional
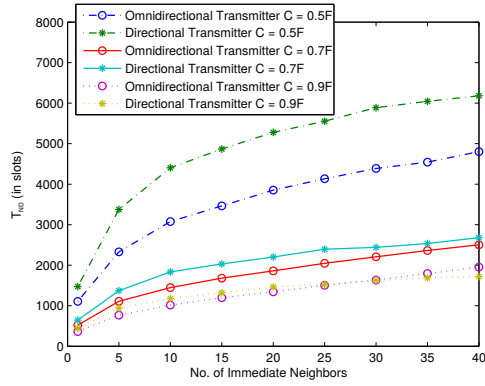
Figure 2.22: Effect of supercapacitor capacity on ND time.
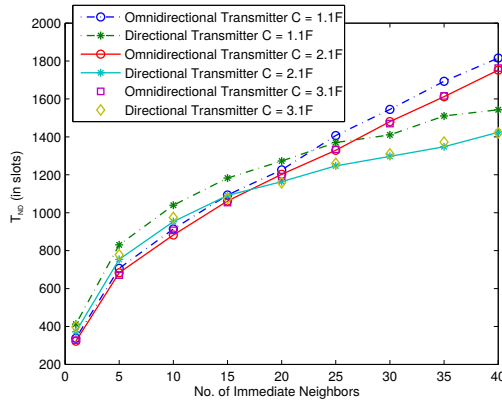
Figure 2.23: Effect of supercapacitor capacity on ND time. ND time does not improve after a threshold capacity.
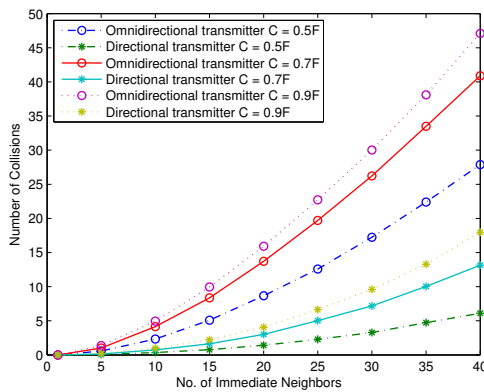
Figure 2.24: Number of collisions for different capacity values.
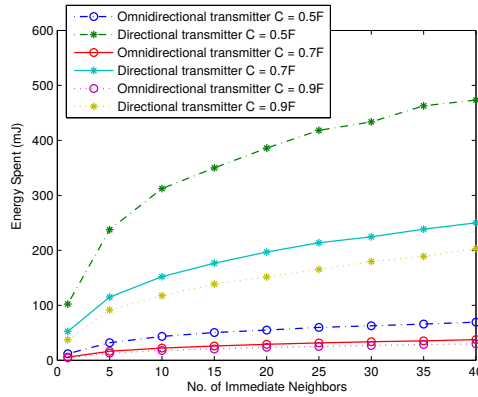
Figure 2.25: Energy cost at different values of C.

finding node is reduced. For the case where C = 0.9 F, the directional finding node matches the performance of the omni-directional one for low values of k and even outperforms it for $k = 35$.

This improvement in performance is not seen beyond a threshold C. We see in Figure 2.23 that there is no improvement in ND time from 2.1 F to 3.1 F and very little improvement from 1.1 F to 2.1 F. It can be seen that the value of k at which the directional transmitter performs better than the omni-directional one reduces from 0.9 F at $k = 35$ (seen in Figure 2.22) to 1.1 F at $k = 25$ and 2.2 F at $k = 20$. Such a reduction is a result of the increased collision count for the omni-directional transmitter as seen in Figure 2.24 at higher values of k.

We observe in Figure 2.24 that the number of collisions keeps increasing as C goes up. This can be explained by the fact that every node in the setup has a better chance of responding to ND packets when the amount of stored energy goes up. This is also supported by the ND energy seen in Figure 2.25. A larger C allows for better use of available energy.

At this point, it is important to discuss the effect of the use of the storage element. We have seen previously, the behavior of the system when there is no storage element present (through numerical results presented in Section 2.5.1). We saw that in the absence of a storage element, the directional transmitter performed poorly and was unable to outperform the omni-directional performance despite the advantage of suffering lower interference. Here, we observe that for the cases where C takes values 0.5 F and 0.7 F, the directional transmitter performs worse than the omni-directional case, but it recovers when the value of C increases.

2.5.3.6. DISCUSSIONS

As we have seen, there are various parameters that have a pronounced effect on the neighbor discovery time in the two-way scheme. We have seen that every parameter setting has advantages and disadvantages, and the tradeoffs need to be considered.

While a directional finding node is capable of better performance due to less interference, at very low energy availability, the directional antenna loses its advantage due to a higher number of ND packets sent and received, hence leading to higher en-

ergy consumption. It must be noted that the high energy consumption is only on the
finding node. Thus, at the cost of energy on the finding node, the neighboring nodes
will need to spend less energy due to reduced collisions.

Furthermore, in adverse conditions, if the finding node has very low energy avail-
ability, we must distribute the burden among the other nodes. From the results we
can understand that there is a threshold energy interarrival time below which it is
advisable to perform directional neighbor discovery. In order to increase the advan-
tages of the directional finding node, a better scheme could be devised by choosing a
wider θ such that the benefits of both lower interference and lower number of HELLO
packets can be enjoyed.

The size of the energy storage element size affects the directional transmitter more
than the omni-directional transmitter. If the available energy in the storage element
is less than the required energy for performing a complete discovery in all sectors,
then the time required for ND increases, rendering the benefits of directional antenna
unattractive. This tradeoff needs to be evaluated in the deployment scenario: in many
deployments, the size of the storage element depends on the source and the expected
amount of energy harvested.

Adapting the duty cycle based on the available energy is a common technique
adopted in energy-harvesting WSNs. If the same harvesting source is used across the
network, then both the extremes need to be considered: all the nodes have too small
a duty cycle when the energy harvested is less or all the nodes are awake and respond
leading to collisions when the energy harvested is more. During the ND process, the
duty cycle of neighbor nodes can be stipulated at a fixed value depending on the node
density and the energy source. We summarize the tradeoffs below:

1. **Node density and antenna beamwidth**. Node densities are chosen in networks
   to provide redundancy in case of failure of nodes. However, we have observed
   that increased node density has an adverse effect on the performance of the
   ND process. A directional finding node is capable of better performance due
   to decreased collisions, but that comes at the expense of more time and energy
   spent.

2. **Antenna beamwidth and available energy**. Omni-directional ND process takes
   less time when the amount of energy harvested and the storage capacity are
   less as compared to the directional antenna ND process. Omni-directional ND
   is also beneficial when the node density is less. However, as the storage capac-
   ity or the amount of energy harvested increases, the directional antenna ND
   process gains advantage due to less collisions.

3. **Node duty cycle and node density**. Increased node density coupled with each
   node having a large duty cycle will lead to an increase in the number of colli-
   sions. One method would be to adapt the duty cycle based on the number of
   collisions.

2.5.4. SIMULATION RESULTS OF ONE-WAY ND

The one-way ND process was described in Section 2.3.3. Once the bootstrapping
phase is complete, we assume that every node is aware of all of its immediate neigh-
bors. However, a continuous ND process is required since nodes die and come to life
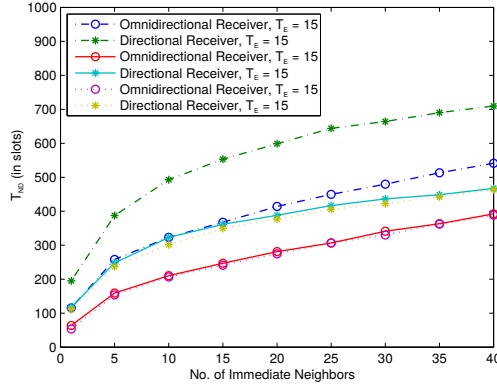
Figure 2.26: ND time for one-way discovery.
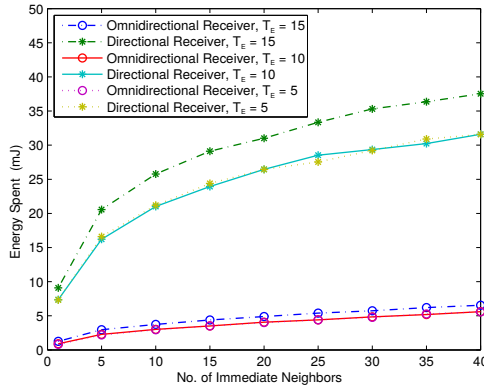
Figure 2.27: ND energy for one-way discovery.

again. In this case, the one-way ND process is beneficial. In this method, the finding node behaves like a simple receiver.

In this section, we present the simulation results. The simulation model and the parameters are as described in Section 2.5.2. Since we propose that this scheme be used for continuous neighbor discovery, we must ensure that this method has the least possible overhead. However, as mentioned earlier, the beaconing that we expect neighbor nodes to perform is multi-purpose and the overhead is not strictly for the neighbor discovery process alone. Hence we focus only on the energy spent at the finding node.

As can be seen from Figure 2.26 the directional finding node (θ=45°) takes a longer time to discover all of its neighbors than the omni-directional node. At longer energy interarrival times, the directional finding node performs worse as all nodes defer listening for an ND packet to a time when energy is available.

The energy consumption at the finding node is seen in Figure 2.27. At T_E of 5
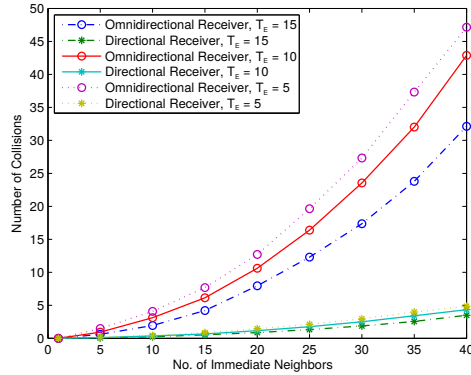
Figure 2.28: ND collisions for one-way discovery.

and 10, the energy consumption for discovery at the directional finding node is the same, whereas the required number of time slots for discovery are more for the $T_E = 10$ condition.

For the omni-directional finding node, the energy consumption is almost the same for all energy conditions. In terms of energy requirement, the omni-directional case provides the best performance with little or no variation with energy condition, but its performance in terms of required number of slots does vary. Thus, we may conclude that this is due to the deferment of beaconing at the neighbor nodes due to lack of energy.

Similarly, the energy requirement at the directional node (θ=45°) is the same for energy interarrival times of 5 and 10, but a little higher for $T_E = 15$ time slots. Oddly, when the node faces infrequent energy arrival, it must spend more energy. The reason for such a behavior can be explained by the rarity of energy in all nodes. This further motivates the importance of better design and choice of storage element size.

The energy requirement in all T_E cases is much larger than that for the omni-directional case. This is inevitable because the directional finding node spends more energy to listen as it scans sector 1 through $\frac{2\pi}{\theta}$. Also, the probability of listening in a sector when a neighbor node transmits a beacon in that same sector is heavily reduced as the nodes no longer respond to a query, which explains the increased number of slots required for discovering all neighbor nodes in the directional case.

The advantage of the directional finding node, in the two-way case, of lower interference is lost here as nodes do not respond to a query and thus there is a lower probability of collision caused by greater variation in the instant at which beacons are transmitted. Thus, the number of collisions as seen in Figure 2.28 is much lower than that observed for the two-way neighbor discovery, even in the omni-directional case.

Discussion: The one-way neighbor discovery scheme can be implemented for neighbor discovery with the finding node acting as an omni-directional receiver. At lower beamwidths, the system performance goes down and cannot be improved. The advantage of the one-way method is that the node attempting to discover its neighbors has a low energy overhead and requires lower neighbor discovery time than the

two-way scheme. However, the scheme is not ideal for the initial discovery in the bootstrapping phase as bi-directional discovery does not occur here. It can be used for continuous neighbor discovery such that the energy overhead across the network is minimized.

2.6. CONCLUSIONS

In this chapter, the importance of performing explicit neighbor discovery in energy-harvesting wireless sensor networks was motivated. The importance of a different approach to ND for bootstrapping and for continuous operation when nodes leave and re-enter the network was emphasized. With the help of an analytical model, the important parameters that influence ND were identified as transmitter beamwidth, node density, node duty cycle and the rate of energy arrival. The exact impact that these parameters have was observed through numerical evaluation and simulations. Based on the results, several tradeoffs were discussed. We summarize a few important implications of this study:

- With an increasing number of neighbor nodes, the interference increases. Thus, neighbor node density has a detrimental effect on ND performance. When the nodes operate at low duty cycles, ND performance decreases. However, an increasing duty cycle with an increasing node density would have the adverse effect of increased energy usage and impacts the ND performance even more. Therefore, an optimal duty cycle must be picked keeping density and energy consumption in mind.

- Antenna directionality offers an advantage in ND. Under certain conditions, it is advisable to use a small beamwidth of transmission to actively discover neighbor nodes.

- Energy availability has a great impact on ND performance. If energy arrives less frequently, the ND performance worsens. The adverse effects of varying energy availability are more pronounced in case of directional discovery. If the variations in energy availability are smoothened with a buffer, performance is positively impacted.

- It is important to differentiate between initial and continuous ND for seamless network operations. A simple one-way scheme can perform continuous ND with relatively low overhead.

While we addressed one specific problem, there are two open questions:

- We considered a specially endowed finding node that performs the initial neighbor discovery. Although this provides us insight into the requirements for ND, in order to present a generalized solution, a model in which every node initiates ND processes of its own must be studied and understood. This homogeneous network would be an extension of the model we have studied here.

- Based on the insights obtained here, a practical, lightweight ND protocol must be developed for energy-harvesting WSNs. Such a protocol must be naturally integrated into the MAC or networking layers.

3

TOPOLOGY CONTROL

3.1. INTRODUCTION

In the previous chapter, we analyzed methods for discovering neighbors in energy-harvesting WSNs. In this chapter, we shall take a step forward towards networking the energy-harvested sensor nodes.

As seen in the previous chapter, energy-harvesting in WSNs introduces new challenges in networking them due to energy variations. Residual energy-levels in nodes vary over time based on harvesting opportunities. Furthermore, the energy-levels vary across the nodes due to different nodes having different harvesting opportunities. Due to this, the nodes switch between *Active* (on) and *Inactive* (off) modes, making them often leave or rejoin the network over time. This implies that the neighbors change over time. Even a statically deployed energy-harvesting network can be considered to be a dynamic network due to energy variations.

In an energy-harvesting WSN, the network lifetime is no longer restricted by the limited energy supply. Even though the nodes in the network are considered to be perpetual, the network is not guaranteed to be always connected. This is illustrated with the example in Figure 3.1.

A common solution in energy-harvesting WSNs is to deploy redundant nodes to ensure sufficient coverage of an area and to protect against the energy variations [62]. While redundant nodes offer advantages due to the dense network deployment, they also bring certain disadvantages: typically the maximum transmission power is used to transmit in order to ensure successful packet reception. However, in a dense network, this leads to many nodes interfering with each other. Furthermore, in a dense network, many routes are possible. With the dynamic network, this may lead to re-computing and discovering new routes.

Some of these problems can be overcome by topology control (TC). TC is a common technique that conserves energy by reducing transmission power and improves the network capacity by reducing interference [63]. TC increases energy-efficiency by restricting the number of communication links. TC algorithms aim to achieve this by choosing the *right* transmission power and neighbors such that the network is connected. The classic trade-off dealt by TC algorithms is shown in Figure 3.2. On one hand conserving too much energy may harm the network connectivity, but on the other hand, increasing redundant routes in may increase interference leading to energy wastage.

In energy-harvesting WSNs, the network is heterogeneous in terms of available energy on the nodes. This implies that the nodes with more energy can help the nodes with low energy to remain connected. Although there is a vast body of literature on topology control for battery-powered WSNs [64, 65], they typically do not consider heterogeneous levels of energy among nodes. Other work that does consider heterogeneous levels of energy takes a static set of nodes to have higher energy-levels [66]. Therefore, we investigate topology control for energy-harvesting WSNs in this chapter. As constructing a new topology every time energy-levels change is expensive in terms of energy consumption, localized TC algorithms are required to keep the energy-harvesting WSNs operating perpetually. In this context, we address the two following questions:

- How should a node select neighbors such that the global topology is connected while the nodes reduces its transmission power?

- How should a node maintain the local topology given the dynamics of energy?

In this chapter, we consider two distinct scenarios for topology construction algorithms that are typical to IoT application:

1. convergecast, where there is a sink and the connectivity is to be maintained to transfer data to the sink;

(a) At time t_1, Node 3 has higher energy while Node 2 has lower energy. All nodes are connected.

(b) At time t_2, Node 3 exhausts energy. Thus the network topology is changed.

(c) At time t_3, Node 3 harvests energy and rejoins, but with limited energy resulting in different roles for nodes, i.e., Node 3 chooses nearer neighbors and Node 2 connects to Node 5 to keep the network connected.

(d) At time t_4, Node 2 leaves the network initiating reconstruction of the link between node 3 & 5.

Figure 3.1: Challenges posed by the varying energy-levels in constructing topology in an energy-harvesting WSN.
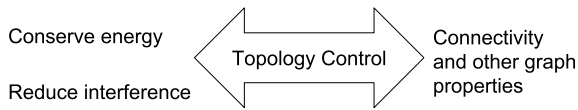
Figure 3.2: The trade-off between node energy conservation and network connectivity in topology control.

2. a generic network where nodes are deployed randomly and have to form a network in order to exchange data between some source-destination pairs.

We propose two localized Energy-Aware Control of Topology (E-ACT) algorithms – E-ACT-s and E-ACT-d corresponding to these two scenarios. In both algorithms, a well-connected topology is constructed and maintained by having each node adjust its transmission power based only on the locally collected information. Specifically, our contributions are as follows:

1. To the best of our knowledge, we are the first to propose implementable, low-complexity topology control algorithms for energy-harvesting WSNs. We propose localized topology control algorithms for two typical scenarios in energy-harvesting WSNs that form a globally connected topology while maximizing the residual energy in every node. While E-ACT-s guarantees well-connectedness, E-ACT-d is probabilistic and well-connectedness property can be tuned as required.

2. We also propose a localized topology maintenance algorithm to handle the dynamic variations in the remaining energy-levels at the nodes.

3. We evaluate the proposed algorithms based on simulations and on real-world deployments. The results show that the proposed algorithms perform better with regard to network connectivity, fault-tolerance, transmission energy consumption and neighbors' remaining energy.

The chapter is organized as follows. Section 3.2 describes the related work. Section 3.3 describes the system model and the two scenarios considered. In Section 3.4, we describe the proposed algorithms. In Section 3.5, we evaluate the algorithms using simulations and testbeds, and discuss the results. The chapter concludes in Section 3.6.

3.2. RELATED WORK

We have summarized the related work with their features in the Table 3.1. Not many works are present that are applicable to the unique challenges of energy-harvesting WSNs. The important one is by Tan et al., who presented a distributed Energy-Harvesting-Aware (EHA) algorithm [67], which models the behavior of sensor nodes as an ordinal potential game where the high harvesting power nodes cooperate with the low harvesting power nodes to maintain the connectivity of the network. Game theory-based algorithms have drawbacks with respect to realizing them. It is apparent that the communication overhead is high since nodes need to send requests and response.

Table 3.1: Summary of related work.

Work	Type of network	Basic idea	Considering node's energy	Fault-tolerance
K-Neigh	WSN	Selects k-closest neighbors	N/A	N/A
CBTC (α)	Nodes with position information	Selects at least one neighbor in each direction	N/A	k-connectivity
FLSS$_k$	k-connected network	Builds the local sub-graph k-connected	N/A	k-connectivity
RESP	Nodes with different energy	Selects neighbors according to a weight function	Residual energy-levels of all nodes	k-connectivity
DPV	Heterogeneous WSN	Selects neighbors such that a node has at least k-vertex-disjoint paths to supernodes	Nodes with limited energy and supernodes with unlimited energy	k-connectivity
EHA	energy-harvesting WSN	Models the behaviors of nodes based on game theory	High harvesting power nodes co-operate with low harvesting power nodes	N/A

3

Moreover, it requires accurate energy harvesting and energy consuming profiles to predict how nodes behave, which is related to the deployment and environment, and may not always be available.

For traditional WSNs, extensive studies have been done, and different algorithms were proposed based on various ideas. Many works consider building a k-connected topology, wherein k disjoint paths exist between every source-destination pair of vertices. This fault-tolerance is important in WSNs, especially if the nodes' energy-levels are not taken into account. Building a minimum-cost k-connected sub-graph is an *NP-hard* problem [68].

Two works that build a fault-tolerant topology are CBTC(α) [69] and Fault-tolerant Local Spanning Sub-graph (FLSS$_k$) [70]. CBTC(α) is an extension of the CBTC algorithm [71], which stands for Cone-based Topology Control, providing a fault-tolerant topology. In this algorithm, each node increases its transmission power, trying to retain connections to at least k neighbors in "every direction", where α is a constant depended on k. FLSS$_k$ is a distributed algorithm that can preserve k-connectivity in a network. Nodes collect local information of its neighbors, sorting them by distance. Then, each node selects enough neighbors such that the local sub-graph is k-connected. Nevertheless, whether the sub-graph is k-connected needed to be tested by communicating with other nodes, which causes the high communication overhead.

A more practical algorithm is K-Neigh [72] protocol. It is a distributed, asynchronous, and localized protocol that maintains k neighbors of each node based on distance estimation. By using distance estimation techniques like Radio Signal Strength Indicator (RSSI) based estimation, it is possible for a node to estimate the distance to another node. The drawback is that K-Neigh does not preserve network connectivity in the worst case. We base our algorithms on K-Neigh due to its simplicity.

There are works that consider the residual energy of nodes such as Residual Energy-aware Shortest Path (RESP) [66]. In this work, a weight function is employed, involving not only the required transmission power but also the residual energy of nodes. With this weight function, the proposed algorithm preserves the minimum-weight path. The construction of k-connected sub-graph part in this algorithm is based on the similar idea of FLSS$_k$, but instead of choosing the closest neighbors, it chooses neighbors in the order of sorted results of the weight function, which also causes high communication overhead. Bagci et al. proposed an algorithm [73] for heterogeneous WSNs consisting of supernodes (with infinite energy) and ordinary nodes. In the settings, route data is collected by sensor nodes to supernodes, proposing a Disjoint Path Vector (DPV) algorithm for topology construction. The authors argue this algorithm works better in the two-tiered heterogeneous network. In this work, supernodes are supposed to have unlimited energy resources, which makes the supernodes and the normal nodes have different tasks in constructing the topology. However, in a typical energy-harvesting WSN, where similar nodes are deployed and have the same energy capacities, it is difficult to satisfy the requirements of supernodes. Before we propose our algorithms, we first describe the system in the next section.

3

3.3. SYSTEM AND SCENARIOS

In this section, we define the system model and definitions. Next, we present the assumptions made. Further, we describe the two scenarios that we consider for designing our algorithms.

3.3.1. SYSTEM MODEL AND DEFINITIONS

We consider an energy-harvesting WSN network consisting of n nodes with omni-directional antennas. Nodes can adjust their transmission power levels in steps from the set $\{0, P_1, P_2, \ldots, P_{max}\}$, which depends on the radio hardware. For instance, the radio CC2420 [74] has 8 power levels with a minimum -25 dBm to maximum 0 dBm. Let the network topology be represented by an undirected graph $G = (V(G), E(G))$, where $V(G) = \{v_1, v_2, \ldots, v_n\}$ is the set of nodes and $E(G)$, is the set of links in the network. In addition, for a node u in the network, it has a unique identifier, denoted as $id(u)$. The network consists of only stationary nodes and do not consider the mobile nodes in this work.

Some terminology that we will use in this work are defined as follows:

Definition 1 (Topology). *The topology generated by an algorithm is a sub-graph $G' = (V'(G'), E'(G'))$ of the original graph $G = (V(G), E(G))$, wherein $G' \subseteq G$.*

Definition 2 (Neighbor Relation). *A node u is a neighbor of node v under a topology, denoted by $u \to v$, if there is an edge (u, v) in the topology.*

Definition 3 (Neighborhood). *The neighborhood of node u, denoted by $N(u)$, is the set of nodes that are the neighbors of node u in the topology.*

Definition 4 (Degree). *The degree of node u is denoted as $Deg(u)$. This is defined as the neighbors of node u in a topology. Obviously, $Deg(u) = |N(u)|$.*

Definition 5 (Physical Degree). *The physical degree of node u is defined as the number of neighbors within the transmission range of node u.*

Definition 6 (Connectivity). *For a topology, node u is said to be connected to node v (denoted by $u \Rightarrow v$) if there exists a path ($p_0 = u, p_1, \ldots, p_{m-1}, p_m = v$) such that $p_i \to p_{i+1}$, $i = 0, 1, \ldots, m-1$, where $p_i \in V(G)$, $i = 0, 1, \ldots, m$. It follows that $u \Rightarrow v$ if $u \Rightarrow p$ and $p \Rightarrow v$ for some $p \in V(G)$.*

Definition 7 (k-vertex Connectivity). *A graph G is k-vertex connected (or k-connected)if for any two vertices $v_1, v_2 \in V(G)$, there are k pairwise-vertex-disjoint paths from v_1 to v_2. Or equivalently, a graph is k-vertex connected if the removal of any $k-1$ nodes (and all related links) does not partition the network.*

Definition 8 (Well-connected Graph). *A graph G is well-connected if for any two vertices $v_1, v_2 \in V(G)$, there is at least one disjoint path from v_1 to v_2.*

Definition 9 (Addition and Removal). *The Addition operation is to add an extra edge (v, u) into G if $(u, v) \in E(G)$ and $(v, u) \notin E(G)$. The Removal operation is to delete any edge $(u, v) \in E(G)$ if $(v, u) \notin E(G)$.*

Each node is equipped with an energy storage buffer such as super-capacitors. We assume that we can measure the state of charge in the storage buffer. For super-capacitors, the voltage across the super-capacitors can be used to measure the energy-level with $E = \frac{1}{2}CV^2$. The nodes may employ adaptive duty-cycling mechanisms [75]. The energy arrival model is not required as we work with the remaining energy on the nodes. We define the state of a node as follows:

Definition 10 (Node's Energy State). *If the remaining energy of a node is less than a predefined value E_{min}, we consider its energy state is Inactive; otherwise its energy state is Active. This is denoted by: $state(u) \in \{$ Active,Inactive $\}$.*

3.3.2. ASSUMPTIONS
We model the network and nodes based on the following assumptions.

1. We assume that the network is connected initially. This assumption ensures that the topology generated by the topology control algorithm can still be connected.

2. We assume that each node knows the distance and minimum transmission power required to reach each of its neighbor. These parameters can be estimated based on RSSI [76].

3. We assume a synchronous medium access control mechanism in which nodes wakeup around the same time and transfer data. This can be implemented with a scheme such as S-MAC [77].

3.3.3. SCENARIOS
We consider two typical scenarios for topology construction in energy-harvesting WSN. Any other scenario can be modeled as a subset of these scenarios.

- A convergecast scenario, wherein there is a dedicated sink node to which all the nodes send their data. This is a typical data collection scenario for IoT applications (see Chapter 1).

- A distributed scenario, which is more generic scenario, where the nodes must exchange data between some source-destination pairs. This scenario can be envisioned in the realm of machine-to-machine communications in IoT applications.

3.4. PROPOSED ALGORITHMS
With the system model and assumptions in place, in this section we first describe our arguments for not constructing a k-connected network, and then list the design constraints for the algorithms. Next, we provide an overview of the working of the algorithms, and describe each one individually. Finally, we describe the topology maintenance algorithm.

3.4.1. FAULT-TOLERANCE IN ENERGY-HARVESTING WSN
While fault-tolerance has been a major research issue in WSNs, it is not worthwhile to investigate k-connectivity in the context of energy-harvesting WSNs. Constructing a

minimum-cost k-connected graph is an *NP*-Hard problem. Approximate algorithms have been proposed to construct k-connected topology. For instance, as described in Section 3.2, FLSS$_k$ is a typical distributed algorithm to build such topologies. However, it has the following drawbacks:

1. Since nodes require local sub-graphs, it implies nodes need multiple hops neighbor information. This brings extra communication overheads, causing high transmission energy consumption.

2. Given nodes know the local sub-graph, whether the sub-graph is k-connected needs to be tested by using network flow techniques. This also results in high time and communication complexities. Jorgic et al. present a work on localized detection of k-connectivity [78], which shows that it is impossible for nodes, based on local knowledge, to be accurate with respect to global connectivity properties.

In energy-harvesting WSNs, where energy is critical for the performance, energy must be spent wisely. Not all or most of the energy must be spent in constructing a fault-tolerant topology. Moreover, since nodes may leave and rejoin the network at any time, reconstructing the k-connected topology becomes unrealistic in terms of energy consumption.

Consequently, instead of constructing a k-connected topology with high energy consumption, we would like to maximize the residual energy in every node of the network. We aim to make higher energy nodes taking more workload than the lower energy nodes, which reduces the faults in the system. We further look to build a well-connected topology with low transmission overhead, which also handles and utilizes the dynamics of energy in the network.

3.4.2. DESIGN GUIDELINES
The algorithms designed for both the scenarios listed in Section 3.3.3 must adhere to these constraints:

(a) the algorithm should be localized, i.e., the algorithm must rely on only one-hop information;

(b) the algorithm should have low communication overheads; and

(c) the global topology should be well-connected.

3.4.3. E-ACT-* OVERVIEW
The basic idea of E-ACT-* (Energy-Aware Control of Topology-*) is that a topology control algorithm in an energy-harvesting WSN should not just select links with low costs, but should also select neighbors according to their energy-levels. Considering the energy issue, we design algorithms based on a greedy strategy to maximize the remaining energy of nodes and select neighbors with high residual energy. The reasoning is that the nodes with higher energy-levels will perform more tasks (due to adaptive duty-cycling). Consequently, since nodes have "high energy neighbors", their neighbors can receive and transmit more messages, resulting in a more sustainable network. This is the main guideline of the algorithms in this work.

Both variants consist of two phases: topology construction and topology maintenance. The key idea in the construction phase is that nodes select neighbors according to the distances of the neighbors and their remaining energy. In this case, the distance is no longer the only factor in selecting neighbors. Topology maintenance is required in energy-harvesting WSN as a mechanism to update the topology whenever nodes leave or rejoin the network. This takes care of the nodes' energy in the heterogeneous network and keeps all the active nodes in the topology.

The first phase of E-ACT-* is topology construction. Nodes first collect neighbor information, including the remaining energy and the distance between nodes. Then each node selects neighbors according to neighbor selection metric based on local information. There are two major differences between E-ACT-s and E-ACT-d:

1. they use different strategies to discover neighbors; and

2. nodes select neighbors based on different criteria.

We discuss and elaborate the two points as follows, explaining how E-ACT-s and E-ACT-d work.

3.4.4. Topology Construction in E-ACT-s

E-ACT-s (Energy-Aware Control of Topology-sink) is designed to guarantee that the topology is well-connected with low communication overhead for the convergecast scenario. E-ACT-s has two steps: (i) Neighborhood information collection and (ii) Neighbor selection. E-ACT-s is described in Algorithm 5.

The topology construction begins when the sink broadcasts a HELLO message. The message includes its energy-level, state and number of hops from the sink, i.e., 0. Nodes that receive the message add the transmitter to their neighbor-list, note down its energy, number of hops from the sink and the minimum required transmission power. The receiving nodes then broadcast their HELLO messages after medium contention with their energy-level, state and number of hops, incremented by 1.

Algorithm 5 E-ACT-s on a node u.

1: **Input:** Node u;
2: **Output:** $N'(u)$ computed neighbors of node u
3: $MessageLevel := 0$
4: **if** *id(u) == id(sink)* **then**
5:     Broadcast HELLO message with *MessageLevel* information at maximum transmission power
6: **else**
7:     When receive HELLO message from node v
8:     *MessageLevel := v.MessageLevel + 1*
9:     Send HELLO message with *MessageLevel*
10:     $N(u) := N(u) \cup \{v\}$
11: **end if**
12: Wait for all nodes to finish neighbor information collection procedure
13: Compute $N'(u)$ using neighbor selection Algorithm 6
14: Construct bi-directional links by adding missing links

After the neighbor information collection phase is complete, in the next step we begin the neighbor selection phase. Here we define the energy threshold E_T, which decides how many neighbors a node should select. Starting from the closest neighbors, a node starts including its neighbors until the sum of neighbors' remaining energy meets the threshold. By using this greedy algorithm, nodes always connect to neighbors that need low transmission power to be reached. This minimizes energy expenditure on the node. Further, by selecting nodes based on energy as the second criteria ensures one of these two: (a) if there are high energy neighbors close to the node, then less number of neighbors are selected; and (b) if there are only low energy neighbors present, then more number of neighbors are selected. In either case, some kind of fault-tolerance is ensured. Note that one of the neighbors selected in E-ACT-s is mandatory to have a lower hop count to the sink than itself. This ensures that all active nodes that have at least one active neighbor with a lower hop count to the sink are connected.

Algorithm 6 Neighbor selection of E-ACT-s on node u.

1: $N(u)$ the neighbor list of node u; E_T the predefined energy threshold
2: $N'(u)$ computed neighbors of node u
3: Sort the nodes in $N(u)$ in ascending order of distance
4: $N_E := 0$; $N'(u) := \emptyset$
5: **for** v in $N(u)$ **do**
6:    **if** $State(v) == Active$ and $N_E < E_T$ and $v.MessageLevel < u.MessageLevel$ **then**
7:       $N'(u) := N'(u) \cup \{v\}$
8:       $N_E := N_E + Energy(v)$
9:    **end if**
10: **end for**
11: Adjust transmission power to the minimum value needed to reach the farthest node in $N'(u)$

In order to give an impression of the topology generated using the proposed algorithms, we show the original topology and the generated topology in Figure 3.3.

3.4.5. TOPOLOGY CONSTRUCTION IN E-ACT-D

E-ACT-d (Energy-Aware Control of Topology-distributed) is for the generic case where there is no hierarchy. It is more challenging to construct a well-connected topology with just one-hop information in this case. If an incorrect set of neighbors is selected, then the resultant global topology will be disconnected. In E-ACT-d, we can set the number of neighbors to be selected, indirectly through the threshold E_T. We shall discuss more about the influence of E_T in Section 3.5.

The algorithm is presented in Algorithm 7. Similar to E-ACT-s, nodes broadcast HELLO messages, collecting the neighbor information. The only difference between this phase of E-ACT-s and E-ACT-d is that there is no need for any hopcount information. Once the neighbor information collection phase is complete, each link is assigned a weight as in Equation 3.1,

(a) The original topology | (b) The topology generated by E-ACT-s | (c) The topology generated by E-ACT-d
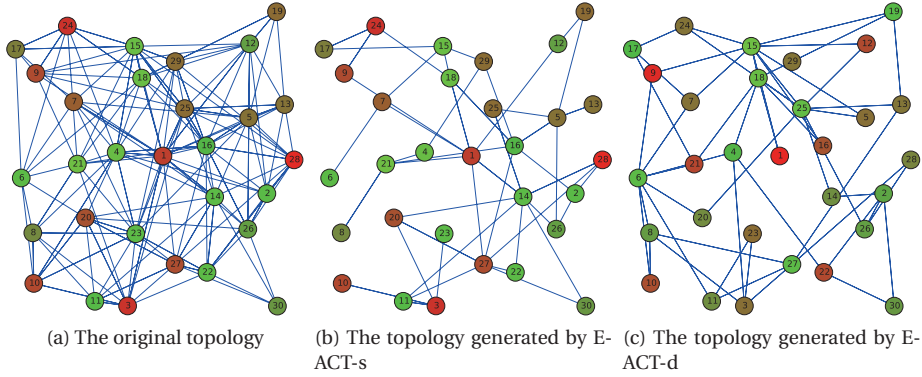
Figure 3.3: Demonstration of the topology generated by E-ACT-s and E-ACT-d. Gradient of colors are used to indicate the energy-levels of the nodes. Green implies higher energy while red is for lower energy-levels. Node 1 at the center is the sink node.

$$w(u,v) = \alpha \cdot \frac{E_v}{E_{max}} + (1 - \alpha) \cdot (1 - \frac{RSSI_{u,v}}{RSSI_{min}}) \qquad (3.1)$$

where, $w(u,v)$ is the weight function of the directed edge (u,v); E_v is the received remaining energy of node v, and E_{max} is the maximum energy capacity of a node. $RSSI_{u,v}$ denotes the RSSI from node v to node u, while $RSSI_{min}$ is the minimum RSSI to ensure connectivity. We also set α, a weight factor, that allows to control the importance level for the remaining energy of the neighbor or for the required transmission power to the neighbor.

The next step is to sort the neighbor list $N(u)$ of node u in ascending order of their weight and select the neighbors until the neighbors' energy is greater than or equal to E_T. Finally, nodes can add missing edges to construct the symmetric neighbor list, making the graph bi-directional.

Algorithm 7 E-ACT-d on node u.

1: **Input:** Node u
2: **Output:** $N'(u)$ computed neighbors of node u
3: Broadcast HELLO message at maximum transmission power
4: Upon receiving message from node v: $N(u) := N(u) \cup \{v\}$
5: Wait for all nodes to finish neighbor information collection procedure
6: Compute $N'(u)$ using neighbor selection Algorithm 8
7: Construct bi-directional links by adding missing links

3.4.6. TOPOLOGY MAINTENANCE

We implement a simple event-triggered (based on energy) procedure to initiate topology maintenance. In E-ACT-*, a node sends notification message when its remaining energy drops or increases above predefined thresholds. After receiving this notifica-

---

Algorithm 8 Neighbor selection of E-ACT-d on node u.

1: **Input:** $N(u)$ the neighbor list of node u; E_T the predefined energy threshold
2: **Output:** $N'(u)$ computed neighbors of node u
3: Sort the nodes in $N(u)$ in ascending order of weight function
4: $N_E := 0$; $N'(u) := \emptyset$
5: **for** v in $N(u)$ in this order **do**
6:      **if** $State(v) == Active$ and $N_E < E_T$ **then**
7:          $N'(u) := N'(u) \cup \{v\}$
8:          $N_E := N_E + Energy(v)$
9:      **end if**
10: **end for**

---

tion, nodes re-select their neighbors according to the metric (for e.g, distance based in E-ACT-s). The topology maintenance algorithm is shown in Algorithm 9.

We set two energy bounds, namely *UpperBound* and *LowerBound*, where $E_{max} > UpperBound > LowerBound > 0$. A node switches its state only when the bounds are crossed. Suppose a node that was *Active* spent most of its energy and the energy-level fell below the *LowerBound*. In this case, it sends a notification message that it is *Inactive*. Although it may harvest energy above the *LowerBound* in due course, the node does not enter *Active* state until its energy-level crosses the *UpperBound*. The reasoning is to avoid the node toggling between the states too often. Toggling between the states often not only wastes energy but also creates unreliable topologies.

Algorithm 9 Topology maintenance on node u.

1: **Input:** $N(u)$ the neighbor list of node u; E_T the predefined energy threshold
2: **Output:** $N'(u)$ computed neighbors
3: Upon receiving broadcast message $(v, Energy(v))$ from node v:
4: **if** $Energy(v) > UpperBound$ or $N_E < E_T$ **then**
5:      Set $(v, Active)$ in $N(u)$
6: **else if** $Energy(v) < LowerBound$ **then**
7:      Set $(v, Inactive)$ in $N(u)$
8: **end if**
9: Compute $N'(u)$ using neighbor selection Algorithm 6 or Algorithm 8

In all the three algorithms, we use broadcast messages. Broadcast messages are unacknowledged making them very susceptible to be lost due to collisions or due to lossy wireless channel. This affects our algorithms severely, resulting in disconnected topologies. To overcome these, we use the topology maintenance algorithm. When a node is *Active* but does not have sufficient number of neighbors, i.e., the sum of neighbors' energy is less than the energy threshold E_T, then the node sends a notification message. All the *Active* nodes in its neighborhood will respond to this message. If the number of neighbors is still insufficient, it waits until the next transmission round of the underlying synchronous MAC protocol.

In practice, either of the topology construction algorithms, E-ACT-*, is executed once at the start in a newly deployed network and the topology maintenance algorithm is executed for the rest of its lifetime.
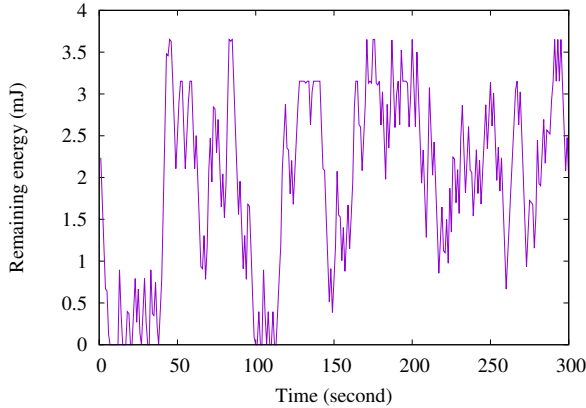
Figure 3.4: Remaining energy on a node harvesting with Bernoulli process.

Table 3.2: Simulation parameters.

Parameter	Value
Deployment area	$500\,\text{m} \times 500\,\text{m}$
Number of nodes	10, 20, 30, 40 and 50
Node distribution	Uniform
Radio	CC2420
E-ACT energy threshold	$E_T = E_{max}$
E-ACT-d weight	$\alpha = 0.5$

3.5. PERFORMANCE EVALUATION

3.5.1. EXPERIMENTAL SETUP

We consider an energy-harvesting WSN in which each node is powered through a solar panel and stores the harvested energy in a supercapacitor of size $15\,m$F. Since a typical low-power sensor node [74] can only operate between 2.6 V-3.4 V, all of the energy in the supercapacitor cannot be used. Therefore, the maximum usable energy is $E_{max} = 36\,m$J.

For our simulations, we model energy arrival as Bernoulli random process [79] with energy arriving in 'packets' of 0.9 mJ. Due to the energy being harvesting only half the time coupled with small storage buffer, the nodes may die or be reborn frequently. This creates a highly dynamic network. Figure 3.4 shows the remaining energy on a node with Bernoulli model.

We perform the simulations on the Cooja simulator [80] in Contiki-OS 2.7 [81]. We simulate energy-harvesting WSN battery model in software. Furthermore, we consider a multipath radio model, collisions and other physical phenomena of wireless communications in our simulations as supported by Cooja. We use the ENERGEST module in Contiki to monitor the energy usage. The other simulation parameters are listed in Table 3.2. The performance evaluation of our algorithms was also done in a real-life testbed and these results will be presented in Section 3.5.5.

3.5.2. EVALUATION METRICS

To evaluate the proposed algorithms, we take two categories of metrics to quantify the results: network metrics and energy-harvesting related metrics.

3.5.2.1. NETWORK METRICS

We first focus on the network properties of the generated topology. Specifically, we evaluate the following metrics.

Node degree: Generally, a node with fewer neighbors means lower interference in the transmission range. On the other hand, a higher node degree improves the fault-tolerance property in a network. Therefore, node degree is an important metric to evaluate.

Computed transmission power: The main goal of a topology control algorithm is to adjust the transmission power of nodes while achieving the desired graph properties. The computed transmission power of a node is the transmission power computed by the node to be used based on our algorithms. It is important as it affects the network connectivity and interference. Consequently, we would like to investigate how the proposed algorithms reduce the transmission power.

Transmission energy consumption: When constructing the topology, the nodes send messages to acquire the neighborhood information. The more messages a node sends, the higher the transmission energy it consumes. Traditional topology control algorithms in WSN rarely consider the transmission energy consumption. Nonetheless, when it comes to an energy-harvesting WSN, where the energy utilization is important, we would like to maximize the energy usage and evaluate the topology control algorithms in terms of this metric. Additionally, it also shows the *energy-*complexity of an algorithm as constructing topology requires exchanging messages among nodes.

Spanner factor: The spanner factor is defined in Equation 3.2. It describes how the lengths of hops in the generated topology are stretched. Since nodes in the generated topology reduce the transmission power, the length of the shortest path to other nodes may consequently be increased. This indicates the number of hops among nodes increases. To evaluate the implication of our algorithm on the network graph, we use this metric.

$$\rho(G_0) = \frac{\sum\limits_{\forall (u,v) \in E(G_0), u \neq v} |\text{ShortestPath}(u, v, G_0)|}{\sum\limits_{\forall (u,v) \in E(G_{max}), u \neq v} |\text{ShortestPath}(u, v, G_{max})|}. \tag{3.2}$$

Interference: As nodes transmit data using the same wireless radio channel, interference occurs when nodes send and receive data at the same time. In order to evaluate the interference in the generated topology, we measure the physical node degree, which shows how many nodes are in the transmission range of every node. This is based on the fact that nodes in the transmission range will suffer interference when

they transmit data at the same time. Therefore, the lower the physical node degree, the lower the interference would occur.

3.5.2.2. Energy-harvesting related metrics

Apart from the metrics mentioned previously, when studying the energy-harvesting WSN, few other metrics are also significant. The following metrics we propose are based on the energy aspect in an energy-harvesting WSN. Considering the heterogeneous energy-levels on the nodes, it is necessary to study the impact of energy on our algorithms.

Remaining energy per neighbor: This metric shows how the nodes select the neighbors with respect to their energy-levels. In a battery-powered WSN, topology control algorithms do not consider the remaining energy of nodes. So when a node selects neighbors, it treats the neighbors without distinction in terms of the energy-levels. However, in our proposed algorithms, they distinguish the energy-levels of nodes.

Connectivity over time: In an energy-harvesting WSN, the constructed topology does not last forever due to the energy changes over time. By looking at the connectivity as time progresses, it helps assess how our algorithms adapt and maintain network connectivity with the energy changes.

3.5.3. Results

We evaluate the performance of E-ACT-s and E-ACT-d against K-Neigh [72] and CBTC [69] with respect to the metrics described in the previous section. The reasons that we compare our proposed algorithms with the classic topology control algorithms are as follows:

1. The number of existing topology control algorithms designed for energy-harvesting WSNs is limited;

2. our proposed algorithms is the first work, as far as we know, which is localized, implementable and focuses on selecting neighbors with high remaining energy.

Therefore, we would like to show how the proposed algorithms achieve the design goals in energy-harvesting WSNs, rather than just comparing the standard topology metrics such as stretch factor or other graph metrics.

Node degree: Figure 3.5 shows the average node degree. As compared to the original graph (shown by "None"), the graphs generated by E-ACT-* are the lowest even among K-Neigh and CBTC. The K-Neigh algorithm first selects a fixed number K of closest neighbors, in this case, we chose $K = 9$ as recommended [72]. Then nodes exchange the neighbor lists to keep symmetric neighbor lists. Therefore, the resultant number of neighbors is less than K. As for the CBTC algorithm, the node degree is bound by select at least one neighbor in every cone. The cone angle is set to $\frac{2\pi}{3}$ as described in [71].

The node degree of E-ACT-* is bound by the energy threshold E_T as mentioned in the algorithm description. Therefore, by adjusting E_T, we can have different results of node degree.
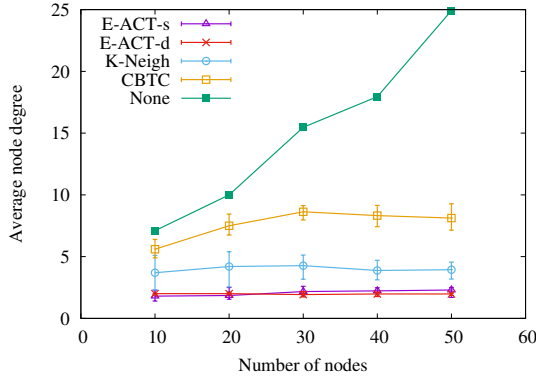
Figure 3.5: Average node degree in the resultant topology of four algorithms. E-ACT-*
have lower average node degree than K-Neigh and CBTC.
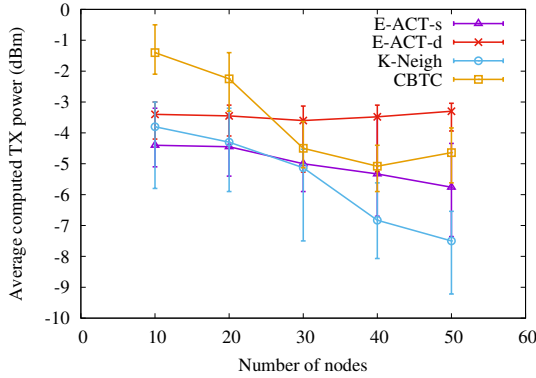
Figure 3.6: Computed transmission power. E-ACT-s reduces more transmission
power because it selects the closest neighbor; the transmission power is more stable
in E-ACT-d, which is a consequence of employing the weight function.

Computed transmission power: Figure 3.6 plots the average computed transmis-
sion power in the topologies generated by the aforementioned algorithms. The re-
sults show that E-ACT-s and E-ACT-d reduce the transmission power. Specifically,
E-ACT-s has less transmission power than E-ACT-d. This is because E-ACT-s gives
more priority to distance, while E-ACT-d balances distance as well as the neighbors'
energy-levels.

Transmission energy consumption: Figure 3.7 depicts the average transmission
energy consumption of each node in topologies generated by various algorithms. The
results show that E-ACT-s and E-ACT-d consume less energy to construct topologies,
which is important in terms of building an energy-efficient network topology. To
quantify the transmission energy consumption, we count the number of messages
needed; each node broadcasts two messages when constructing the topology: the
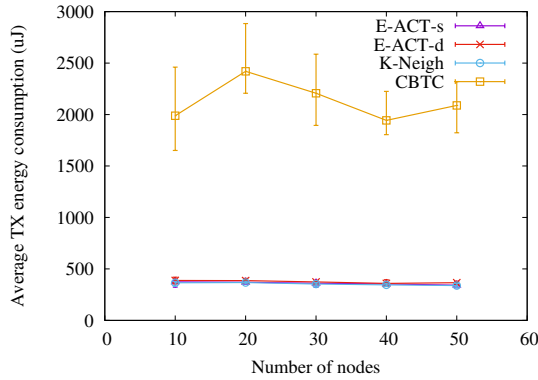
Figure 3.7: Transmission energy consumption for various algorithms. E-ACT-* and K-Neigh use fewer messages to construct topologies than CBTC.
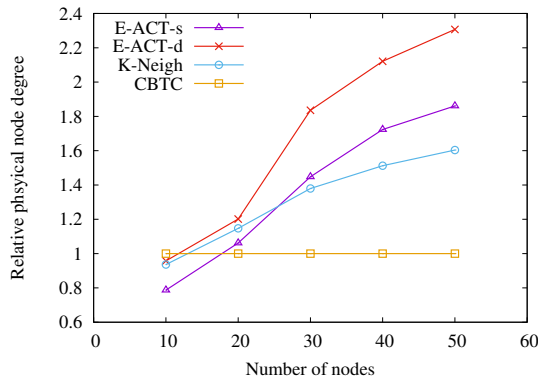
Figure 3.8: Relative physical node degree with CBTC as the baseline.

HELLO message and the neighbor list message.

Interference: As shown in Figure 3.8, the average physical node degree of E-ACT-* is relatively higher. This is the implication of selecting neighbors based on not only the distance but also the energy-levels. The E-ACT-* do not deviate much from that of K-Neigh. The deviation however is due to the trade-off between selecting high energy neighbors and reducing the interference.

Spanner factor: Figure 3.9 shows the spanner factor in the generated topology of various algorithms. Firstly, we observe that the spanner factors in all algorithms is greater than 1, which means the shortest paths in all generated topologies are stretched. Secondly, E-ACT-* have higher values of spanner factor. Revisiting the algorithms, we know that the nodes with higher remaining energy are selected frequently, which form the backbones in the topology. Consequently, nodes with less remaining energy are made to communicate via the high energy nodes. This is the main reason why the
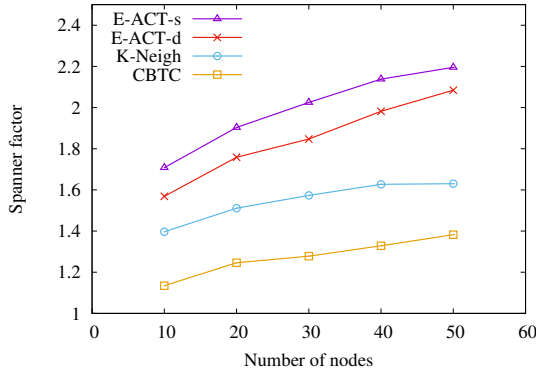
Figure 3.9: Spanner factor of the generated topologies.

shortest paths become longer in E-ACT-*.

Remaining energy per neighbor: Figure 3.10 illustrates the average remaining energy per neighbor of the topologies derived under different algorithms. The average remaining energy per neighbor of E-ACT-d is always higher compared to other algorithm, while the value of E-ACT-s is higher than K-Neigh and CBTC in most cases. This results demonstrate the basic idea of E-ACT: nodes select neighbors that are with high remaining energy.
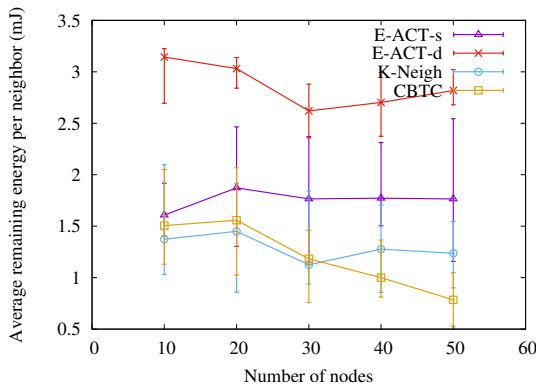
Figure 3.10: E-ACT-* select neighbors with higher remaining energy, other algorithms select neighbors without considering the energy-levels.

Connectivity over time: Apart from the topology construction phase, we also evaluate the network connectivity issue in the topology maintenance phase. With the topology maintenance procedure described in Algorithm 9, the network has the ability to maintain a dynamic topology. We consider every time the topology is changes as an *iteration*.
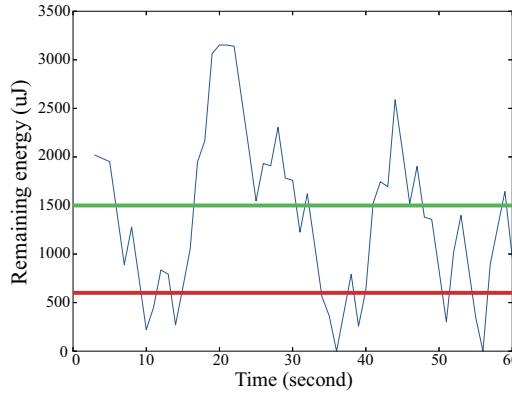
Figure 3.11: The remaining energy on a node with the two bounds: *UpperBound* (green line) and *LowerBound* (red line), which decide if the node is *Active* or *Inactive*.

For the given capacity of 15 mF for the storage buffer, we set the two bounds as shown in Figure 3.11. We chose the *LowerBound* to be $600\mu J$, which is the energy required for transmitting three full payload (128 B) messages in TelosB nodes. For the *UpperBound*, we chose the value as $1500\mu J$, which allows a node to transmit at least 4 full payload messages before switching to *Inactive* state.

Figure 3.12 shows how the connectivity changes when the topology iterates. The results show that the network may be disconnected for some iterations. The reasons could be that the notification message is lost, or there are no active neighbors at the given time. Though these reasons are inevitable, with the help of the topology maintenance mechanism, the network has the ability to recover the connectivity. In addition, Figure 3.13 shows the connectivity over time, where 0-connectivity means the network is disconnected. The first few iterations can be disconnected because the topology construction phase is asynchronous, making some nodes still building their local topology. After the topology is connected, which implies the topology construction phase is done, and the topology is stable, we can see that the topology is updated over time. The topology is well-connected for most of the iterations, and it also shows that the topology maintenance mechanism is valid and efficient as it can recover the connectivity.

3.5.4. DISCUSSION

As described in the algorithms, we provide two parameters that can be tuned in order to generate topologies with the desired graph properties.

3.5.4.1. INFLUENCE OF α IN E-ACT-D

E-ACT-d employs a metric to quantify and select neighbors, which is affected by the weight of α. α can give weight to either energy of the neighbor or the distance, making the weight function generic. Here, we study the influence of α.

Figure 3.14 shows the average remaining energy per neighbor in terms of different values of α for a fixed E_T. We notice that giving more weight to remaining energy of neighbors leads to higher remaining energy per neighbor. Additionally, as
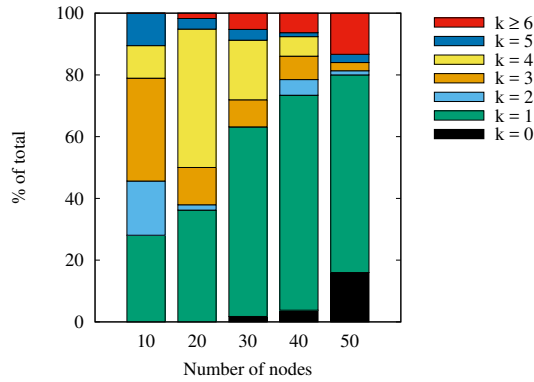
Figure 3.12: The *k*-connectivity property in the topology maintenance phase with E-ACT-d.
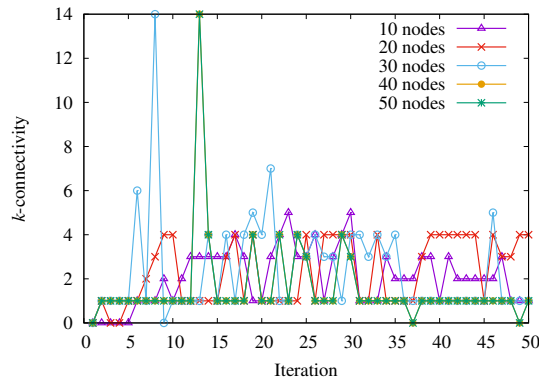
Figure 3.13: The connectivity in a network over time with E-ACT-d.
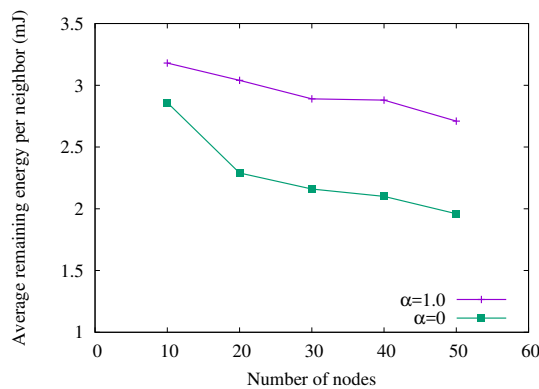
Figure 3.14: The average remaining energy per neighbor is related to the weight function in E-ACT-d. A higher α implies that E-ACT-d gives more importance to the neighbor's energy.
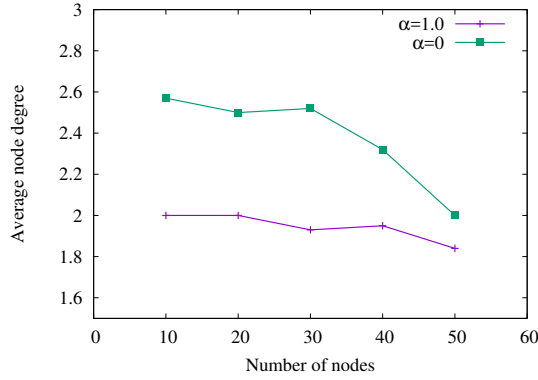
Figure 3.15: Average node degree with respect to $alpha$ in E-ACT-d for a fixed E_T. A higher α selects fewer neighbors.
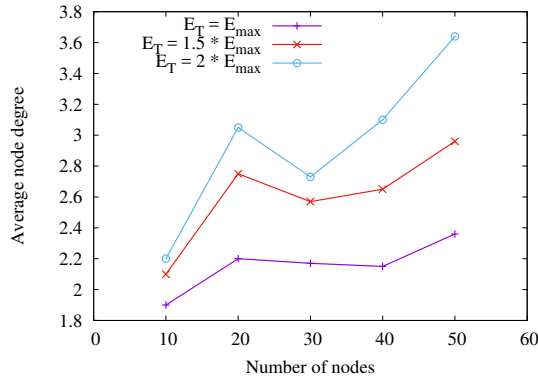
Figure 3.16: Average node degree in the resultant topology of E-ACT-d. The topology was well-connected.

shown in Figure 3.15, low values of α result in a high average node degree. Each node can choose its own α giving it the flexibility to either have more neighbors (be well-connected) or choose higher energy neighbors who can route packets for the nodes.

3.5.4.2. ENERGY THRESHOLD E_T

Since the node degree in our algorithms is based on energy threshold E_T, the obvious question is how guaranteed is the connectivity. This is more important in the case of E-ACT-d, since in E-ACT-s a link to one of its parents is always added. A simple solution is to choose a high E_T value. However, as shown in [82], if a node connects to $\Theta(\log n)$ nearest neighbors, the graph will be connected. Based on this, we evaluate the topology construction for various E_T.

As shown in Figure 3.16, the average node degree increases with higher E_T. According to the simulations, we found that value of $E_T \geq E_{max}$ made the graph well-connected irrespective of the number of nodes. The distribution of the network con-

Table 3.3: Experiment results on the Indriya testbed.

Algorithm	E_T	Avg. node degree	Avg. TX power	% of connected	Spanner factor
E-ACT-s	E_{max}	2.03	-19.07 dBm	61.40%	2.66
	$1.5\,E_{max}$	2.54	-18.22 dBm	90.42%	2.54
	$2\,E_{max}$	3.04	-15.08 dBm	96.29%	1.78
E-ACT-d	E_{max}	2.17	-7.60 dBm	85.29%	1.54
	$1.5\,E_{max}$	2.75	-6.07 dBm	91.43%	1.47
	$2\,E_{max}$	3.80	-4.97 dBm	96.80%	1.26

nectivity is shown in Figure 3.17.

3.5.5. TESTBED RESULTS

We conducted experiments on the Indriya [83] and FlockLab [84] WSN testbeds. When testing the proposed algorithms on the testbed, the following limitations exist: (a) As the deployment is fixed and some nodes in the network are unavailable, the connectivity issue is more important than the other metrics; and (b) Due to the complexity of the indoor environment, the wireless channel is lossier compared to the simulation setting. Therefore, we tested the E-ACT-* algorithms mainly to evaluate the connectivity issue in the generated topology.

We observed that broadcast messages got lost more often in the realistic deployment compared to the simulated radio channel. Thus, the generated topology was not always connected. Nonetheless, since our proposed algorithms enable the network to be fault-tolerant, the connectivity can be recovered over iterations. In addition, we know that the fault-tolerance is related to the value of E_T, as E_T decides how many neighbors to select.

3.5.5.1. RESULTS FROM THE INDRIYA TESTBED

The Indriya testbed consists of 96 available nodes, where nodes in this testbed are deployed across three floors. The type of nodes is TelosB, which consists of TI-MSP430 microcontroller and equipped with CC2420 radio. We evaluated the results of the generated topology in the E-ACT-s and the E-ACT-d algorithms. Table 3.3 shows several evaluation metrics based on the testbed results. In this table, average node degree, average computed transmission (TX) power and spanner factors are similar to the results that are based on simulations. Furthermore, *% of connected* means network connectivity over iterations. The results from the table show that though the network experiences disconnection, the network has the ability to recover connectivity. Particularly, by tuning the value of E_T, the probability that the network is connected is increased. By setting $E_T = 2\,E_{max}$, the connectivity over iterations is greater than 96% on the given testbed deployment.

3.5.5.2. RESULTS FROM THE FLOCKLAB TESTBED

As the Bernoulli energy arrival model does not really model a real-world source effectively, we can consider models to emulate energy-harvesting sources such as the solar
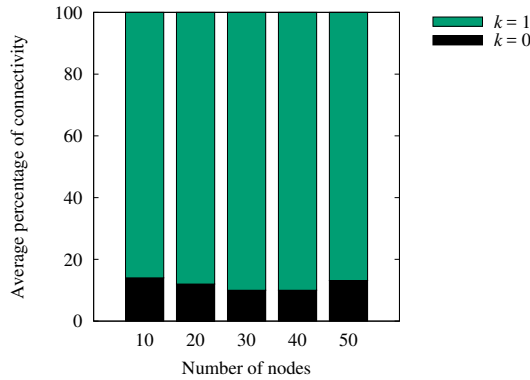
(a) The k-connectivity in a network with $E_T = 0.5E_{max}$.
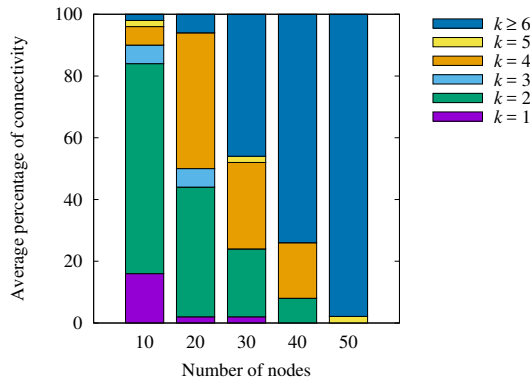
(b) The k-connectivity in a network with $E_T = E_{max}$.
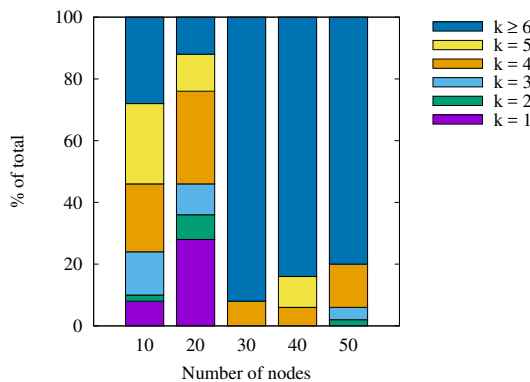
(c) The k-connectivity in a network with $E_T = 2E_{max}$.

Figure 3.17: Network connectivity in E-ACT-d with different values of E_T. The topology generated by E-ACT-d is always well-connected when $E_T \geq E_{max}$.

(a) With Gaussian distribution

(b) With Uniform distribution
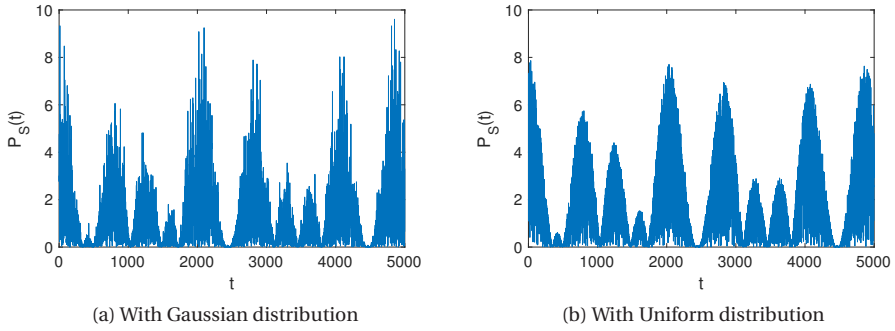
Figure 3.18: Power trace with Moser's model

Table 3.4: Experiment results on the FlockLab testbed.

Algorithm	E_T	Avg. node degree	Avg. TX power	% of connected	Spanner factor
E-ACT-s	E_{max}	2.10	-18.27 dBm	70.20%	2.5
	$1.5\,E_{max}$	2.46	-16.42 dBm	92.52%	2.02
	$2\,E_{max}$	3.24	-14.10 dBm	97.90%	1.74
E-ACT-d	E_{max}	2.05	-8.45 dBm	80.29%	1.84
	$1.5\,E_{max}$	2.64	-5.95 dBm	91.43%	1.57
	$2\,E_{max}$	3.52	-4.57 dBm	96.80%	1.36

model proposed by Moser [85]. This model generates energy given by the following equation.

$$P_S(t) = |10\,\mathcal{N}(t)cos(t/70\pi)cos(t/100\pi)|, \tag{3.3}$$

where $\mathcal{N}$ denotes a normally distributed random variable with mean 0 and variance 1. The power harvested from this model is shown in Figure 3.18(a). The obtained power trace $P_S(t)$ exhibits both stochastic and deterministic with periodic behavior, and simulates patterns of day and night periods similar to those experienced by solar cells in an outdoor environment. A similar power trace can be generated even when the normally distributed random variable is substituted by a uniform random variable with mean 0 and variance 1. Such a power trace is shown in Figure 3.18(b). We shall make user of this model for experiments in the Flocklab testbed.

We used 25 TMote Sky nodes in the Flocklab testbed for our experiments. Table 3.4 shows several evaluation metrics based on the testbed results. The results are similar to the Indriya testbed results despite energy arrival from the harvester not being completely random. This shows the effectiveness of E-ACT-* algorithms when deployed in real-world scenarios.

3.6. CONCLUSIONS

We investigated topology control – a topic that has been studied extensively in battery-powered WSNs but has not been fully explored in energy-harvesting WSN. We investigated the new challenges and constraints in topology control in energy-harvesting WSN setting. Since the nodes harvest energy from the ambiance, number of nodes that are alive at a given instant keeps varying. This poses a bigger challenge in re-using the topology control algorithms proposed hitherto. Thus we proposed two localized topology control algorithms, namely E-ACT-s and E-ACT-d, and a topology maintenance algorithm. We evaluated the proposed algorithms based on simulations and on real-world deployments—the Indriya testbed and the Flocklab testbed. As for the complexity, E-ACT-* algorithms take only around 80 lines of code to implement.

With respect to the performance, simulation results show that compared to classic algorithms that do not take neighbor's remaining energy into consideration, our proposed algorithms increase at least 33% in the remaining energy per neighbor. In terms of energy consumption and fault-tolerance, our proposed algorithms typically achieve 1-connected topology using 74% less energy compared to K-Neigh. Furthermore, by choosing the right parameters, a fault-tolerant k-connected topology can be obtained. The average spanner factors of E-ACT-s and E-ACT-d are 1.99 and 1.84 respectively, which shows that the average lengths of shortest paths among nodes are increased but not by much. As for interference, the number of physical node degree is increased by at most 30% in E-ACT-* algorithms compared to K-Neigh.

The increase in spanner factors and the interference are acceptable trade-offs for selecting neighbors based on distances and energy levels. With regard to topology maintenance, results show that E-ACT-* are adaptable to the changes in energy levels, and it preserves a connected network in at least 96% of iterations over time. Testbed results demonstrate that in a real-world and complex indoor environment, by increasing the value of E_T , our proposed algorithms still can keep the network connected over time, which proves that E-ACT-* are flexible and implementable algorithms that meets the requirements.

In a nutshell, we can conclude our work suggests:

1. Nodes in energy-harvesting WSN should be assigned with different roles based on their energy levels;

2. topology control algorithms in energy-harvesting WSNs should select neighbors based on nodes' energy levels to keep the network connected;

3. as for fault-tolerance, by choosing neighbors based on energy-levels instead of targeting at achieving a k-connected topology, the network will be well-connected also achieve a high value of k-connectedness.

E-ACT-* algorithms are only the beginning and it has opened up many problems to be solved. Foremost work is to determine the threshold E_T that will render the graph connected. We only evaluated for different values of E_T but a value must be determined theoretically. The second work should be to incorporate energy-prediction in the algorithms in order to reduce the toggling between node energy states. Finally, integrate E-ACT-* algorithms with routing protocols in energy-harvesting WSN such as Collection Tree Protocol [49].

4

UNFOLDING AND IMPROVING THE PERFORMANCE OF CONSTRUCTIVE INTERFERENCE

4.1. INTRODUCTION

Many WSN applications rely on network flooding. Typical uses of network flooding are to disseminate data through the network and time-synchronize the nodes. Data dissemination is used to query sensor values or perform network housekeeping tasks such as distributing configuration parameters and updating software codes. Apart from using synchronized time values for time stamping in messages, it is also used by real-time, high-rate data collection systems [86]. Thus building an efficient network-flooding technique is essential. Several techniques for flooding have been proposed in [87, 88, 89], which aim to minimize latency or achieve energy-efficiency. Recently, Ferrari et al. [90] made a major contribution through their flooding technique called Glossy. It achieves latency close to the lower theoretical limit and also implicitly synchronizes the nodes with sub-microsecond accuracy and with high reliability.

The constructive interference (CI) phenomenon is used by Glossy to eliminate the need for contention to access the wireless medium. CI occurs when two or more nodes transmit the same data concurrently, which makes the signals superpose. Hence, receivers can decode the packet successfully with high probability due to, supposedly, the increased signal power at the receivers. To achieve CI successfully with IEEE 802.15.4 radios operating in the 2.4 GHz band, the maximum tolerable temporal displacement by the concurrent transmissions is one chip duration, which is $0.5\,\mu$s. Ferrari et al. [90] achieve this tight bound with radio-triggered synchronization mechanism and demonstrate this on Tmote Sky wireless sensor nodes.

Ferrari's work generated huge interest in the research community to study CI. However, from the previous studies, there appears an inconsistent and often contradicting picture about the working of CI. For example, while it is claimed in [90] that CI does not depend on the number of transmitters in the network, Noda et al. [91] report otherwise, namely, a significant decrease in packet reception when the number of transmitters increases. Another instance is that Ferrari et al. [90] claim that out-of-phase carrier waves from three or more concurrent transmitters do not hamper the

(a) Aligned signals

(b) Signals with a large phase offset

(c) Signals with different Tx power

(d) Signals from imperfect radio clock

4
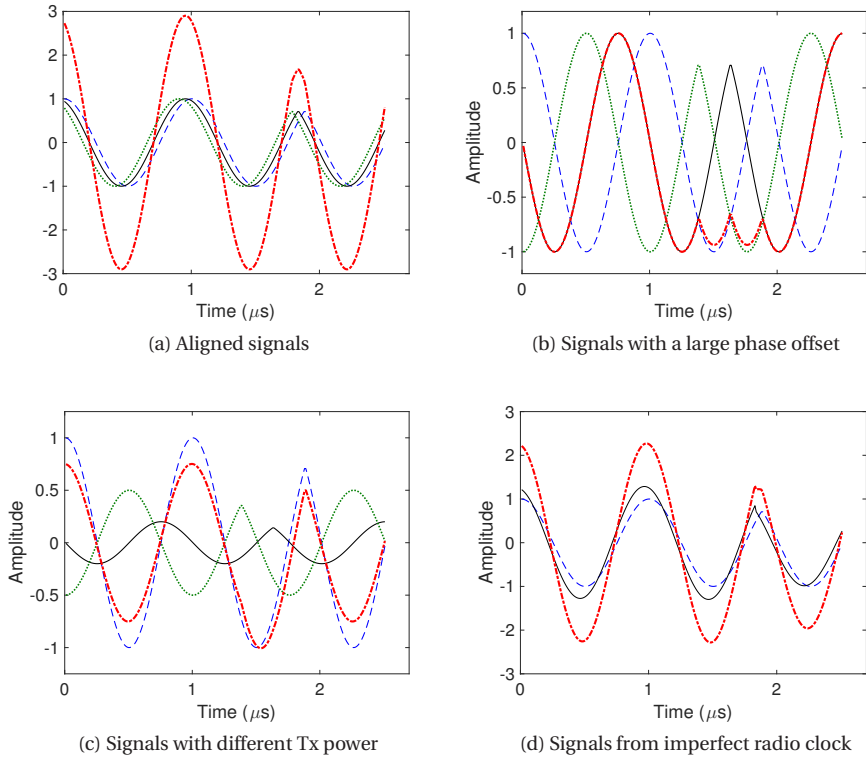
Figure 4.1: The resultant signal (in red) when individual signals are aligned, have a temporal offset, have varying transmit powers and are subject clock errors on the radio.

decodability of the received signal although Wang et al. [92] derive a sufficiency condition for the phase of the concurrent signals such that they interfere constructively. This clearly demonstrates that we lack a complete picture of the CI phenomenon.

Several factors influence the performance of CI as commercial off-the-shelf IEEE 802.15.4 hardware is designed to work with a single carrier.

1. There is a high chance that the signals arrive with different phase offsets at the receiver for several reasons, including, distance between the transmitters and physical phenomena such as multipath, leading to failures in decoding the signals.

2. Furthermore, if nodes transmit with different powers, then the phase of the resultant signal is influenced by the strongest signal.

3. Clocks on the radio are allowed to have large drifts since compensating for drifts within one signal is easy. However, this can hamper CI.

4. Since sensor nodes are designed to be inexpensive, they have low accuracy crystals for the CPU clocks. Clock drifts can creep in to hinder CI.

Figure 4.1 shows the resultant signal under the influence of some of these factors. Figure 4.1(b) shows that the signal is not decodable when there is a large phase offset between the concurrent transmissions. However, the resultant signal can be decoded although the concurrent transmissions have a large phase offset when one signal overpowers the others as shown in Figure 4.1(c). An example of signal from an imperfect radio clock is shown in Figure 4.1(d).

The above aspects have not been studied holistically. This chapter aims to provide comprehensive insights into the impact of these factors with rigorous experimentation in different scenarios. Each scenario offers different radio propagation characteristics. We show that the performance of CI can be quite unreliable since it depends on several factors. Since protocols based on CI have been shown to be highly energy efficient coupled with very low latencies, the performance of CI should be improved. Based on the insights obtained from our experiments, we design Destructive Interference based Power Adaptation (DIPA), a transmit power adaptation based algorithm that improves the performance of CI. Protocols such as Glossy can benefit from DIPA to improve both performance, specifically bit error rates and packet losses, and save power on the nodes. This chapter makes the following contributions:

1. We derive the resultant signal obtained from superposition of several concurrent transmissions in order to study CI from a receiver's perspective. Based on the resultant signal, we derive the maximum tolerable phase offset for achieving effective CI. Furthermore, we show the influence of various parameters from the expressions of the resultant signal.

2. We conduct an exhaustive experimental study of CI considering minute details in real-life settings. We validate the dependency on the factors through these experimental results.

3. One important result that we establish is that varying transmit powers can be beneficial to improve packet reception. Based on this, we propose DIPA, a localized algorithm that adapts transmit power based on feedback.

4. We propose to use *destructive* interference as a negative feedback mechanism for DIPA. We evaluate this algorithm on real-life sensor network testbeds. We show the improvement in the performance of CI due to DIPA as well as improvement in energy efficiency.

The chapter is organized as follows. Section 4.2 summarizes the theory of constructive interference and related work. We also list the claims and counter-claims made in the literature about the working of CI. Section 4.3 describes the experimental setup. In Section 4.4, we give expressions for the resultant signal and show through these equations, how CI depends on various parameters. We corroborate these with experimental results and draw our conclusions about CI also in Section 4.4. We establish that obtaining an optimal transmit power set has exponential complexity, and propose our algorithm with its evaluation in Section 4.5. We make concluding remarks in Section 4.6.

4.2. Constructive Interference

In this section, we first summarize the theoretical background of constructive inter-
ference, and then briefly describe the literature that has studied CI and applications
that use CI.

4.2.1. Theory of Constructive Interference

When two nodes transmit the same packet simultaneously on the same frequency
band to a receiver within their transmission ranges, the transmitted signals super-
pose leading to *constructive* interference at the receiver. On an IEEE 802.15.4 node
operating in the 2.4 GHz band, the data to be transmitted is first split into 4-bit groups
each forming a symbol. Each symbol goes through a Direct Sequence Spread Spec-
trum (DSSS) modulation. Every symbol is modulated with a pseudo-random noise
(PN) sequence of 32 chips. The symbol-to-chips mapping is defined in the IEEE
802.15.4 standard [93]. This baseband signal is then modulated onto the carrier with
Offset-Quadrature Phase Shift Keying (O-QPSK), which is transmitted over the wire-
less medium.

At the receiver, a coherent detection method is used to demodulate the carrier
signal. The signal is down-converted into chips, which are then mapped back to the
symbols. Redundancy introduced by the PN sequence allows for coping with errors
caused on the channel. This redundancy improves the receiver sensitivity level at the
cost of a reduced data rate.

For CI to occur, the tolerable temporal displacement between signals is $0.5\,\mu$s [90],
since the chips in quadrature-phase (Q-phase) are delayed by the chip time, $T_c =
0.5\,\mu$s with respect to the in-phase (I-phase) carrier. As in [94], let the O-QPSK signal
be represented by,

$$S(t) = I(t)\cos \omega_c t - Q(t)\sin \omega_c t. \tag{4.1}$$

Here, $I(t)$ is the I-phase, $Q(t)$ is the Q-phase component, and $\omega_c = \pi/2T_c$ is the radial
frequency of half-sine pulse shaping. The resulting constructively interfered signal is
given by,

$$S_r(t) = \sum_{i=1}^{K} A_i S_i (t - \tau_i) + N_i(t), \tag{4.2}$$

where, K is the number of concurrent transmitters, A_i is the amplitude and τ_i is the
temporal offset of the ith transmitted signal. $N_i(t)$ is the noise added to the signal.

4.2.2. Related Work

We group the related work on CI into two categories: articles that study or analyze the
CI phenomenon, and articles that use CI for protocol development in WSN.

Work on CI: With concurrent transmissions, a packet can be decoded by the re-
ceiver even in the absence of the capture effect. For concurrent transmissions to in-
terfere constructively, precise timing requirements need to be imposed on the trans-
mitter nodes. Ferrari et al. [90] analyze these requirements and outline a method to
achieve them on CC2420 radios, specifically trying to make overall delay determin-
istic in nodes that have low accuracy clocks. Furthermore, they propose Glossy, a
mechanism to flood the network within a few milliseconds. Importantly, they show
through experiments on testbeds that (i) as the number of concurrent transmitters

increases the packet reception ratio (PRR)[1] increases; (ii) the only factor that affects CI is not meeting the temporal offset constraint of $\leq 0.5\,\mu$s among concurrent transmissions.

Wang et al. [94] studied the scalability of CI. They argue that PRR of CI decreases with an increasing number of nodes due to non-deterministic delays. They show scalability is an issue, and propose an algorithm to handle it. The scalability issue has also been studied in [91], which demonstrates, with experiments, that more transmitters will affect the received signal severely.

A model for computing the success of packet reception under both CI and capture effect is proposed in [95]. Improving PRR in CI has been considered in [92] and [96]. Increasing the power difference among transmitters combined with the use of a forward error correction scheme is the method proposed in [96].

It is claimed in [92] that signals transmitted within $0.5\,\mu$s is not enough for CI due to the noise in the received signals. Further, they propose algorithms to achieve chip-level synchronization and select only those transmitters that improve the received signal power, with simplifying assumptions. From these studies, we make some observations.

Claim 1: Temporal offset among concurrent IEEE 802.15.4 transmitters not exceeding $0.5\,\mu$s will generate constructive interference with high probability [90].

Contradicting claim: Concurrent transmission with delay less than $0.5\,\mu$s is insufficient to guarantee CI due to noise in the radio signals [92].

Claim 2: Out-of-phase carrier waves allow correct detection with high probability, when the number of concurrent transmitters is greater than or equal to three [90].

Contradicting claim: Not all out-of-phase carriers allow the decoding of the packet correctly. A maximum tolerable phase offset to generate CI is derived in [92].

Claim 3: The number of concurrent transmitters have little impact on PRR [90].

Contradicting claim: CI does not scale with the number of transmitters due to the lack of coherence among carrier signals [91].

Claim 4: Non-deterministic delays are present and affect CI negatively [94].

Claim 5: Power imbalance greater than $5\,$dBm improves the PRR [91], where power imbalance is defined as two concurrent transmitters having transmission power levels that differ by a certain value. A similar claim is made in [96], in which power imbalance greater than $2\,$dBm improves the PRR.

Claim 6: PRR decreases when packets become longer [90].

It is apparent that there is an inconsistent view on the working of CI, and some claims are not completely explained and need substantiation. In this chapter, we shall establish how these parameters affect CI and perform experiments to validate them in various real-world scenarios.

Work on the use of CI: A node density estimation algorithm by counting the number of combined signals in CI based on the received power is proposed in [97]. The Splash protocol pipelines transmissions for parallel data dissemination over a tree using Glossy [98]. This work also demonstrates certain weaknesses of CI such as lower reliability of CI with larger packet sizes and that not all tightly synchronized transmissions are helpful. Splash uses several techniques, such as diversity in transmis-

---

[1]Packet reception ratio is the ratio of the number of data packets successfully delivered to the number of packets transmitted regardless of the number of transmissions involved in delivering each packet.
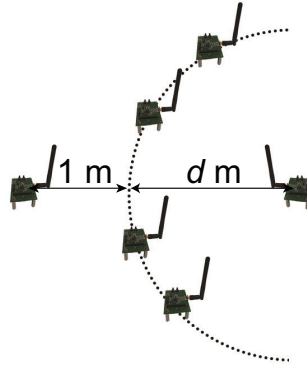
Figure 4.2: Data collection setup in which concurrent transmitters are placed on an arc to make them equidistant from the receiver.

sion density, opportunistic overhearing, channel cycling and XOR coding, to improve PRR. Ferrari et al. [99] propose a protocol utilizing Glossy to convert the multi-hop WSN to a shared, low-power wireless bus. This bus supports one-to-many, many-to-one and many-to-many traffic. Another work [100] modifies Glossy to make it a data collection protocol. While such protocols require all nodes to participate in concurrent transmissions, the authors of [101] propose a method to reduce them by selecting the nodes only in the direction of the destination. These protocols require reliable working of CI, which we investigate in this chapter.

4.3. Design of Experiments

We study the characteristics of CI both analytically as well as with experiments in real-life settings with twelve identical nodes. In this section, we describe the experimental setup used and the locations where experiments were conducted.

4.3.1. Experimental Setup

The setup is shown in Figure 4.2. An initiator node is placed 1 m away from the set of relay nodes that also act as the concurrent transmitters. These nodes are placed on an arc, formed by the circle of radius d. A receiver is placed d m away, i.e., at the center of the circle, making receiver equidistant from the concurrent transmitters.

The distance between the receiver and the concurrent transmitters is chosen such that the network remains connected when any of the concurrent transmitters sends a packet at -6 dBm. That is, d is the threshold distance at which all the packets from a transmitter reaches the receiver successfully when transmitted with the specified power. Note that d varies across locations due to different radio propagation characteristics. In each location, we verified that connectivity exists and all packets were received between every concurrent transmitter node and the receiver. We used the CC2530 system-on-chip solution from Texas Instruments [43], which supports IEEE 802.15.4 radio. CC2530 is controlled by an industry-standard 8051 microcontroller unit in the chip. The chip has a low-power consumption along with high receiver sensitivity (-97 dBm) and allows to choose transmit powers from -28 dBm to +4.5 dBm in

Figure 4.3: Experimental setup in an empty office.

17 predefined steps. The radio also allows us to choose payload sizes from 1 B to 127 B. For our experiments, we used $\lambda/4$ antennas[2] with a reverse polarity SMA connector. We chose external antennas to eliminate any dependency of the performance of CI on the chip antennas. We implemented CI following the guidelines given in [90], and validated its proper working. That is, we ensured that the concurrent transmitters would transmit within a temporal offset less than 0.5 μs.

All nodes were powered by batteries that provided sufficient voltage levels throughout the experiments. We ensured that batteries had not caused any problems, by checking the voltage levels before and after the experiments to confirm that the measurements made were in good order.

Before each experiment, we ascertained that we used a channel (channel 26 of IEEE 802.15.4) in which there was no external interference from nearby WiFi or Bluetooth devices. No microwave appliances were nearby as well.

4.3.2. LOCATIONS
We conducted experiments at four different locations.

A model of an airliner fuselage: The fuselage is of dimensions 12 m × 3 m. The curved enclosure is made up of tin, and has wooden flooring. In this location, the radius of the arc, d, was 10.5 m.

Corridor: The corridor is 2 m wide and 27 m in length. Here, d was 23 m.

Office space: An empty office was another location for our experiments. It is 10 m × 7 m. In this location, d was 8 m. Figure 4.3 shows the setup in the office space.

Soccer field: An outdoor location free from any construction was chosen. In this case, the radius of the arc was 8 m. Figure 4.4 shows the setup in the field.

---

[2]http://www.lsr.com/downloads/products/330-0016.pdf
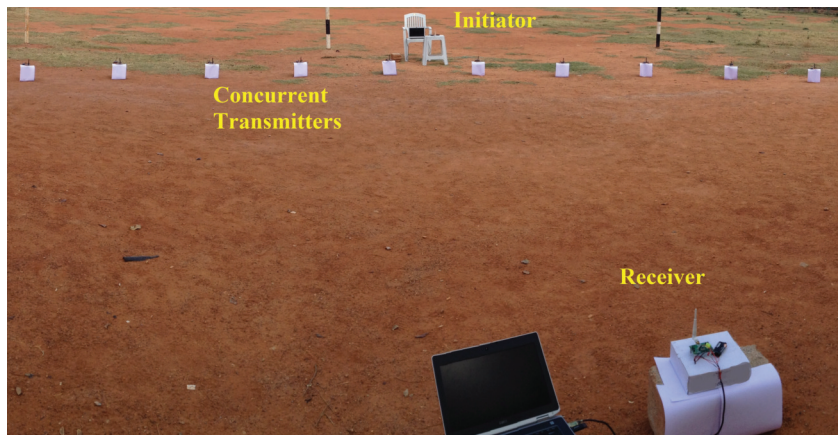
Figure 4.4: Experimental setup in the field.

As mentioned before, each location offers different radio propagation character-
istics. The signals reflect in the fuselage and the corridor locations, while the office
space has less reflections since there are no obstacles. In the soccer field scenario, the
signals are reflected only by the ground.

4.3.3. DATA COLLECTION SCENARIOS

All the experiments were conducted in a line-of-sight setting. We created seven sce-
narios for experimentation. At each location, we collected data with at least 10,000
packets for various packet sizes in each scenario. Below is the list of scenarios.

Scenario 1: We started off with data collection with one transmitter and one re-
ceiver. At each step, we added one more transmitter. The transmission power of each
concurrent transmitter was set to -6 dBm. This scenario studies the effect of the num-
ber of concurrent transmissions on a receiver.

Scenario 2: Scenarios 2–5 are created to study the effect of power imbalance
among concurrent transmitters. In this scenario, alternate nodes were set to -6 dBm
and -3 dBm.

Scenario 3: In this scenario, alternate nodes were set to transmission powers of
-6 dBm and 1 dBm.

Scenario 4: In this scenario, every node chose a random transmission power be-
tween -10 dBm and +4.5 dBm.

Scenario 5: In this scenario, we considered 9 nodes out of which we created groups
of three nodes. In each group, nodes transmitted at -6 dBm, -3 dBm and 1 dBm.

Scenario 6: In this scenario, 9 nodes were used. Alternate nodes were displaced by
a distance of $\pm\lambda/2$ from the circumference of the circle, while the other nodes were
on the circumference. Here, λ is the wavelength of the carrier wave. This scenario
studies the effect of the distance between transmitters on the phase difference. The
distance $\lambda/2$ was chosen since this would create a 180° phase offset between carrier
signals of adjacent nodes.

Scenario 7: This scenario is similar to the previous scenario wherein the alternate
nodes were displaced by $\pm\lambda/4$ instead of $\pm\lambda/2$. This scenario too studies the effect of
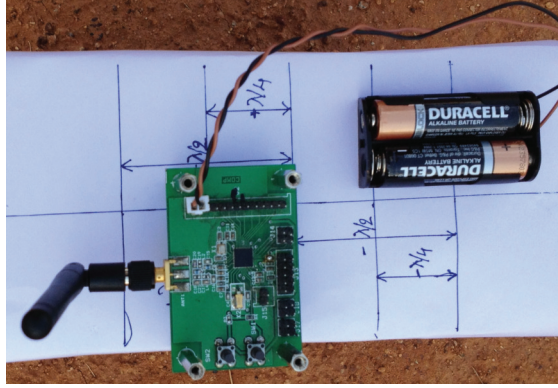
Figure 4.5: Node movement for scenarios 6 and 7.

the distance between transmitters on the phase difference as $\lambda/4$ separation would cause a 90° phase offset between carrier signals of adjacent nodes.

4.4. Unfolding CI

In this section, we derive the amplitude and phase of the resultant signal. By phase, we refer to the phase of the carrier signal, unless mentioned otherwise. Based on these expressions, we analyze an exhaustive set of parameters on how they impact CI. Furthermore in this section, we corroborate this study with experimental results obtained from the setup and different scenarios described in the previous section. With these results, we present a holistic picture about CI.

4.4.1. Phase Offset

Carrier phase offset among the interfering signals can hinder constructive interference. Wang et al. [92] state that for CI to occur, the individual signals must also satisfy a sufficiency condition: for signals to interfere constructively, the phase offset of the ith arriving signal should not exceed $|\phi_i| \leq \arccos\left(\sqrt{\frac{P_i}{P_S}}\right)/\omega_c$ from the strongest arriving signal with power P_S. Here, P_i is the power of the ith signal. This implies that the maximum tolerable phase offset is $\pi/2$. While the condition seems intuitively correct since the I and Q components are offset by $\pi/2$, it is not completely realistic especially when the powers are different. We will show that even if P_i is only slightly less than P_S, but has a $\phi_i > \pi/2$, the signal can be decoded correctly.

To obtain the correct sufficiency condition, we take a more holistic approach to compute the phase, i.e., we derive the resultant signal and the tolerable phase offset.

Lemma 1. *Constructive interference has occurred when the carrier phase offsets are within $\pm\pi/4$ with respect to each of the received signals at the receiver.*

Proof. Equation (4.2) can be represented as $S_r(t) = \sum_{i=1}^{K} A_i \cos(\omega_f t + \phi_i)$, where ω_f is the carrier frequency, ϕ_i is the phase of the ith signal. For the sake of understanding the influence of the phase differences, we neglect noise from this equation. However, the negative influence from noise in phase detection and symbol recovery is an

essential and basic element of the CI phenomenon, which is difficult to quantify.

From the Harmonic Addition theorem, the summation is given by,

$$S_r(t) = \sum_{i=1}^{K} A_i \cos(\omega_f t + \phi_i) = B \cos(\omega_f t + \hat{\phi}), \qquad (4.3)$$

where,

$$B^2 = \sum_{i=1}^{K} A_i^2 + 2 \sum_{i=1}^{K} \sum_{j>i}^{K} A_i A_j \cos(\phi_i - \phi_j), \qquad (4.4)$$

$$\text{and } \hat{\phi} = \arctan \frac{\sum_{i=1}^{K} A_i \sin \phi_i}{\sum_{i=1}^{K} A_i \cos \phi_i}. \qquad (4.5)$$

Here B is the amplitude of the resultant signal and $\hat{\phi}$ is the phase of the resultant carrier signal. This resultant signal is downconverted to baseband signal. There are two possible cases for this baseband signal.

Case 1: The signal is not decodable because the summation of several signals with different phase offsets produced a signal with invalid baseband phase information (see Figure 4.1(b) for an example).

Case 2: The signal is decodable, i.e., CI has occurred. Even if the baseband phase offset of this decodable signal is greater than zero, the phase lock loop in the receiver attempts to correct the offset. This may be seen as the constellation being rotated by the baseband phase offset. Practically, this is possible for any phase offset if the preamble is sufficiently large.

In many implementations of O-QPSK based receivers (e.g., [102]), symbol recovery is done by taking hard decisions with respect to the axes of the constellation. In order to be correctly decodable, the symbols must be in the right quadrant to avoid detection errors. This is only possible if the baseband signal has a maximum phase offset of $\pm\pi/4$ with respect to the ideal constellation. This implies that this case is only possible if the phase offset of the resultant carrier, $\hat{\phi}$, is less than or equal to $\pm\pi/4$ with respect to each of the received signals at the receiver. Therefore, to decode correctly, the arriving signals are said to be interfering constructively when the maximum phase offset is $\hat{\phi} \leq \pm\pi/4$. □

We now look at various sources that can alter the phase even if the temporal offset among transmitters is less than $0.5\,\mu$s.

4.4.1.1. Clock Errors and Number of Transmitters

There is a heavy reliance on the on-board clock to maintain synchronization. Typically, a crystal oscillator sources the clock for the microcontroller to execute instructions. In Tmote Sky nodes, a digitally controlled oscillator (DCO) acts as the source, which operates at a maximum of 8 MHz. However, this DCO is subject to errors of about $\pm20\%$ from the nominal value, and temperature and voltage cause deviations of about $-0.38\%/°$C and $5\%/$V respectively [90].

Wang et al. [94] state that there can be uncertainty in time due to software delays, radio processing delays and clock drifts in each hop.

Let p_e be the probability mass function (pmf) of the uncertainty of time delays on a node. With K concurrent transmitters, each being independent from the other

transmitters, the effective pmf will be $p_e * p_e * \ldots K$ times $= p_e^K$. The probability that there are no clock drifts, i.e., no phase offsets with K concurrent transmitters decreases exponentially with increasing number of transmitters. The exponential curve represents the lower bound of success, i.e., occurrence of no clock drifts. Therefore, we can conclude that non-deterministic delays are present and can influence the resultant phase.

4.4.1.2. DISTANCE BETWEEN TRANSMITTERS

The phase of the resultant signal is given by the following relation when two concurrent transmitters (assuming transmission powers are equal) are placed at distances d_1 and d_2 from the receiver respectively,

$$\phi = \frac{2\pi(d_1 - d_2)}{\lambda}, \tag{4.6}$$

where, λ is the wavelength. It is apparent that if these two transmitters are separated by a distance of $\lambda/2$, then they cancel each other. A generalization of this statement is that path differences between transmitters cause phase offsets, which in turn affects the resultant amplitude and hence, the decodability of the signal. For 2.4 GHz radios, the wavelength is ≈ 12.5 cm. Hence, small path differences can create undesirable phase offsets.

4.4.1.3. TRANSMISSION POWER

Intuitively, the signal with more power should dictate the amplitude and phase of the resultant signal. This is evident from Equation (4.4) and (4.5), i.e., when there is a stronger signal $S_i > S_j$, the value of B and $\hat{\phi}$ tends towards the value of A_i and ϕ_i. We demonstrate this with the following example. We consider two concurrent transmitters. We fix the amplitude and phase of one signal to constant values, namely $A_1 = 1\,V$ and $\phi_1 = \pi/4$. We fix only the phase of the second signal at $\phi_2 = 5\pi/6$ and vary only the amplitude from 0.00 V to 2.00 V in steps of 0.01 V. Figure 4.6 shows the amplitude and phase of the resultant signal computed from Equation (4.4) and (4.5). There is a point of discontinuity in the phase at a certain point, and it begins tending towards the second signal, as it gets stronger.

When there is a stronger signal even with a phase offset, current receivers can compensate this phase offset by using phased-lock loops, hence decoding correctly. In the example in Figure 4.6, when the powers of the two signals vary, the resulting signal can be correctly decoded although A_2 has a phase offset greater than $|\phi_2| > \pi/2$. For the example in Figure 4.6, we computed the regions in which the resultant signal can be decoded as either S_1 or S_2. The resultant signal is taken to be decoded when it has a correlation coefficient greater than or equal to 0.99 of the decoded signal with either S_1 or S_2. The region between these two points do not correspond to either of the transmitted signals and cannot be decoded. However, we have demonstrated that concurrent transmissions with varying powers and phases can still be decoded, which is in contradiction with the sufficiency condition from Wang et al. [92].

4.4.1.4. PHYSICAL ENVIRONMENT

Another factor that affects the phase of the resultant signal is the physical environment where the sensor nodes are deployed. Multipath is unavoidable in many real-

(a) Resultant amplitude   (b) Resultant phase
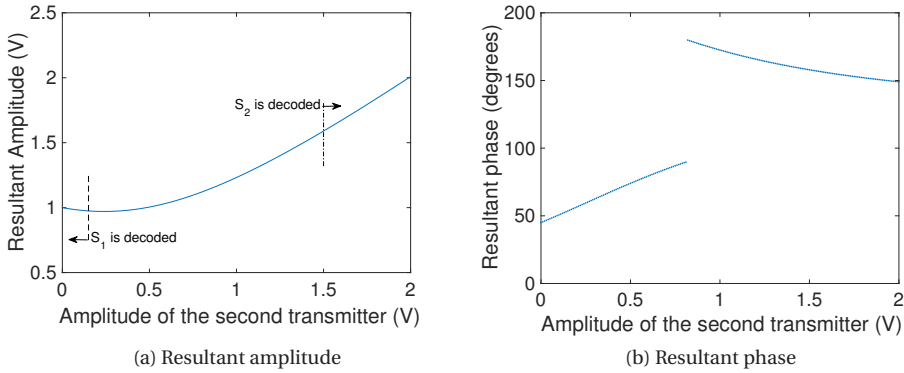
Figure 4.6: Resultant amplitude and phase when $A_1 = 1\,\text{V}$ and $\phi_1 = \pi/4$. Amplitude A_2 is varied from 0 to $2\,\text{V}$ in steps of $0.01\,\text{V}$ and its phase is $\phi_2 = 5\pi/6$.

world deployments. Due to this effect, concurrently transmitted signals travel different path lengths. Therefore, the receiver will see different phase offsets of the signals. Although several channel models exist, it is difficult to quantify the exact influence of multipath signals on the received signal. Nevertheless, it should not be neglected and can clearly be seen in an actual deployment. We shall demonstrate this in the following section.

Lemma 2. *A packet can be decoded with high probability when concurrent transmissions of the same packet have (a) the temporal offset between transmissions $\leq 0.5\,\mu s$; (b) the phase offset of the resultant signal $\leq \pm\pi/4$ with respect to each other for the received signals; (c) different transmission powers for the individual transmissions.*

Proof. Conditions (a) and (b) are the necessary and sufficiency conditions for constructive interference. Condition (a) has been proven in [90] and condition (b) has been proven in Lemma 1. The necessary and sufficiency conditions hold when the transmission powers employed by the concurrent transmitter are equal. Condition (c) specifies the special case when either (a) or (b), or both are not met. With Lemma 1 and the discussions thereafter, it is clear that when transmission powers of the individual concurrent transmissions are different, the phase offset is determined by the stronger arriving signal and has higher chances of being decoded. When the transmission powers of the individual signals vary with time offsets of transmissions close to $0.5\,\mu s$, which is much lower than the preamble time, there is a non-negligible chance of (power) capture taking place [89], i.e., the ability of the radio to receive a strong signal regardless of other concurrent transmissions. When the tight time synchronization of $0.5\,\mu s$ cannot be met due to synchronization errors or clock drifts, there is still a high probability of the packet being decoded correctly. □

The significance of Lemma 2 is as follows: concurrent transmissions increase the probability of packet reception either through constructive interference or capture effect (when different transmission powers are employed). However, it is difficult to
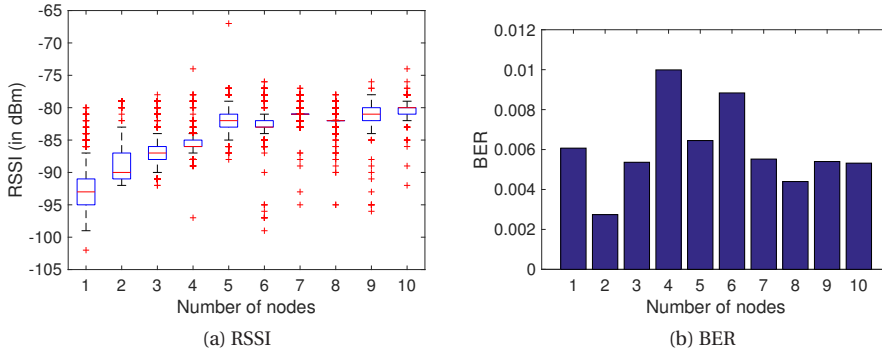
Figure 4.7: RSSI and BER values in an empty office.

quantify the probability of correct reception analytically due to noise and other various parameters affecting the signal.

4.4.1.5. OBSERVATIONS

Since we are investigating the phenomenon of CI over one hop, we look at statistics of each transmitted packet rather than the PRR.

Here, we are interested in received signal strength (RSSI), bit error rate (BER) and packet loss. We present selected data from different scenarios to best describe the effect of parameters on CI. The inferences drawn here are applicable to data from all scenarios since the trends were similar. While some conclusions can be derived from previous work, we present them here for the sake of completion. Together with our inferences, this work provides comprehensive insights into CI.

Figure 4.7 shows the RSSI and BER values at the receiver in the empty office scenario. The RSSI increases with increasing number of concurrent transmitters before saturating at a certain power. However, when we look at the BER, we see that BER does not follow the nice trends as the RSSI; nor does a high RSSI imply less errors. We also placed an additional receiver in this scenario at 1 m distance from the concurrent transmitters. The RSSI and BER values at this receiver (see Figure 4.8) also depict the same trends. Figure 4.9 shows the RSSI and BER in the fuselage location when the nodes are kept at 10.5 m distance. In this case, we observe that the RSSI does not follow the nicely increasing trends especially with 4 and 5 concurrent transmitters. We speculate that the some signals were not contributing to the decoded signal and hence lower RSSI. BER, in this experiment too, does not show any relation with RSSI. The causes for lower BER could be due to one or more of the factors discussed in the previous section. From this figure, we infer the following:

Inference 1: CI increases the energy in the wireless channel.

Inference 2: Higher RSSI does not imply lower BER of the packet.

Inference 3: Temporal offset $\leq 0.5\,\mu$s is necessary for CI to occur with high probability. However, achieving this tight synchrony is not always sufficient to reap the maximum benefits of CI.

Inference 4: There is no relationship between BER and the number of nodes, i.e., we cannot conclude that the number of concurrent transmitters will influence the

(a) RSSI

(b) BER
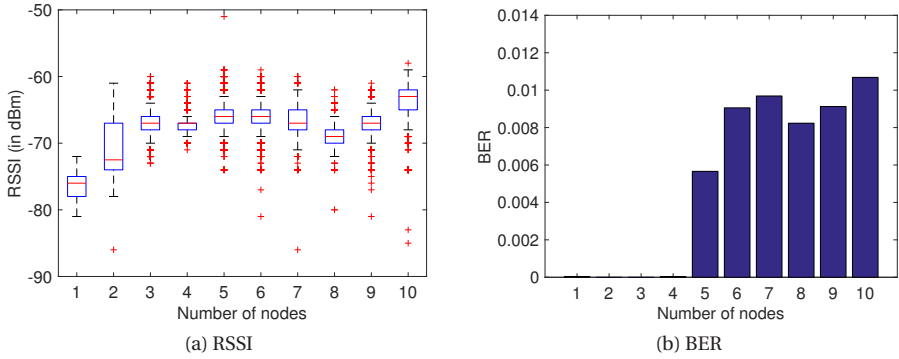
Figure 4.8: RSSI and BER values in an empty office with receiver at 1 m from concurrent transmitters.

(a) RSSI

(b) BER
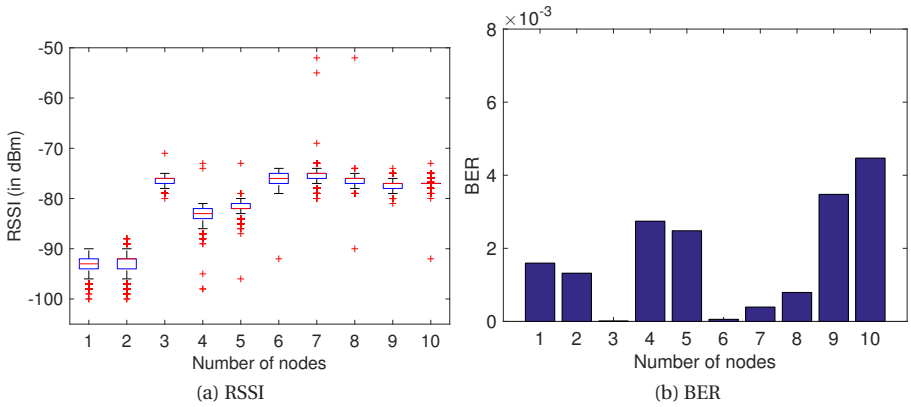
Figure 4.9: RSSI and BER values in a model airliner fuselage with receiver at 10.5 m from concurrent transmitters.

PRR.

Although we achieved a tight synchronization of $0.5\,\mu$s on the nodes, we saw that the BER shows variation in performance. This leads us to the third inference. The sufficiency condition in Lemma 1 was probably not satisfied here. We will now illustrate the fourth inference better with another dataset.

Figure 4.10 shows the RSSI and BER for varying number of transmitters in the corridor environment. We strongly suspect that multipath is influencing the received signals. In a corridor with one transmitter, multipath will mostly be beneficial as the corridor will act as a waveguide. However, in order to realize CI, both the conditions for the temporal and phase offsets as stated in Lemma 1 must be satisfied. Although the concurrent transmitters may be well synchronized, the path lengths traversed by the individual transmissions may be different. This leads to a new problem that arises with concurrent transmissions. The influence of multipath with concurrent trans-

(a) RSSI
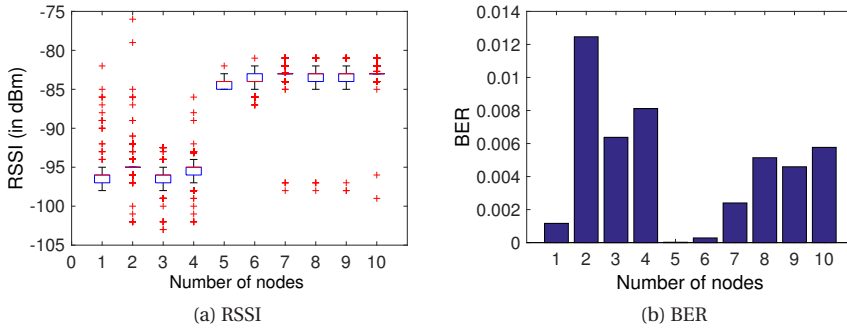
(b) BER

Figure 4.10: Multipath effects in corridor.
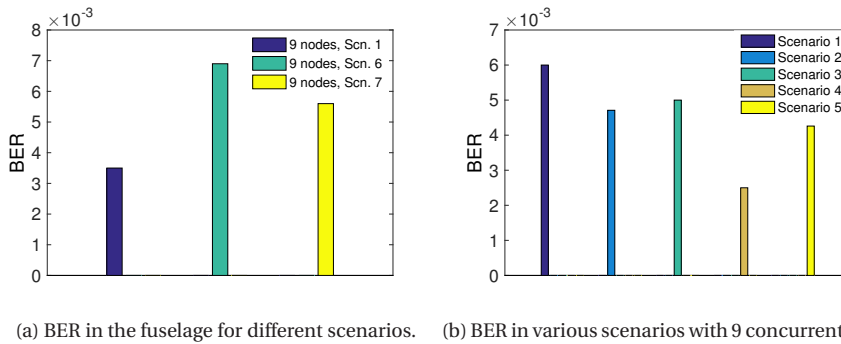
(a) BER in the fuselage for different scenarios.

(b) BER in various scenarios with 9 concurrent transmitters in the soccer field for a payload size of 127 B.

Figure 4.11: BER in various scenarios in two different locations.

mitters can be seen in Figure 4.10(b), which shows that multipath can significantly impact the BER. It seems that the signal from the fifth node is more 'influential' since the RSSI suddenly steps up after the fifth node is added and BER reduces as well. Note that all nodes used the same transmit power. The fifth node was the third node from either side of the walls, in different experiment trials, much closer to the walls than nodes 1 to 4. We can therefore infer the following:

Inference 5: There is a definite influence of the set of transmitters on CI that are participating in concurrent transmissions.

Inference 6: The phase of the resultant signal is influenced by multipath.

Inference 5 is easily observable in Figure 4.10(b), wherein adding the fifth node performed better than even with a single transmitter. When signals are bounced off, they take varied path lengths, which is one of reasons for Inference 6 (Inference 6 is also in line with the discussions in the previous section). We will illustrate it with another experiment.

Figure 4.11a shows the BER for different scenarios when the nodes are displaced by $\lambda/2$ (Scenario 6) and $\lambda/4$ (Scenario 7). Here it is apparent that the change in path length has increased the bit errors.

Inference 7: The phase of the resultant signal is influenced by the distance between concurrent transmitters.

The last study is about the transmit power difference among transmitters. For this study, we pick the data from the soccer field scenario with a payload of 127 B (worst BER case). We see the BER from various scenarios in Figure 4.11(b). It is clear that different transmit powers have a positive effect on CI, as described in Section 4.4.1. Across experiments, it was difficult to infer whether 3 dBm or 7 dBm difference in transmit power performed better. But in all cases, when the transmit powers were randomly chosen (Scenario 4), the obtained BER was the least. Clearly, a power imbalance is effective, but it is difficult to find a common threshold of the imbalance that improves the performance of CI.

Inference 8: Transmitting at higher power usually results in better packet reception. However, power imbalance among concurrent transmitters can also aid packet reception.

4.4.2. Clock Drifts on the Radio and Packet Size

It is well-known that the bit error rate increases with increasing packet size. In the case of a single transmitter, this observation is attributed to the error-prone wireless channel. However, with CI, there is another factor that causes the increase in bit error rates with increasing packet size even if the channel is coherent throughout the transmission.

Apart from the DCO on the microcontroller, there is another oscillator in the radio module. IEEE 802.15.4 specifies that the radio can tolerate up to ±40 ppm clock drifts [93] when receiving the carrier signal. That is, the total frequency offset between two concurrent transmitters can be up to 80 ppm. This causes the signals to be distorted (an example is shown in Figure 4.1(d)). While an automatic frequency control unit can be employed for compensating the frequency offset, this is not employed due to additional circuitry and cost in the radios. This offset is fine when receiving a single carrier signal since it can be recovered easily at the cost of decreased sensitivity level. However, with CI given that the signals have non-zero phase offsets, the frequency offsets start impeding the signal and the bits are decoded in error.

Figure 4.12 shows the BER for different packet sizes from the experiments in the soccer field. As expected, longer packet sizes are prone to error. To illustrate the clock errors on the radio, we plot the bit error rate per bit position in a payload of 127 B (1016 bits) in Figure 4.13. We see huge variations in errors for 3 nodes and the trend of errors seems to increase with subsequent bit positions. To capture this trend, we fit a line to the data which is shown in bottom plot of Figure 4.13. The slope is increasing in both the cases of two and three nodes but seems negligible for the two node case, while it is clear the errors are increasing with three nodes.

Inference 9: Bigger packet sizes are prone to more errors due to both the wireless channel and higher carrier frequency offset caused by low accuracy clocks in the radio.

Inference 10: The number of concurrent transmitters will influence the BER for bigger packet sizes due to erroneous clocks on the radio.

(a) Average of all packet sizes

(b) Packet size 16 B

(c) Packet size 32 B

(d) Packet size 64 B

(e) Packet size 96 B

(f) Packet size 128 B
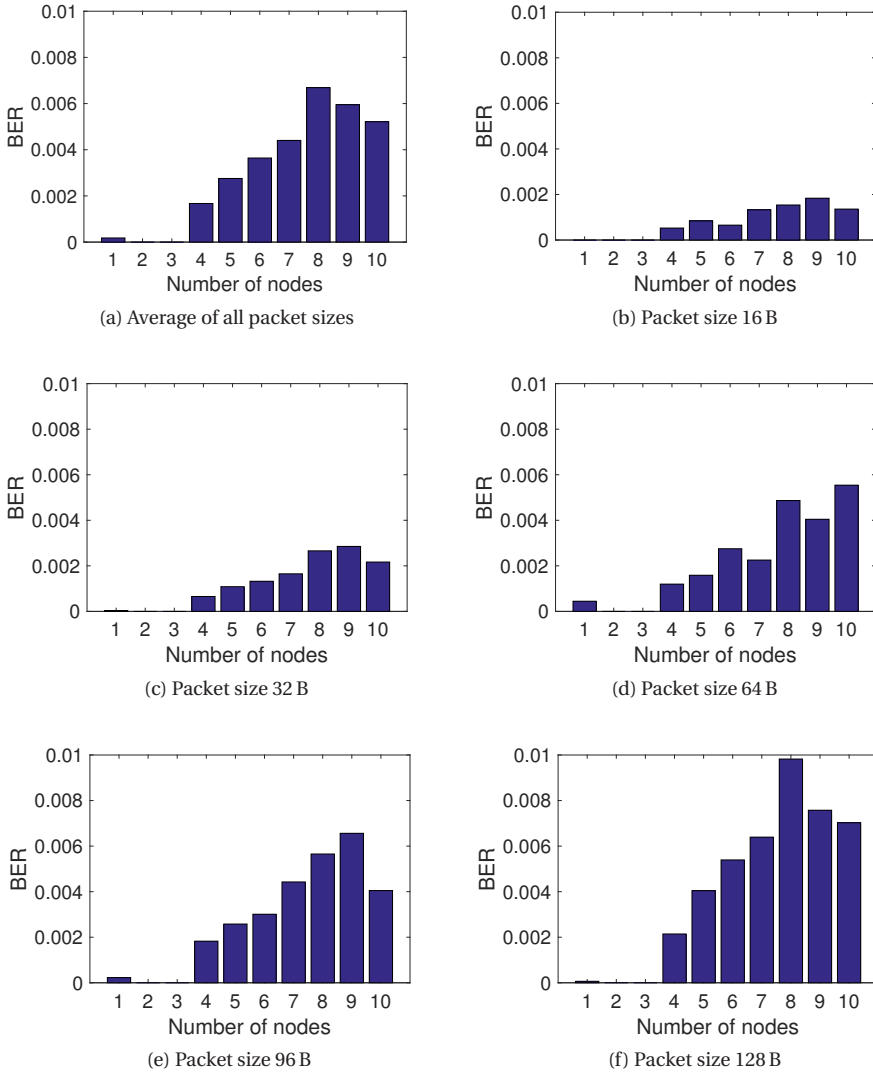
Figure 4.12: BER in the soccer field for different packet sizes.
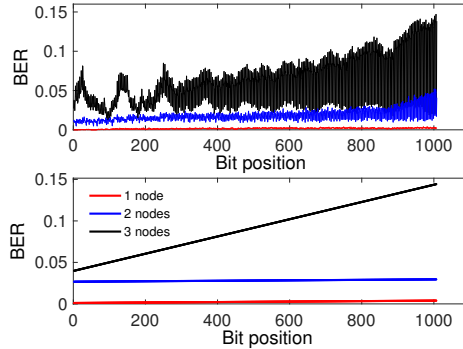
Figure 4.13: Top: BER per position for a 127 B payload with varying number of concurrent transmitters. Bottom: Linear fitting to show the slope of BER at different bit positions.

4.5. Improving the Performance of CI

Many works such as the ones mentioned in Section 4.2.2 employ CI over multihop wireless sensor networks. For example, Low-power wireless bus [99] builds a collection and dissemination protocol over Glossy that is demonstrated to be highly energy-efficient as compared to other similar protocols. These works, including Glossy, transmit the packets more than once to ensure reliable packet delivery. Since CI can have a bad performance, it is important to improve the performance of CI that also increases the energy-efficiency of CI without impeding the benefits of CI.

As demonstrated in the previous section, minimum BER from CI can be obtained only when all the parameters are just *right*, which is almost impossible due to many associated practical difficulties. Furthermore, in a random deployment, which is typical of a WSN, each receiving node may see a different BER. Nevertheless, there are two methods to improve CI: (a) reducing non-deterministic delays on the nodes; (b) choosing the transmission powers for each node that maximize CI. There has been considerable work to improve the performance of CI by reducing non-deterministic delays [92, 94]. However, while synchronization is necessary, the performance is still limited by the deployment as we have seen in the previous sections. To this end, setting transmission powers for each node is more beneficial (see Inference 8).

The problem of choosing the set of transmission powers for all concurrent transmitters that maximize CI, while achieving energy efficiency, in the network has an exponential number of combinations. Energy efficiency is important since the nodes are battery-powered. Let each node have Γ transmission power levels to choose from. With K concurrent transmitters, in the worst case number of combinations that need to be evaluated are of the order $O(\Gamma^K)$. Furthermore, given that the wireless channel changes over time, a static set of transmission powers will not help in the lifetime of the network. A limitation of a real-life deployment with Glossy or other CI based protocols is that there are no ACK packets; nor can ACK packets be introduced since the transmissions are not unicast.

Under these conditions, we propose an algorithm Destructive Interference based Power Adaptation (*DIPA*) that adapts transmission power based on the performance

Figure 4.14: Decoded symbol after destructive interference for different combination of symbols from two concurrent transmitters. The number in each cell indicates the decoded symbol.

of CI. The performance is obtained through *feedback*. To this end, we utilize *destructive interference* (DI) to gather feedback from the neighboring nodes. We first describe how DI works, before describing the algorithm.

4.5.1. DESTRUCTIVE INTERFERENCE OF SYMBOLS

Given that CI achieves tight synchronization at chip level, we can achieve DI at a symbol level. At the receiver, if many dissimilar symbols overlap then symbol recovered can be any symbol from the set of all symbols. However, if two dissimilar symbols overlap at the receiver, then the decoded symbol is probably going to be either of them. For example, if symbols 0x0 (or S_0) and 0x1 (or S_1) are transmitted, the receiver demodulates and uses a soft-decoding procedure to get the chip sequence. This sequence may not correspond to any of the symbols. A hard-decision procedure follows to map the decoded sequence to one of the symbols, wherein symbol with the highest correlation to the decoded sequence is used as the decoded symbol. In this case, the "distance" from 0x0 is lower than that of 0x1.

We simulate DI between all combinations of symbols taking two at a time in MAT-LAB and derive the decoded symbol as shown in Figure 4.14. When we look at the upper triangular matrix of this symmetric matrix, we observe that symbol S_0 is the most likely symbol to be decoded when it interferes with any other symbol (except in five cases). In general, the first eight symbols are more *robust* than the last eight symbols [103]. The last symbol, S_{15} is the least likely symbol to be itself.

In order to exploit this as a feedback mechanism, we make use of the above observation: we select S_{15} to represent ACK. When nodes have to send NACK, they send S_0. We take a conservative approach here, i.e., the symbol representing ACK is the symbol that is least likely to be itself when it overlaps with another symbol. In contrast, the

NACK is the most robust symbol, i.e., S_0. There can be multiple concurrent transmitters sending either of these two symbols. The feedback symbols experience the same phenomena as CI, therefore the decoded symbol depends on several parameters such as number of transmitters, clocks, multipath, transmission powers and capture effect. In order to be even more conservative, at the receiver, if the feedback is any symbol other than S_{15}, then it is considered to be NACK. Thus, DI allows us to capture the feedback of the channel and other errors well.

With the feedback mechanism in place, we first describe the algorithm for a single hop case, and then show how to integrate it into Glossy for more practical applications.

4.5.2. DIPA Algorithm

We designed the DIPA algorithm considering a random deployment of nodes, wherein each receiving next hop node can experience a different BER and packet reception with the same set of concurrent transmitters. The intuition behind the algorithm is simple: increase transmit power if packets are not being received successfully, and slowly decrease the power if the packet reception is stable. The idea is to make transmissions as reliable as possible while conserving energy.

One byte (i.e., we choose two symbols since we lose only four bits) is used as feedback and is appended to the data. Each concurrent transmitter takes this decision locally and independently, based on the feedback it receives from the neighboring nodes. Note that each concurrent transmitter might also see a different feedback due to the same effects as on CI and the probability of correct detection. A caveat to the working of this mechanism is that the CRC of the packet should be computed in software except for the feedback. At the receiver, the CRC should be checked except for the feedback. This software based CRC computation is allowed in most radios [43].

To explain the algorithm, we consider a one-hop setup similar to Figure 4.2. The algorithm is equally applicable when the concurrent transmitters are randomly placed, and when there is more than one receiver. Here, the source sends a packet, which is forwarded by the concurrent transmitters to the receivers. The receivers validate the packet reception by checking its CRC. ACK is sent if the packet is received correctly, otherwise a NACK is sent. If no packet is received, i.e., even with an invalid CRC due to noise or insufficient transmit power, then a timeout occurs on the concurrent transmitters. In this case, a NACK is sent in the subsequent packet that is to be forwarded. The algorithm for adapting the power based on feedback on a concurrent transmitter is given in Algorithm 10. The function OnReceiveTimeOut is called when ACK packet is not received, which can occur when: (a) the packet sent not received by any receiver; (b) the packet sent was received but could not pass the CRC check or (c) the receiver's transmission power is too low to be received correctly. The function OnReceive is called when a packet is received. This implies that at least one receiver was able to decode the sent packet correctly. A negative feedback implies that earlier sent packets were not being received correctly, therefore, transmit power is increased for the subsequent packets. Nodes decrease their transmit power only when they observe G_{TH} consecutive successful reception. If transmission fails or time out occurs, the transmit power is increased. When the maximum transmit power fails to get ACKs, then the nodes resort to a random power level, hoping for the best.

In a multihop case where Glossy is used, every node receiving a packet will re-

---

Algorithm 10 DIPA algorithm on a concurrent transmitter

1: // Let p_s be the next packet to be sent, and p_r be the packet that is received
2: Initialize $nSuccess \leftarrow 0$

3: **function** ONRECEIVETIMEOUT
4:      $nSuccess \leftarrow 0$
5:      **if** $GetTxPower()$ == MAX_TX_POWER **then**
6:          $ChooseRandomTxPower()$
7:      **else**
8:          $IncreaseTxPower()$
9:      **end if**
10:      $p_s.SetFeedback(\text{NACK})$
11: **end function**

12: **function** ONRECEIVE(Packet p_r)
13:      **if** $p_r.IsCRCValid()$ == FALSE **then**   // Incorrect Tx power from the receiver
14:          $p_s.SetFeedback(\text{NACK})$
15:      **else**
16:          $nSuccess \leftarrow nSuccess + 1$
17:          $p_s.SetFeedback(\text{ACK})$
18:          **if** $p_r.GetFeedback()$ == NACK **then**   // Previous packets were not being received
19:              **if** $GetTxPower()$ == MAX_TX_POWER **then**
20:                  $ChooseRandomTxPower()$
21:              **else**
22:                  $IncreaseTxPower()$
23:              **end if**
24:          **else**   // Everything is just fine
25:              **if** $nSuccess \geq G_{TH}$ **then**
26:                  $DecreaseTxPower()$
27:                  $nSuccess \leftarrow 0$
28:              **end if**
29:          **end if**
30:      **end if**
31: **end function**

4

broadcast it a predefined number of times. To use DIPA here, we simply include the feedback into the Glossy payload. The only change is in the notion of ACK in Algorithm 10, i.e., the concurrent transmitters wait for actual data packets instead of ACK packets from the neighboring nodes.

The worst case running time of DIPA is O(1) as can be seen in Algorithm 10. While DIPA should not cause any timing issues, however in case there arises such an issue, then the feedback can be collected for every packet but power adaptation can be executed after every few packets to suit the needs of the protocol.

4.5.3. EVALUATION

We used an implementation of Low-power Wireless Bus [104] in Contiki, which bases its working on Glossy, for our evaluation purposes. Although original Glossy transmits each packet at least twice to guarantee a high PRR, we modify this aspect of Glossy to make only one transmission of each packet since we are interested to evaluate the performance of CI. We also incorporated DIPA into this Glossy (henceforth we call this variant as DIPA) for evaluation purposes. We set G_{TH} to 5, and use {-5 dBm, -3 dBm, -1 dBm, 0 dBm} as the set of transmission powers on the nodes. We compare the performance of CI in Glossy and DIPA with respect to BER, packets loss ratio and the transmission powers used, for different packet sizes. Packet loss is said to occur when a transmitted packet fails to reach the receiver or when the CRC check on the received packet is reported as failure.

We evaluate our algorithm in two real-life testbeds w-ilab.t [105] and Indriya [83]. We used 45 nodes on the third floor of the w-ilab.t office testbed, and 37 nodes on the first floor of the Indriya testbed. Both the testbeds contain sensor nodes with CC2420 radio. The nodes are randomly deployed in both testbeds, and have a mixture of both line-of-sight and non line-of-sight links. We choose the testbeds since such a scenario is more common in real-life deployments. In order to make a fair comparison, we restricted the transmission power set so that the number of hops does not differ when the least and/or the highest transmit powers is chosen in both the testbeds.

We first present results from w.iLab.t testbed. In this testbed, we compare DIPA with Glossy transmitting at two different powers. All values are averaged over the data from all the nodes and experiments, and are normalized with respect to Glossy with high transmission powers (Glossy (HP)). Glossy (LP) represents the case where all the nodes employ lower transmission power. We consolidate our results in Table 4.1 and Figure 4.15.

Glossy trades off energy for better BER and packet reception, which is evident from Figure 4.15 when compared between Glossy (LP) and Glossy (HP). DIPA adapts power based on the feedback in order to achieve lower packet losses than Glossy. This can be seen from the table and the figures that our method performs as good as Glossy with respect to BER, reduces packet losses and consumes lower power than Glossy for a better performance. Compared to Glossy with 16B packets, DIPA achieves better BER with 25% lower packet loss and around 48% savings in transmission powers. Similarly, for 32B packets, DIPA achieves a better BER with 10.5% lower packet losses and 42% of power savings. While BER increased negligibly with 64B packets, we used 40% lower power to achieve 12% lower packet losses.

Based on the above results, we set Glossy (HP) as the benchmark and only compare DIPA against it in the Indriya testbed. We see in Figure 4.16(a) that DIPA results

Table 4.1: Transmit Powers in w.iLab.t testbed.

Algorithm	Tx Power Consumed (in %)
Glossy (HP)	100
Glossy (LP)	40
DIPA (16B)	52
DIPA (32B)	58
DIPA (64B)	60
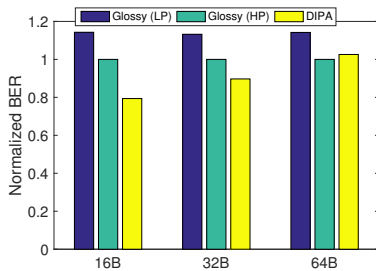
(a) Normalized BER
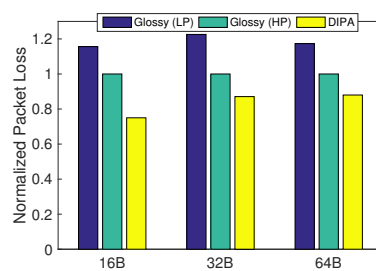
(b) Normalized Packet Loss

Figure 4.15: Comparison between Glossy and Glossy with DIPA in w.iLab.t testbed.

Table 4.2: Transmit Powers in Indriya testbed.

Algorithm	Tx Power Consumed (in %)
Glossy (HP)	100
DIPA (16B)	36
DIPA (32B)	38
DIPA (64B)	40
DIPA (128B)	47
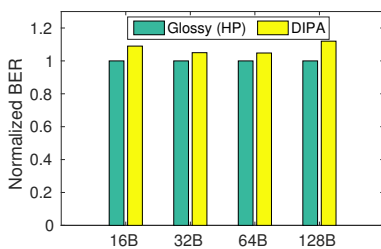
(a) Normalized BER
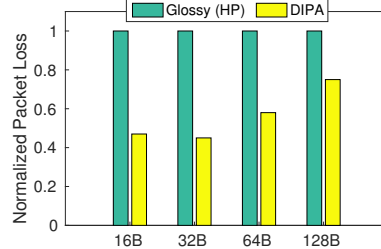
(b) Normalized Packet Loss

Figure 4.16: Comparison between Glossy and Glossy with DIPA in Indriya testbed.

in higher BER than Glossy (HP). However, the higher BER does not result in higher packet losses. In fact, the packet losses with DIPA are much lower than Glossy (HP) for all packet sizes as can be seen in Figure 4.16(b). This is because packets experienced bursty errors with DIPA. When concurrent transmitters send with different transmission powers that result in a decodable packet, the packet has no or minimum errors due to the influence of one or more high power signals. However, when the packet is undecodable, the packet contains bit errors. DIPA tries to maximize successful packet reception. This leads to the bursty errors.

Compared to DIPA, Glossy achieves better BER between 5-12% over different packet sizes. However, DIPA outperforms Glossy with only 53%, 54%, 42% and 25% lower packet loss for 16 B, 32 B, 64 B and 128 B packets. The savings in transmission powers can be computed from Table 4.2.

4.6. Conclusions

Constructive Interference (CI), due to its simplicity, has redefined services and applications, and opened up new avenues in wireless sensor networks. Various studies, hitherto, on CI portrayed an inconsistent view of its working, limitations and benefits. In this chapter, we extensively studied CI from the point of view of receivers both analytically and experimentally. Specifically, we derived the expressions for resultant signal and listed the parameters that affect CI. We established how these parameters influence performance of CI and validated our arguments with results from exhaustive experiments considering minute details, such as half wavelength distance differences among the transmitters, power, etc. Finally, we drew inferences on the working of CI in real-life settings capturing various situations. We believe that our work is one of the first to provide a holistic view of CI and its effects in various scenarios. While the experiments were conducted in a line-of-sight scenario, they are applicable to other settings as well.

Further, we proposed *DIPA*, a distributed algorithm that is energy-efficient. It improves packet reception by adapting transmission powers, and enhances reception due to power capture. This algorithm leverages destructive interference to gain feedback about packet reception with CI. We evaluated our algorithm on two real-life testbeds against Glossy, and showed significant energy savings and better packet reception in these evaluations.

The major learning from this chapter are listed below.

1. Despite CI being useful due to its simplicity and low-latency guarantees, it is quite unreliable.

2. Low-cost components hitherto not known to have caused any problems in communication affect CI, sometimes severely.

3. Only two parameters under an application's control that affects CI are clock and transmission power.

One fundamental question remains: when a packet is received when transmitted by concurrent transmitters, is it due to CI or capture effect as claimed by Ferrari et al. in [106]? We dig more into this aspect in the next chapter.

5

UNDERSTANDING CONCURRENT TRANSMISSIONS IN IEEE 802.15.4 RADIOS

5.1. INTRODUCTION

Concurrent transmissions have been successfully used in wireless sensor networks (WSNs) to design energy-efficient networking protocols. The Flash flooding [89] and Chaos [107] protocols make use of packet capture to disseminate data to all nodes in the network. Glossy [90] and Splash [98] utilize the constructive interference (CI) phenomenon to flood data, and low-power wireless bus [99] uses CI for data collection.

CI occurs when multiple nodes transmit the same signal simultaneously and superposing at the receiver, which helps the receiver to decode the resulting signal successfully with high probability. Packet capture occurs when one of the several simultaneously transmitted signals is cleanly decoded by the receiver. In the previous chapter, we investigated the working of constructive interference (CI) and the various factors that affect its performance. While CI is a recent entrant into concurrent transmissions for wireless networking, packet capture, or simply capture effect (CE), is the more well-known concurrent transmission phenomenon. Due to significant similarities between the phenomena, CI has often drawn speculation if the underlying physical phenomenon is just CE. That is, the receiver decodes the strongest of the transmitted signals with the other signals not interfering destructively [92, 108, 109].

We explain this speculation with an example shown in Figure 5.1. Figure 5.1(a) shows the case when the signals are misaligned but are transmitted with different transmission powers. This is a classical example for power capture, wherein the 'blue' signal is most likely to be decoded since it has the highest transmit power. The receiver is said to lock onto a signal with the most power and ignore the rest. Figure 5.1(b) shows the case when the signals are completely synchronized. If CI occurs, the decoded signal must be a sum of the amplitudes. On the other hand, if CE is the phenomenon behind successful reception of the signal, then the receiver is said to lock onto the phase of one of the signals and ignore the other signals.

Efforts such as [95] have attempted to answer this question with experiments. The

(a) Transmissions with temporal offset and varying transmit powers

(b) Synchronized Transmissions
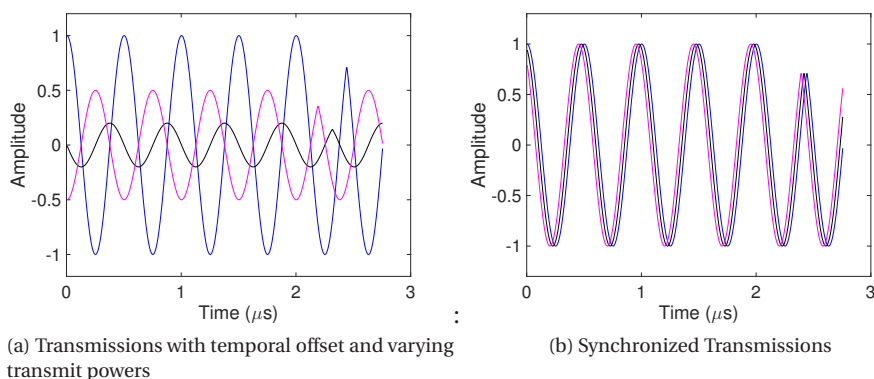
Figure 5.1: Example scenarios where (a) power capture can occur and (b) CI can occur.

authors conclude CI is too difficult to achieve on commodity hardware. The reason mentioned for this conclusion is that the signals from concurrent transmitters can completely superpose with a probability as low as 0.066. Since one of the signals arrives earlier than the rest, the authors conclude it must be capture. However, observations by researchers employing both CI and CE is that CI seems to be 'too good' to be just capture effect [90, 99, 107].

The speculation is not just of academic interest but also has a practical implication. While CI has quite stringent conditions on concurrent transmissions, CE, on the other hand, is quite relaxed: firstly, each concurrent transmitter can send a different packet and secondly, the temporal difference can be upto preamble time ($128\,\mu s$) of the first packet. If CI is no different from CE then the strict constraints can simply be dropped. Therefore, it is necessary to understand the actual working of concurrent transmissions.

In this chapter, we try to gain deeper understanding on the CI and CE phenomena through experimentation in almost ideal conditions. Our contributions in this chapter:

1. We conduct an exhaustive set of experiments on CI in near ideal conditions in order to study why and how it works. We conclude that CI is not CE with non-destructive interference.

2. We explain what exactly *locking* to one of the many transmitted signals means in packet capture. The current understanding of CE is that the receive locks on to the phase of one signal, while the others are ignored. We conclude that this only a part of the explanation; we add the missing part – the power of the locked signal is strong enough so that its phase is not influenced by the interfering signals.

An overview of CI and CE are provided in Section 5.2. The relevant literature that has analyzed these phenomena are described in Section 5.3 along with the speculations made on the two phenomena. The experimental setup is described in Sec-

tion 5.4, followed by the experiments and observations in Section 5.5. The discussions in Section 5.6 presents a clearer picture of the CI and CE phenomena. We conclude the chapter with final remarks in Section 5.7.

5.2. An Overview of Concurrent Transmissions Techniques

In IEEE 802.15.4 radios operating in the 2.4 GHz band with the Direct Sequence Spread Spectrum (DSSS) physical layer, constructive interference (CI) and capture (CE) are the two techniques that can provide successful packet reception despite two or more concurrent transmissions. We provide an overview of them in this section.

5.2.1. CI

A common notion is when two or more nodes transmit at the same time, the interfering signals from different sources causing a significant number of bit errors, and recovering either of the signals correctly becomes impossible for the receiver. However, if multiple nodes transmit the same signal simultaneously, the resulting signal superimposes and allowing the receiver to decode the signal. This is termed as the constructive interference (CI) phenomenon. If $S(t)$ is the transmitted signal by each of the K concurrent transmitters, then the resultant signal at the receiver is given by $S_r(t) = \sum_i^K A_i S_i(t - \tau_i) + N_i(t)$. Here, A_i is the amplitude and τ_i is the temporal offset of the ith transmitted signal. $N_i(t)$ is the noise added to the signal by the wireless channel.

The necessary and sufficiency conditions to achieve CI are that the temporal difference between concurrent transmissions is one symbol period ($0.5\,\mu$s) and the phase offset at the arriving signals at the receiver must be less than $\pi/4$ compared to the transmitted signals, respectively. The factors affecting CI have been discussed in detail in Chapter 4.

5.2.2. CE

Another synchronous transmission technique is packet capture: it is the ability of a radio on the receiver to successfully decode one of the signals even in the presence of several ongoing transmissions. The differences between CI and CE are that the concurrent transmissions need not be the same signal, and the temporal offset between the transmissions need not be strictly within one symbol time. The maximum tolerable temporal difference between the concurrent transmissions for CE to occur is the preamble time ($\leq 128\,\mu$s). These make CE easier to implement.

Two types of CE can occur in the IEEE 802.15.4 radios [110], which are described below.

1. **Power capture**: In power capture, the radio on the receiver successfully decodes the the strongest signal among several ongoing transmissions. In other words, if the power of one of the signals exceed the sum of interference from the remaining signals by a certain threshold, the receiver still be able to receive or capture the strongest transmission successfully. Simply put, if $S_s(t)$ is the

strongest signal at instant t, then it will be decoded due to capture if

$$\frac{S_s(t)}{\sum_i S_i(t)} > \delta_{SIR},$$

where δ_{SIR} is the threshold signal-to-interference ratio for capture to occur. This equation is simplified and does not consider noise or interference that is correlated (such as colliding packets).

2. **Delay capture**: In delay capture, there is a time delay between the overlapping transmissions. The receiver successfully decodes the strongest signal even if the receiver has 'locked' onto the weak signal that arrived first.

Every IEEE 802.15.4 frame begins with a preamble. This helps the receivers to detect the beginning of a frame and synchronize the code. A start of frame delimiter (SFD) follows the preamble in the transmitted frame. This indicates that the bytes following SFD contain the payload.

A common understanding of how packet capture works is as follows [111]. The receiver continuously tries to find the preamble. Once found, the local oscillator locks on to the phase of this signal. All other signals arriving at other phases are supposedly ignored. Therefore, only one of the several ongoing transmissions get decoded.

In this chapter, we focus more on the power capture phenomenon than the delay capture as the former is closer to the CI phenomenon.

5.3. Related Work

In this section, we shall describe the existing literature on CI and CE, and also the works that have looked at both together. Furthermore, we shall describe the need to distinguish between these two phenomena.

5.3.1. Work on CI

Ferrari et al. presented the necessary condition for the constructive interference phenomenon to occur (i.e., the temporal offset should be less than one symbol period), and demonstrated it successfully on Tmote Sky nodes [90]. Wang et al. [94] questioned the scalability of CI as demonstrated by Ferrari et al. due to the presence of non-deterministic delays that are caused by clock drifts. They analyzed its effect on carrier phase offset from the transmitter's perspective, and derived the sufficiency condition for CI to occur. The sufficiency condition allows the concurrent transmitters to have a maximum carrier phase offset of $\pi/2$. Furthermore, they presented an algorithm to fix the clock drifts. This was improved in their subsequent work [92], where they try to achieve chip-level synchronization. Noda et al. present another piece of work that questions scalability of CI by experimentation with software-defined radios [91]. On the other hand, König et al. [112] show that they obtained an increase in signal strength of at least 2 dB in 60% of the cases with 2 concurrent transmitters sending the same packet. Furthermore, the packet reception ratio also increased by 20-35%. They present a mechanism to maintain clock synchronization in order to reap the benefits of CI.

In the previous chapter, we presented that the receiver's viewpoint matters the most. Therefore, we derived the sufficiency condition of carrier phase offset with respect to the receiver. We further analyzed the factors that influence the performance

of CI with rigorous experimentation. Furthermore, we presented an algorithm to increase the chances of successful decoding of the concurrent transmissions despite the factors that may be detrimental to CI.

There are also other pieces of work on the CI phenomenon, some of which overlap with the packet capture concepts. These will be presented in Section 5.3.3.

5.3.2. WORK ON CE

The phenomenon of packet capture has been known and utilized for some decades (e.g., [89]). One of the first studies about the capture effect was by Leentvaar et al. [113] with FM receivers in 1976. Since then several works have investigated the phenomenon, particularly with IEEE 802.11b and IEEE 802.15.4 radios. Here, we shall describe the works that have studied capture effect on IEEE 802.15.4 since they are more relevant for our work.

Son et al. studied capture effect through a series of experimentation. They found that occurrence of the capture effect can be guaranteed if the power difference between concurrent transmissions is large enough, which is around 6 dB. Anything below that falls into a gray zone wherein some packets may get decoded successfully, chances of which reduces as the power difference reduces.

Wilhelm et al. [110] provided a detailed study on CE analyzing various parameters that effects it. The parameters they considered were power difference (or power ratio as they call it), timing, packet contents and carrier phase offsets. They provided a model to generalize the conditions under which CE can occur and verified the model with rigorous simulations and experimentation. With the model, they presented zones when capture can occur (time offset or power offset) for different payloads as well as same payload contents (similar to CI). They found that with the same payload contents, the capture zone is much bigger and successful decoding begins at a lower power ratio as well. However, they are skeptical to identify if the decoding was due to CI or CE.

5.3.3. SPECULATIONS ON CI AND CE

There have been two major claims on the working of Constructive Interference (CI) and Capture Effect (CE). We present them here.

Claim 1:   CI is almost non-existent, and the reception is due to packet capture.

Yuan et al. [95] established with experiments that precise synchronization of signals from concurrent transmissions can happen with a probability of 6.6%. Therefore, they conclude that most CI happens only due to CE, i.e., the strongest signal gets locked onto the receivers and others interfere non- destructively.

Another question that some works present is, "is non-destructive interference (NDI) constructive?". While the benefits of CI are observed by the authors [92, 109, 108], they are skeptical to claim that CI occurs when the concurrent transmitters transmit their packets within 0.5μs temporal offset due to the presence of clock drifts, propagation delays and radio processing delays on the nodes. This question suggests that packet capture may be the underlying phenomenon for CI.
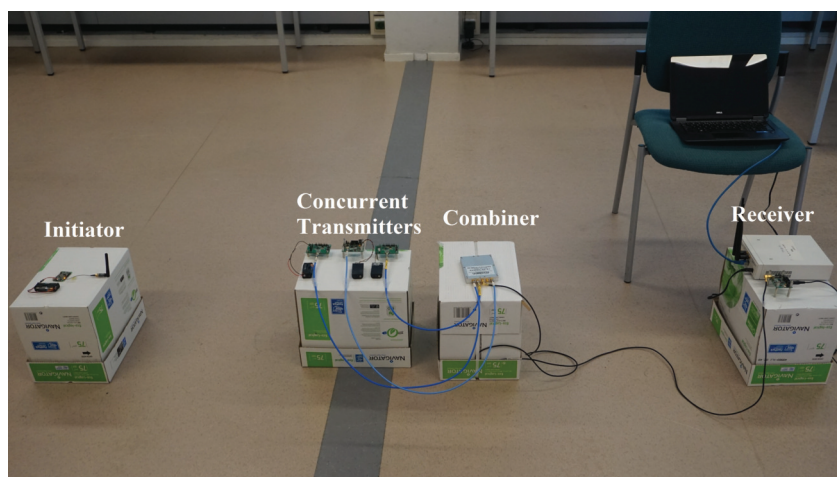
Figure 5.2: Experiment setup with CC2530 nodes, power combiner (channel) and receiver.

Claim 2:   In packet capture, a receiver locks onto one of the several synchronous transmissions [110, 111].

We found that this is the common understanding of the working of packet capture. It is considered that a receiver locks onto a transmission and ignores the other on-going transmissions of lower power. However, when a higher power signal than the current one arrives (within a specified duration), the lock is released and the receiver locks onto the stronger signal. While the observation is correct, the underlying phenomenon needs more explanation. We provide this later in the chapter.

5.4. EXPERIMENTAL SETUP

The experiment setup is shown in Figure 5.2. We used the CC2530 system-on-chip solution from Texas Instruments [43], which supports IEEE 802.15.4 radio. CC2530 is controlled by an industry-standard 8051 microcontroller unit in the chip. The chip has a low-power consumption (consumes 24 mA in active-mode receive operation with CPU idle) along with high receiver sensitivity (-97 dBm) and allows to choose transmit powers from -28 dBm to +4.5 dBm in 17 predefined steps. The radio also allows us to choose payload sizes from 1 B to 127 B.

In our experiments, we used power levels in the range of -4 dBm to -16 dBm, which results in a signal through the combiner well above receiver sensitivity of -97 dBm. We also used a software-defined radio, USRP N210 from Ettus Research, in order to visualize the signal properties such as amplitude and power spectral density. A Software defined radio transceiver on USRP which inter-operates with IEEE 802.15.4 radios was implemented as described in [102]. We repeated all our experiments to collect at least 2500 or more packets in each experiment for the analysis.

Some of our nodes supported USB power and the other nodes required batteries for the experiments. For the battery powered nodes, we ensured that the batteries do not cause any problems by regularly checking the voltage levels before and after

the experiments in order to confirm the validity of the measurements. Furthermore, before each experiment, we ascertained that we used a channel in which there was no external interference from nearby WiFi or Bluetooth devices. No microwave appliances were nearby as well.

To achieve tightly controlled conditions, we used a power combiner from Mini Circuits [114] that supports frequencies of 2 to 6 GHz. The power combiner is a passive device that adds each signal *singularly* from connected ports of the device. The vector sum of the signals will appear as a single output with an insertion loss of 6 dB. The RF cables will shield any external interference and RF propagation effects. The power combiner provides the channel model with all senders sharing a single collision channel, and outputs a scaled superposition of all signals.

For the experiments in this setup, we found that when the initiator (shown in the figure) blasts a high-power beacon, it is captured by the concurrent transmitters because of the high transmission power. This helped us to simplify the setup and work with the nodes without any change. The transmissions from the concurrent transmitters would go through the RF cables as shown in Figure 5.2.

5.5. EXPERIMENTS AND OBSERVATIONS

Four sets of experiments are designed to analyze CI and CE:

1. The first set of experiments studies power capture when the transmissions are completely synchronized.

2. The second set of experiments studies the CI phenomenon.

3. The third set of experiments studies the packet capture in the presence of time offsets.

4. The final set of experiments studies how symbols are decoded in the radio.

In all these experiments, the nodes are synchronized to have temporal offset less than $0.5\mu s$ unless otherwise mentioned. We describe the experiments followed by key observations from them. We mainly look at two metrics: packet reception ratio (PRR) and symbol error rate (SER).

Experiments on power capture: The first four experiments are designed to study the effect of power capture.

   Exp. 1. In this experiment, we considered two concurrent transmitters nodes (say node A and node B) transmitting at the same power level (-10 dBm). The nodes send different data (no symbols in common) and are completely synchronized to cause 'perfect' collisions.

   Exp. 2. This experiment is similar to the previous one, except that node B transmits at -8 dBm, i.e., 2 dBm higher than node A.

   Exp. 3. This experiment is similar to the previous one but now the power difference between nodes A and B is set to 4 dBm.

   Exp. 4. A modification is done to Exp. 3., wherein a third node (node C) is introduced with different data (again no symbols in common with the other transmitters).
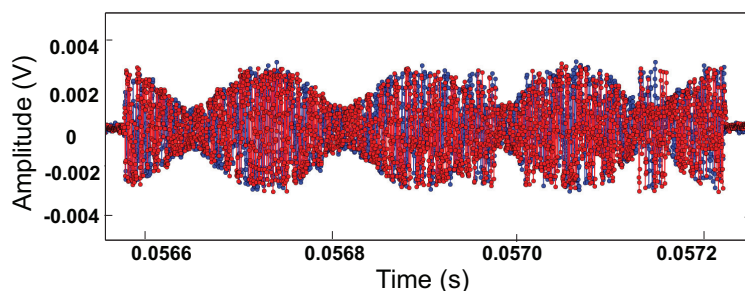
Figure 5.3: Amplitude of perfect collision when nodes send different data at the same power level. The red and blue signals indicate the I- and Q-components of the received signal.

Experiments	Node A	Node B	Node C
Exp. 1	32.40	16.60	NA
Exp. 2	0.96	73.95	NA
Exp. 3	0.05	88.87	NA
Exp. 4	88.82	0.00	0.00

Table 5.1: Bytes received in percentage from different nodes in Exp. 1-4. The percentage of bytes unaccounted in each experiment implies that the bytes did not belong to transmitted bytes by any of the nodes.

Nodes B and C have the same power levels (-10 dBm) while node A is set to -6 dBm. This modification allows us to see if power capture always occurs.

Observations. Table 5.1 shows the percentage of bytes correctly received at the receiver sent from the nodes despite collisions. Figure 5.4(a) shows the symbol error rate (SER) for these experiments. Symbol error rate (SER) corresponds to the ratio of the number of decoded symbols that were not corresponding to any of the transmitted symbols to the total number of symbols transmitted by all the nodes.

As expected, Exp. 1 has the most losses as well as high SER since the transmissions powers were the same but with different data (perfect collisions). Figure 5.3 shows the resultant signal as captured by the USRP. An interesting aspect about the result of this experiment is that some of the symbols were recognized to be one of the transmitted symbols by either of the nodes. This could be attributed to pure chance that when the signals added up resulted in one of the transmitted symbols or that radio clock drifts helped in this cause (see Chapter 4).

Exp. 2 and 3 show that power capture occurs with higher power difference aiding the decodability of the higher power signal. Therefore, the SER also decreases as the power difference increases. In Exp. 4, although there was more 'noise' created by nodes B and C, we see that the transmission power of node A was high enough leading to power capture. Figure 5.5 shows the PRR for power capture (nodes transmitting
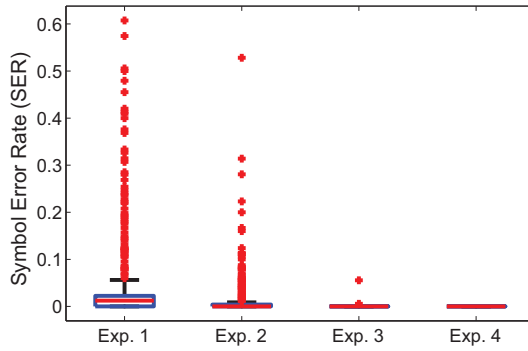
(a) SER for Exp. 1-4
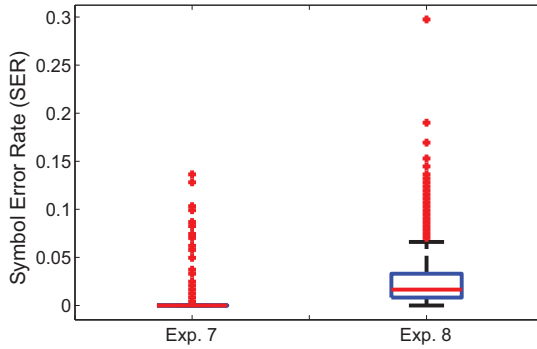
(b) SER for Exp. 7-8
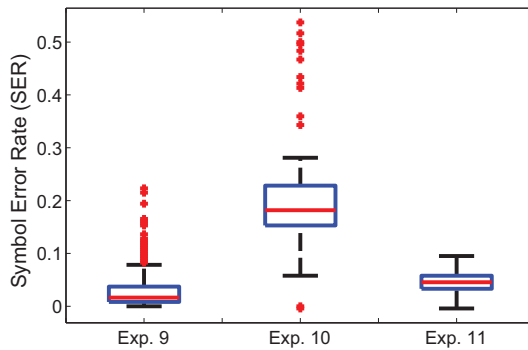
(c) SER for Exp. 9-11

Figure 5.4: Symbol error rates (SER) obtained from different experiments.
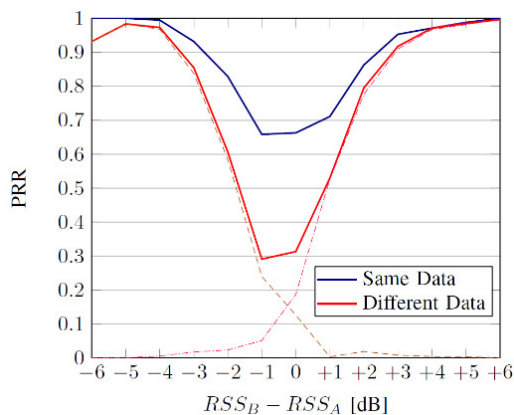
Figure 5.5: Concurrent transmissions by two nodes with varying transmission powers [112].
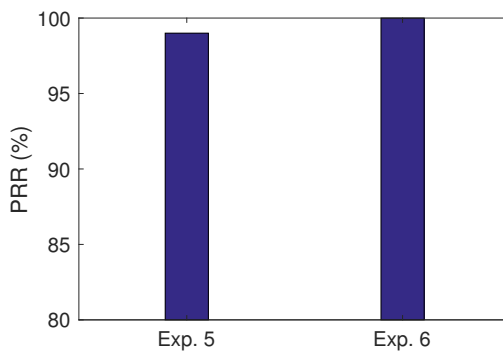
Figure 5.6: Packet reception ratio (PRR) for Exp. 5 and 6.

5

different data) for varying transmission powers based on the experiments by König et al. [112]. At a power difference of 4 dBm, they achieve PRR of around 95%. However, getting one signal to completely dominate the other can be done only when the power difference is very large. Based on these results, we arrive at the following inference.

Inference 1: Power capture occurs when one of the signals is much stronger than the other concurrently transmitted signals.

Experiments on Constructive Interference: The next set of experiments replicate the CI phenomenon as described by Ferrari et al. [90].

Exp. 5. In this experiment, nodes A and B send the same payload with equal power levels of -10 dBm. This experiment allows to see if CI occurs with two nodes.

Exp. 6. Here, node C is added to the setup with the same power level and the same payload. This experiment allows to see if CI occurs with three nodes and if there is any boost in received power due to the newly added node.

Observations. In both the experiments, all data was successfully received with al-

(a) PSD for Exp. 5
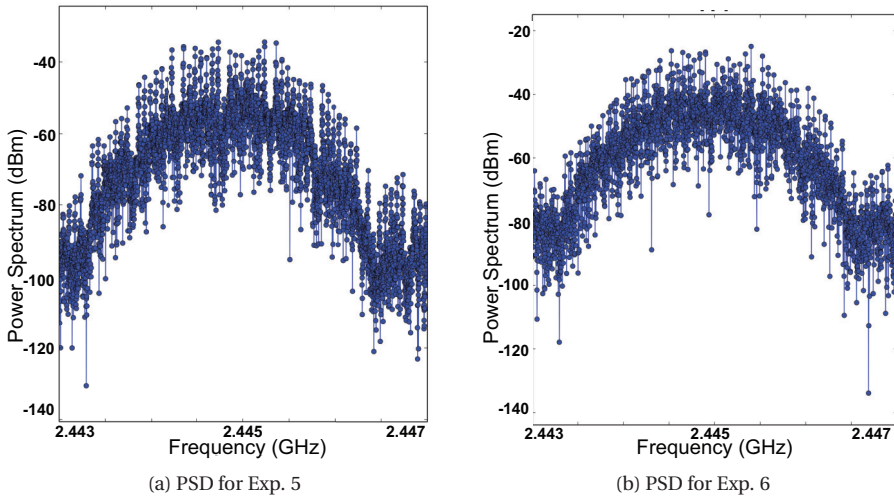
(b) PSD for Exp. 6

Figure 5.7: Power Spectral Density (PSD) for Exp. 5 and 6 as captured by the USRP. When a new concurrent transmitter is added in Exp. 6, we see approximately a 3 dBm improvement due to CI.
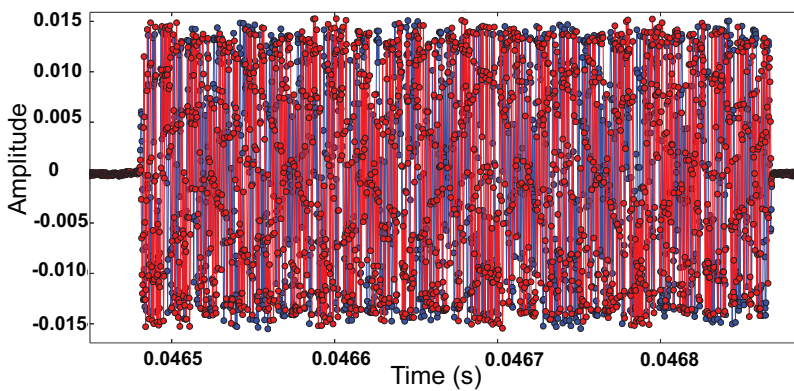
Figure 5.8: A successfully decoded packet under CI.
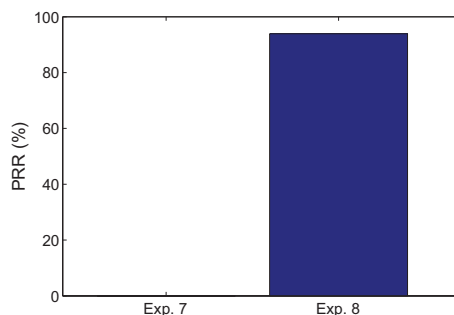
Figure 5.9: PRR for Exp. 7 and 8.

most no packet losses. This is shown in Figure 5.6, which present the packet reception ratio (PRR) for both the experiments. Since these are almost ideal conditions, the addition of one or more concurrent transmitter will boost the resultant power by 3 dBm. This is shown in the power spectral density obtained from the USRP in Figure 5.7. A time domain snapshot of the successful packet reception via USRP is shown in Figure 5.8. It can be seen that the amplitude of the decoded signal is significantly higher than the collided packet (Figure 5.3). Based on these results, and the results from the previous chapter and König et al.'s experiments (see Figure 5.5), we infer that CI works in practice.

Experiments on packet capture with delay: The next set of experiments are designed to study the effect of time offset between signals for delay capture. Instead of doing a tightly time-spaced experiments as in [110, 111], we chose two extreme cases.

Exp. 7. In this experiment, node A and B send the same payload at -10 dBm but are misaligned. The signals are separated by a few hundred nanoseconds with a phase offset close to π. This experiment allows to see if the receiver locks onto one of the signals to decode.

Exp. 8. In this experiment, node A and B send different payloads at -10 dBm but are time offset by a few μs (around 5 μs). Node A's transmissions were delayed. This experiment allows to see if packet capture occurs, and which one is preferred as both nodes transmit with the same power.

Observations. Exp. 7 resulted in severe packet losses (shown in Figure 5.9). In fact even incorrect symbols were not being decoded. This implies that the preamble itself was corrupted/not decoded. However, when different signals are separated by relatively large delays within the preamble time, packets are successfully received in Exp. 8. Of the decoded packets in Exp. 8, 18% of the packets were from node A and 72% from node B. The corresponding SERs for these experiments are shown in Figure 5.4(b).

From Exp. 8, we know that if two signals are transmitted with equal power but transmitted with a temporal offset, then the first arriving signal is most likely to be decoded. This may be said to occur due to 'locking' to the first signal. However, from Exp. 7, we see that the first arriving signal was not 'locked' onto by the receiver and not decoded. If CI were to be based on capture, then the first signal must have been

Experiments	Marker	0xFF	0x33
Exp. 9	53.00	7.87	12.14
Exp. 10	47.2	0.69	0.07
Exp. 11	40.52	9.39	9.41

Table 5.2: Percentage of marker (0x77), 0xFF and 0x33 bytes decoded from Exp. 9-11.

decoded. We draw the following inference based on this:

   Inference 2: CI is not due to packet capture.

Experiments on symbol decoding: The final set of experiments are designed to understand how symbols get decoded in the IEEE 802.15.4 radio receivers.

   Exp. 9. We set node A to send a payload of 121 B in which the odd-indexed bytes are 0x77 and the even-indexed bytes are 0xFF. Similarly, node B has a payload of 0x77 and 0x33 filled in odd- and even-indexed bytes respectively[1]. 0x77 acts as the 'marker' byte. Nodes A and B transmit at -10 dBm. This experiment should confirm if the signals are synchronized then the marker should be decoded almost always.

   Exp. 10. This experiment is similar to the previous one, except that node A is made to transmit at slightly higher power level i.e., -8 dBm. Node C is added which transmits the same payload as node B but at -16 dBm. This experiment gives node A approximately 1 dBm power advantage over the other two senders. While this is not significant, there is a non-negligible chance of power capture to occur (see Figure 5.5).

   Exp. 11. This experiment is similar to Exp. 9, except that node C is added to transmit at -16 dBm. Node C boosts the power of the signal of node A and node B alternatively. That is, the even-indexed bytes of the payload alternates between 0xFF and 0x33. This experiment allows use to get an insight on the influence of power over decoding individual symbols.

   Observations. This set of experiments indicate what exactly happens in the case of power capture when there are high interference spikes. Furthermore, these experiments demonstrate the tight synchronization achieved if we are able to decode the marker bytes.

   Table 5.2 shows the percentage of bytes decoded successfully in these experiments. Indeed many marker bytes were decoded (transmitted markers were 50%). Due to the same power levels in Exp. 9, there is no chance of decoding the complete packets successfully.

   In Exp. 10, although power levels on the node A's payload is higher, they were not decoded. Most of the decoded bytes were just markers. In Exp. 11, the markers and the bytes that had more power were received more often successfully. Figure 5.10 shows the PRR and Figure 5.4(c) shows the corresponding SER for these experiments. The PRR is quite low as expected for all three experiments.

   Inference 3: In case of concurrent transmissions and overlapping symbols, the symbols that have higher power get decoded successfully.

---

[1]The data to be filled were chosen randomly.
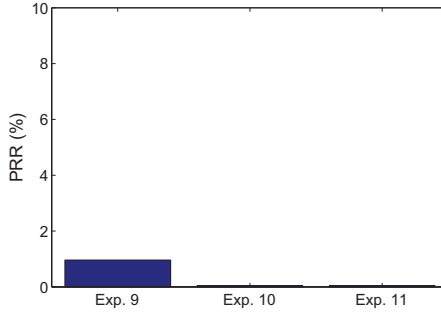
Figure 5.10: PRR for Exp. 9-11.

5.6. DISCUSSIONS

5.6.1. ON CONSTRUCTIVE INTERFERENCE

Based on the observations and inferences from our experiments, we shall try to address the claims mentioned in Section 5.3.3. Claim 1 can be split into questions: (a) is CE the underlying phenomenon for CI to occur?, and (b) given the delays and low-accuracy clocks, how can CI occur? Is it just NDI?

The first question is answered by Inference 2 (based on Exp. 7 and 8) that CI is not due to packet capture. While more experimentation is required here, we substantiate this conclusion with theory. Based on our understanding of CI as presented in the previous chapter, let $S_r(t) = \sum_{i=1}^{K} A_i \cos(\omega_f t + \phi_i)$, where $S_r(t)$ is the signal received due to K concurrent transmissions, and ϕ_i is the phase of the ith signal. From the Harmonic Addition theorem, the summation is given by,

$$S_r(t) = \sum_{i=1}^{K} A_i \cos(\omega_f t + \phi_i) = B \cos(\omega_f t + \hat{\phi}), \tag{5.1}$$

where,

$$B^2 = \sum_{i=1}^{K} A_i^2 + 2 \sum_{i=1}^{K} \sum_{j>i}^{K} A_i A_j \cos(\phi_i - \phi_j), \tag{5.2}$$

$$\text{and } \hat{\phi} = \arctan \frac{\sum_{i=1}^{K} A_i \sin \phi_i}{\sum_{i=1}^{K} A_i \cos \phi_i}. \tag{5.3}$$

Here B is the amplitude of the resultant signal and $\hat{\phi}$ is the phase of the resultant signal.

From the premise of these equations, we know that the signals add up at the receiver. This implies that it is not just one concurrent transmission that the receiver latches onto, but the receiver receives the sum of all the transmissions.

This leads us to the second question. Several solutions have been proposed to tackle the presence of clock drifts, propagation delays and radio processing delays [92, 112, 94]. These increase the chances of temporal offset being less than 0.5μs.

Another important reasons for the working of CI despite has been attributed to the robustness of Direct Sequence Spread Spectrum (DSSS) modulation to errors in
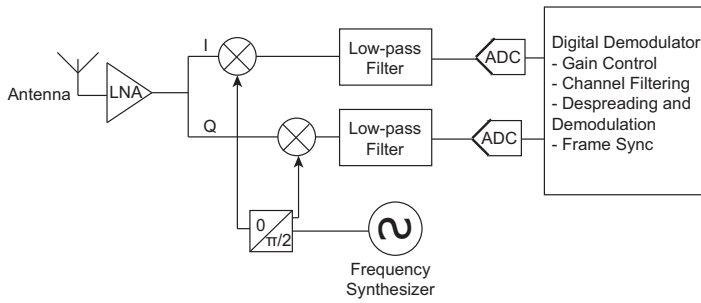
Figure 5.11: A simplified IEEE 802.15.4 receiver block diagram [74].

the IEEE 802.15.4 radios [90]. In this modulation, every 4 bits is spread with a 32-bit pseudo-random noise (PN) (or chip) sequence. The spread signal is then modulated onto the carrier. The PN sequences add redundancy as each 4 bits of the actual data are mapped to 32-bit chip sequences. Each PN sequence is constructed by a procedure to minimize its similarity to the other 15 sequences. This is done using cyclic shifts and conjugation of chips. At the receiver, the carrier is demodulated to a baseband signal with chips, which is de-spread to obtain symbols. Radios make soft decision for each chip, i.e., the received PN sequence may contain non-binary values between 0 and 1. Then this sequence is matched to one of the 16 PN sequences that has the highest correlation using hard decision. In essence, the coding gain of DSSS helps recover from small timing errors and errors caused by the channel.

The philosophical question of whether CI is non-destructive interference (NDI) remains to be answered. It is important to understand the difference between NDI and CI: non-destructive interference is the one where the interfering signals do not hamper the decodability of the signal if not aid it. On the other hand, CI requires that all the interfering signals aid the decodability. In ideal conditions, as in our experiments 5 and 6, we do observe that the signals interfere constructively and boost the power on the received signal. However, given the observations made in Chapter 4 in a real-world scenario, it is difficult to claim whether all the signals interfered constructively, non-destructively or some interfered constructively and some destructively but the communication was successful.

5.6.2. ON PACKET CAPTURE

Given that the signals add up at the receiver, how do we explain the capture effect where in a receiver locks onto one of the several synchronous transmissions (claim 2)?

While the observation is correct in CE that one of the transmissions is decoded successfully among several concurrent transmissions, we hypothesize that the premise of receiver locking the phase of the successfully decoded transmission is flawed.

A simplified IEEE 802.15.4 receiver block diagram is shown in Figure 5.11. Such receivers are commonly used in commercial products such as TI CC2420 [74]. In this receiver, the received RF signal is amplified by the low noise amplifier (LNA) and down-converted in quadrature (I and Q) to the intermediate frequency (IF). At IF, the complex I/Q signal is filtered and amplified, and then digitized by the analog to digital

converters (ADC). Automatic gain control (not shown in the figure), channel filtering, de-spreading and demodulation, symbol correlation, and byte synchronization are performed digitally. A phase-lock loop (PLL, not shown in the figure) is also used before the digital demodulator.

A common assumption in explaining CE is that the PLL latches onto the strongest signals among several on-going transmissions. However, the signals add up at the receiver's antenna and the PLL gets one carrier signal. The PLL then tries to recover the carrier frequency, and the signal is then passed onto the demodulator.

Based on the observations of Exp. 11 and the Equations 5.1- 5.3, we can conclude that a signal that is strong enough to influence the amplitude and the phase of the resultant signal effectively wins the channel. Therefore, there is a non-negligible chance that CE happens when a signal has just 1 dBm more power than the other signals. Also, depending on the phases, there is a non-negligible chance that the resultant is not decodable even though the stronger signal is 4 dB more powerful than the others (see Figure 5.5).

A couple of follow-up questions arise: what happens when a stronger signal arrives after the receiver has 'locked' onto (a) within preamble time, and (b) after preamble time? The arguments presented above can be extended to answer these questions. In case (a), if the stronger signal can influence the resultant signal favorably such that the receiver sees the beginning of the preamble, then the stronger signal gets decoded. If the stronger signal does not influence much, such that the errors introduced by the stronger signal on the weaker signal can be recovered due to DSSS, then the weaker signal gets decoded. If stronger signal corrupts the resultant, then this results in a collision.

Case (b) will result in a collision if the stronger signal can influence favorably or corrupts the resultant. Otherwise, the weaker signal gets decoded.

5.7. Conclusions

Concurrent transmissions is gaining huge interest in multi-hop wireless sensor networks due to their high network throughput, low latency and energy-efficiency. Capture effect (CE) and constructive interference (CI) are the two phenomena that enable successful transmissions when two or more nodes transmit simultaneously. While CI has been shown to be very effective, it has also drawn speculations if it really is CE happening in the background.

We answer this question with rigorous experimentation in real-world settings and ideal wireless conditions. We conclude that CI is not CE albeit closely related. With the experiments, we have shown every symbol is decoded independently. Through these experiments we have extended the understanding of capture effect.

While these experiments are quite helpful, they are an indirect way to infer about the phenomena. We are on the search to find a method that can conclusively differentiate CE, CI and non-destructive interference.

6

TOWARDS LOW-LATENCY AND HIGH-RELIABILITY ROUTING IN ENERGY-HARVESTING WSNS

6.1. INTRODUCTION

Many Internet of Things (IoT) applications require low latency and high reliability[1] to enable closed-loop control [115]. For example, monitoring and controlling appliances of a smart-home over the Internet require such a closed-loop control, that involves both collecting sensor data and commanding actuators. Furthermore, the traffic patterns in these applications are mainly many-to-one (data collection at sink) and one-to-many (data dissemination from sink), which are periodically executed. These must be supported by the networking protocols. Thus, low end-to-end latency, increased reliability and longer lifetime of the network are the critical parameters that determine the usability and success of the IoT deployment.

Although IoT (or sensor) devices are required to last for a long time, batteries limit the lifetime of the devices, and in turn that of the network and the applications. As described in Chapter 1, we tap into the harvesting opportunities in the ambiance while making the nodes self-sustained with respect to energy. Also, we look to eliminate batteries completely and replace them with more sustainable energy storage buffers such as supercapacitors. Furthermore, merely replacing the batteries with energy harvesters is insufficient due to the variations in energy harvested spatially and temporally. An example network with nodes having varying energy-levels and a dynamic topology is shown in Figure 6.1.

Given the stochastic nature of energy arrivals, existing networking protocols for energy-harvesting WSNs target only reliable packet delivery [116, 117, 118] by adapting to the variations in energy rather than ensuring low latency. Though these protocols are useful for some applications, they do not offer the solution that was sought with ambient energy-harvesting techniques - longer (or perpetual) lifetimes with performance similar to the battery-powered WSN protocols. Since harvested energy is

---

[1]We define reliability as Packet Reception Ratio (PRR), which is the percentage of packets that are successfully received at the destination.
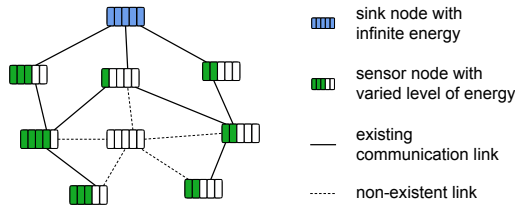
Figure 6.1: Varying energy-levels and dynamic topology in energy-harvesting WSN.
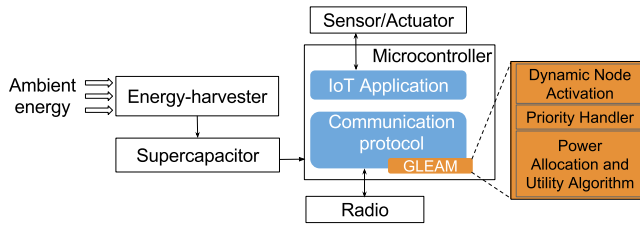
Figure 6.2: The GLEAM power-management module for an energy-harvesting node.

usually less,energy has to be expended judiciously reducing or even avoiding network related overheads, e.g., discovery and routing.

Challenges. A significant number of challenges lie in making the energy variations transparent to the higher layers in energy-harvesting WSNs. Specifically, (a) low harvesting energy and finite energy buffers make it difficult to keep the nodes active periodically; and (b) varying amounts of harvested power makes the network topology dynamic. Therefore, the discovered routes become stale quickly. Furthermore, the unreliability in the wireless channel aggravates the burden on the available energy. Consequently, energy-harvesting in these devices necessitates a redesign of algorithms, and networking protocols to achieve close to perpetual operations while satisfying the application requirements. The most plausible conclusion from the current literature is that the energy-harvesting WSNs cannot support low latency operations, at least to a reasonably satisfiable extent. Thus, the ambition is to avoid overheads, achieve low latency and high reliability under challenging conditions, i.e., low energy-harvesting conditions.

Approach. Instead of adding a new protocol to the already existing plethora of networking protocols for WSNs, we propose an energy-management module called GLEAM to offer low latency and high reliability in energy-harvesting WSNs. To prove our point, we use Low-power Wireless Bus (LWB) [99] as the *de facto* routing protocol and develop GLEAM around it. LWB offers guaranteed latency and high energy-efficiency without any topological information. While high reliability is also guaranteed by LWB in battery-powered WSNs, it remains a non-trivial challenge in energy-harvesting WSNs as nodes do not have sufficient energy as required by LWB. In particular, in low energy harvesting campaigns, nodes need to be intelligent to use the available energy wisely.

The crux of GLEAM is to achieve better reliability through efficient energy-management strategies. Figure 6.2 shows the GLEAM module and its components. GLEAM maxi-

mizes the energy utilization by

- allocating an optimal amount of energy to spend in every data transmission slot,

- spending energy on the most important slots,

- saving energy by reducing transmission power as and when possible, and

- utilizing the redundant nodes deployed in the network efficiently.

Specifically, our contributions are as follows:

- To the best of our knowledge, this is the first work that attempts to provide guarantees on latency and improves reliability considerably in energy-harvesting WSNs that are completely powered by ambient energy sources. This practically important aspect is novel and has not yet received its due attention. To this end, we propose a distributed, energy-management module called GLEAM.

- We formalize the energy allocation problem as a Markovian decision problem and we propose a policy. We prove that this policy is indeed a threshold policy, therefore optimal.

- We propose a set of protocol optimization in GLEAM to make better use of the available energy.

- We outline a method to calculate the critical density required in order to achieve performance similar to battery-powered WSNs using stochastic random geometric graphs.

We evaluate the performance of GLEAM on Indriya and FlockLab, two real-world testbeds with CC2420 radios [83, 84] considering different scenarios with varying number of nodes and different data collection intervals. We show that in one of the worst case scenarios – where harvested energy rate is as low as $50\mu J/s$ with 20 nodes in the network with transmission of $100\,B$ every $30\,s$ – we even get an improvement of 2.5 times higher packet reception ratio, with $6\,mJ$ higher remaining energy on the average compared to the LWB based greedy algorithm.

The organization of this chapter is as follows. We provide an overview and benefits of LWB along with its limitations for energy-harvesting WSN in Section 6.2. Section 6.3 provides an overview of GLEAM. Then, we state the energy allocation problem, formulate it as a Markov Decision Process (MDP), compute the optimal policy, and prove its optimality in Section 6.4. Further, we describe the GLEAM module, energy utilization algorithms, and the protocol optimization to improve reliability in Section 6.5. Section 6.6 evaluates and discusses the performance of GLEAM. We present the density estimation overview also in Section 6.6. We present the related work in Section 6.7 before concluding the chapter in Section 6.8.

6.2. Overview of Low-power Wireless Bus (LWB)

To achieve highly reliable data transmission with least overheads, we use LWB to start with as an implementation tool. LWB uses Glossy [90] for tight time-synchronization

(a) Communication rounds in LWB.   (b) Communication slots within a round.
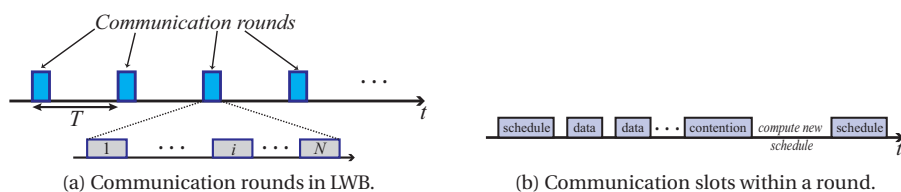
Figure 6.3: Time-triggered operation of LWB.

and flooding its packets across the network. We first provide a brief overview of Glossy and then proceed to describe LWB. We refer the reader to [99, 90] for complete details.

GLOSSY

When two nodes transmit the same packet simultaneously on the same frequency band to a receiver within their transmission ranges, the transmitted signals superpose leading to constructive interference (CI) at the receiver. CI can aid in increasing the decodability of the packet due to increased energy per symbol at the receiver. The tolerable temporal displacement between concurrent transmissions for IEEE 802.15.4 in 2.4 GHz is 0.5 μs. Glossy uses CI for flooding and implicitly provides time-synchronization. In Glossy, nodes turn on their radios, listen for packets on the wireless medium, and relay the received packets immediately after receiving them. Since all the potential receivers receive a packet at the same time, they also start to relay the packet at the same time. This again triggers other nodes in the next hop to receive and relay the packet. In this way, Glossy benefits from concurrent transmissions and quickly propagates a packet from a source node (initiator) to all other nodes (receivers) in the network as a ripple. Every packet is transmitted η times (the default value is five), in order to ensure high reliability. Note that all events are initiated by radio events. Since the medium contention is eliminated, Glossy achieves very low-latency flooding, and nodes are synchronized in the process.

6.2.1. LOW-POWER WIRELESS BUS (LWB)

LWB uses Glossy fast-flooding primitive to deliver data. Since the packet is flooded through out the network, it eventually reaches the destination(s). In order to avoid different packet insert from different source nodes within the same flood, LWB uses a centralized scheduler. It assigns a unique slot to every data source within a communication round, and only the slot owner initiates a flooding in that slot. Communication rounds are periodically scheduled, which is shown in Figure 6.3(a). Since every packet is flooded, LWB does not require any topological information. A superframe in LWB is shown in Figure 6.3(b). Nodes requiring a slot will use the contention access period to send in their requests. The scheduler, usually on the sink, will compute a new schedule and disseminate it at the beginning of the superframes. The analogy here is similar to a bus, wherein one node (initiator) puts the data on the bus that can be read by all other nodes. All nodes participate in all the floods to exploit CI.
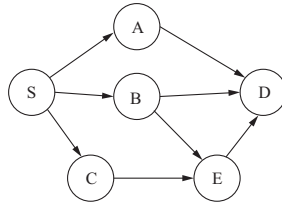
Figure 6.4: An examle of reducing forwarders. The nodes A and B are sufficient for sending between the nodes S and D.

Hop count	1	2	3	4	5
Delay (ms)	6	9	12	15	18

Table 6.1: Latency obtained over different hop counts.

EXISTING OPTIMIZATIONS FOR LWB

Several optimization schemes are proposed for LWB to reduce energy consumption. The important ones are listed below.

Long-run conditions   During the bootstrap phase, the sink can learn about the source nodes and data periodicity. After a certain duration, the traffic pattern can stabilize. In such situations, LWB minimizes the overheads by increasing the round-trip time without violating the maximum latency that can be tolerated.

Forwarder Selection   Carlson et al. [101] proposed a method that selects the set of forwarders falling in the shortest path between a source and destination pair in LWB. This reduces energy consumption and unnecessary flooding of packets in the entire network. A small overhead is incurred as the set is determined by flooding messages between the source and destination nodes. An example of forwarder selection is shown in Figure 6.4.

Apart from the above, minor improvements could be done, such as, nodes piggybacking their requests for additional slots in their data packets to reduce contention and the contention period during long-run conditions. These improvements, however, are *highly insufficient* on nodes powered by harvesting energy.

ADVANTAGES OF LWB

LWB has been shown to offer guarantee latency and high reliability due to the Glossy floods. The average latency values for several hops from our experiments is shown in Table 6.1. Furthermore, due to the absence of medium access contentions, the nodes have low duty-cycles leading to high energy efficiency. It has been shown that LWB outperforms *de facto* protocols such as CTP [49] and Dozer [119] for periodic data collection scenarios. Due to flooding, neighbor discovery is not required anymore making LWB work even when nodes move.
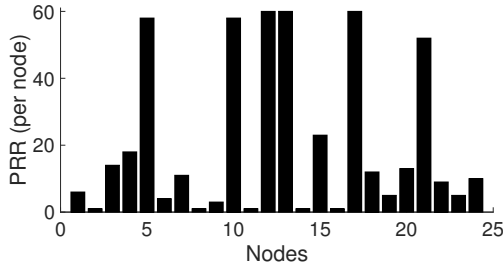
Figure 6.5: Packet Reception Ratio (PRR) per node after 60 rounds.

6.2.2. CHALLENGES FOR USING LWB IN ENERGY-HARVESTING WSNs

While LWB seems ideal, it does not work as is. We experimented with 25 Tmote Sky nodes wherein each node harvested energy in 'packets' (of $50\,\mu$J) according to uniform distribution. The storage buffer could store up to a maximum of $180\,$mJ. We measure the reliability through packet reception ratio (PRR), which is defined as the ratio between the number of packets that are successfully received at the sink and the number of packets transmitted. Figure 6.5 shows the PRR for a periodic collection of every $60\,$s from every node after 60 rounds. It is evident that the performance is not acceptable barring a few nodes. The reasons for such a performance is due to spending energy unwisely. Further,

- Not enough energy on the nodes to participate in all the slots, sometimes for its own data transmission slot.

- Each packet is sent five (η) times in order to overcome the unreliable wireless channel, which leads to draining the energy faster.

- Unequal energy-harvesting opportunities leading to some nodes having good performance and many others not.

Therefore, we propose GLEAM to manage energy wisely in energy-harvesting WSNs. In the next section, we present an overview of the GLEAM module, its design, and operation.

6.3. THE GLEAM MODULE

The goal of GLEAM is to make better use of the harvested energy in a distributed manner. That is, each node has to make its own decision on spending energy in slots and collectively achieve a high reliability in data collection and dissemination from sources to a destination. GLEAM has three major components, namely, dynamic node activation, priority handler, and energy allocation and utility (shown in Figure 6.2). Please note GLEAM is fine tuned for LWB but can be easily extended to any slot-based communication protocol.

Figure 6.6 shows the flowchart of GLEAM. At the beginning of a communication round, the node wakes up and determines if it needs to be active in this slot. This is pertinent to the nodes deployed as redundant nodes to ensure connectivity when the energy-harvesting possibility is low. The source nodes, however, will choose to
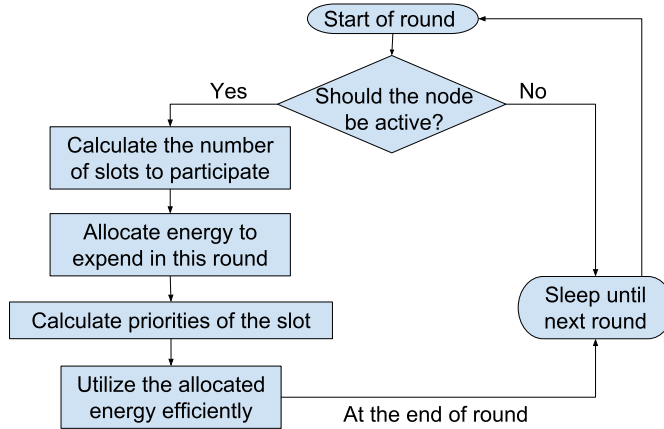
Figure 6.6: Working of the GLEAM energy-management module.

be active as long as they have sufficient energy in their buffer. Nodes choosing to be inactive go to sleep until the next round. This is further described in Section 6.5.

The next step for the active nodes is to note down the slots to participate from the LWB schedule. After that, the energy allocation module has two questions to address: *how much energy to expend in the current round?* and *how to utilize this energy efficiently?* GLEAM looks at maximizing the node's utility over an infinite horizon. The former question is addressed in Section 6.4 wherein an optimal allocation policy is proposed. For the latter question, we tweak LWB to provide feedback from the sink, and use it to prioritize the slots using the priority handler. Then, the allocated energy is used in as many slots as possible starting from the highest priority ones. A protocol optimization is proposed here: instead of transmitting all the packets at the highest transmission power, the node will reduce its transmission power if packets are being delivered successfully. The advantages are that energy is being better used and the performance of the underlying CI phenomenon is improved (see Section 6.5). With all these components and protocol optimization, the nodes utilize the available energy with higher efficiency as will be shown in Section 6.6. In the next section, we formalize the power allocation problem and provide an optimal policy for the same.

6.4. OPTIMAL ENERGY ALLOCATION

In this work, we consider LWB with forwarder selection since it is already an improved version of LWB. Henceforth, when we refer to a node that should participate in a slot implies that the slot is either one of the forwarder selected or its own slot. While the slot schedules are distributed from the sink, each node will have to manage its energy expenditure on its own. Every node must adopt an energy-aware policy to balance the available energy for expenditure in the future and in the current slot. To this extent, two fundamental questions need to be answered:

1. How much energy should be expended in the current time period? and

2. How to utilize this allocated energy maximally?
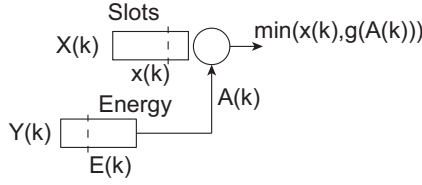
Figure 6.7: The MDP model.

Intuitively, if a node aggressively participates in all its forwarder selected slots, the energy gets depleted soon. On the other hand, if the node is too conservative, then the PRR is low because of its non-cooperation within the network.

In this section, we address the first question. To this end, we propose to use Markov Decision Process (MDP) with which we develop distributed policies. Though there have been several works that propose to use MDP for determining the optimal transmission policies per packet [120, 121, 122], we differ from these works in the following aspects: (i) we cannot 'queue' slots for the future as in some of those models and (ii) we do not decide to transmit in a particular slot but rather allocate energy for the whole communication round.

6.4.1. System Model

We consider an energy-harvesting WSN network consisting of N nodes with omni-directional antennas. Every node u in the network has a unique identifier, denoted as $id(u)$. Here, we focus on a single sensor node, and a communication round k. We consider that the harvested energy between k and $k+1$ follows an *i.i.d.* represented by $Y(k)$. For instance, a Markov chain model for the solar source is presented in [28]. Each node has a supercapacitor as a storage buffer as its remaining energy can be estimated by $E \approx \frac{1}{2}CV^2$, where C is the capacitance of the supercapacitor and V is the voltage.

We assume that the slot arrival process, $X(k)$, also follows *i.i.d.* Let the number of slots to be allocated in the kth round be $x(k)$. A decision must be taken as to how many of these slots will be allocated energy. The remaining slots will be discarded. We model the energy buffer by quantizing it into states $\varepsilon = \{E_0, E_1, \ldots E_{max}\}$. Each state holds energy enough for one slot with maximum transmission power (including transmitting for η times). We assume that all the packets transmitted are of equal size. The energy for round $k+1$ can be computed as,

$$E(k+1) = \min\{E(k) - A(k) + Y(k), E_{max}\}, \tag{6.1}$$

where $A(k)$ is the energy allocated in k. We assume that the energy buffer is much bigger than the average amount of energy harvested. If the buffer is smaller, then the use of an energy buffer is limited. Our model can be represented as shown in Figure 6.7.

We consider a concave, monotonically non-decreasing function, g with $g(A(k))$ indicating the number of slots allocated if $A(k)$ amount of energy is used.

6.4.2. OPTIMIZATION PROBLEM AND OPTIMAL POLICY

Given a state $\{E(k)\} \in S$, value $\{v(k)\} \in \mathbb{R}^+$, a policy π implemented by the node is defined by the probability $\pi(\varepsilon, v)$ of selecting $x(k)$ slots in the communication round k. The optimization problem can be stated as follows: determine the optimal policy π_* such that

$$\pi_*(s) = \arg\max_{\pi} V^\pi(s_0), \tag{6.2}$$

where s_0 is the initial state. The corresponding Bellman's equation [123] is,

$$V^\pi(s) = \max_{\pi} \left\{ V^\pi(s, a) + \sum_{l \in S} Pr(l|s, a) V^{\pi_*}(l) \right\}. \tag{6.3}$$

Here, $Pr(\cdot|s, a)$ represent the conditional probability, and a is the action taken in the corresponding state.

Optimal policy. We begin with the necessary condition for designing an optimal policy.

Lemma 3. *Given g, a concave function and the Markov chain with the state space S is stationary and ergodic, for $\{A(k)\}$ to be asymptotically stationary, a policy that makes $\{x(k)\}$ asymptotically stationary with a stationary distribution π, it is necessary that $\mathbb{E}[X] < \mathbb{E}_\pi[g(A)] \leq g(\mathbb{E}[Y])$.*

Proof. Let the start state be $s_0 = E_0 = 0$. Here $\mathbb{E}[\cdot]$ is the expectation operator. Then for each j, $1/j\Sigma_{k=1}^{j} A(k) \leq 1/j\Sigma_{k=1}^{j} Y(k) + \frac{Y_0}{j}$. The first term, $1/j\Sigma_{k=1}^{j} A(k)$ is $\mathbb{E}[A]$ almost surely (a.s.) as $j \to \infty$ and the second term, $1/j\Sigma_{k=1}^{j} Y(k) + \frac{Y_0}{j}$ is $\mathbb{E}[Y]$. Similarly, $1/j\Sigma_{k=1}^{j} g(A_k) \to \mathbb{E}[g(A)]$ a.s.

It has been shown that $\mathbb{E}[g(A)] > \mathbb{E}[X]$ is needed for the stationarity of $x(k)$ [124]. Since g is concave, we need $\mathbb{E}[X] < \mathbb{E}[g(A)] \leq g(\mathbb{E}[A]) \leq g(\mathbb{E}[Y])$. Thus, $\mathbb{E}[X] < g(\mathbb{E}[Y])$ is a necessary condition to get the desired stationary sequence. $\square$

We present a policy that satisfies this condition. Let

$$A(k) = min(E(k), \mathbb{E}[Y] - \epsilon), \tag{6.4}$$

where ϵ is a small positive constant with $\mathbb{E}[X] < g(\mathbb{E}[Y] - \epsilon)$. We show in Theorem 1 that it is indeed a throughput optimal policy by showing that a stationary (or a threshold vector) does exist as this satisfies the conditions in Lemma 3.

Theorem 1. *The policy given in Equation 6.4 has a unique, stationary, ergodic distribution, and therefore optimal.*

Proof. For any arbitrarily small $\epsilon > 0$, $E(k) \to E_{max}$ a.s. from Equation 6.4 and $A(k) \to \mathbb{E}[Y] - \epsilon$ a.s. Since g is monotonic, we get $g(A(k)) \to g(\mathbb{E}[Y] - \epsilon)$ a.s. Thus, $\{g(A(k))\}$ is asymptotically stationary and ergodic. For the policy $A(k) = min(E(k), \mathbb{E}[Y] - \epsilon)$, $\mathbb{E}[X] < g(\mathbb{E}[Y] - \epsilon)$ is a sufficient condition for $\{x(k)\}$ to be asymptotically stationary and ergodic whenever $\{X(k)\}$ is stationary and ergodic [124]. $\square$

Intuition: The policy indicates that all slots be allocated if the average energy is higher than the required energy. In case, the required energy becomes more, then
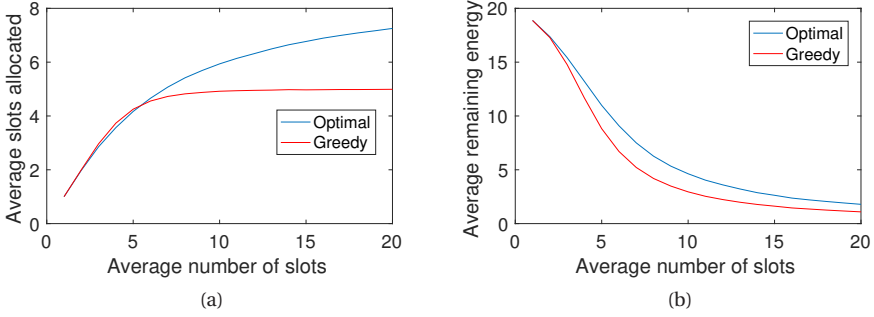
Figure 6.8: (a) Average number of slots allocated for a varying average number of slots arrivals. (b) Average remaining energy for a varying average number of slot arrivals.

only the average amount of energy harvested will be spent. Therefore, the number of slots that are allocated will be $g(\mathbb{E}[Y] - \epsilon)$. This leads to cautious spending of energy when energy is low. This ϵ may represent the minimum energy required to at least send data in its own slot. With this adaptive energy expenditure policy, all the nodes will try to be active as much as possible in the infinite horizon.

6.4.3. NUMERICAL EVALUATION

We evaluate the optimal policy by comparing it with a greedy policy as given in Equation 6.5. The greedy policy attempts to allocate energy for participating in the maximum number of slots possible with the available energy. We evaluate the policies through numerical simulations.

$$A(k) = min(x(k), E(k)). \tag{6.5}$$

We consider g to be linear ($g(x) = x$), which is monotonically non-decreasing. Furthermore, $X(k)$ (slot arrival process) and $Y(k)$ (energy arrival process) are *i.i.d.* with exponential and uniform processes, respectively. We choose the uniform distribution as it models an indoor ambient light harvesting source [125]. Without the loss of generality, we set one unit of energy to participate in a slot. Lastly, we set $\mathbb{E}[Y] = 5$ with the maximum energy storage size of 20 units, and $\mathbb{E}[X]$ is varied from 1 to 20.

Figure 6.8 shows the results for two metrics: average number of slots allocated and average remaining energy in the node. Figure 6.8(a) shows that the node can participate in more slots by using the optimal energy allocation than the greedy policy. The reasoning is simple and obvious: while the greedy policy tries to participate in as many slots as possible at the cost of energy exhaustion, the optimal policy is energy aware and adapts its expenditure according to the energy being harvested. This increases the utility of the node in the infinite horizon. Figure 6.8(b) shows that both the policies spend almost the same amount of energy to participate in a slot, while optimal policy makes better use of the energy.

6.5. ENERGY UTILIZATION

While we saw that the optimal policy outperformed the greedy policy, we notice that only 7 out of 20 slots were assigned to transmit data. This is due to the amount of energy harvested being quite low compared to the consumption rate. In order to handle such situations, we propose several solutions. The way GLEAM executes these solutions is shown in the flowchart in Figure 6.6.

Dynamic Node Activation. Since the available energy on the nodes is quite low, a commonly adopted solution is to deploy redundant nodes [62]. This is particularly helpful when there are no secondary power sources such as batteries. We assume that deploying redundant nodes is possible. This plays an important role as shall be demonstrated in Section 6.6.

However, the purpose is not served if all the nodes, including the redundant nodes are always on. These helper nodes must be dynamically switched on when required. Though the authors of [62] propose policies to activate nodes, it is assumed that the redundant nodes can check the neighborhood status. Such an assumption does not hold in our scenario. Therefore, we design a simple distributed policy. A non-source node is activated according to the policy given in Equation 6.6 for a communication round k on a node i. A source node is always activated if it has a minimum amount of energy, E_{min} to at least participate in its own slot.

$$\mathcal{A}_i(k) = \begin{cases} \text{no activation} & \text{if } E(k) < E_{min} \\ \text{activate with prob. } p & \text{if } E_{min} < E(k) \leq E_{th} \\ \text{activate with prob. } 1 & \text{if } E(k) > E_{th} \end{cases} \quad (6.6)$$

Priority Handler. Since the nodes may not always have sufficient energy to participate even in all its forwarder selected slots, it is important to quantify the importance of slots. By defining weights, the nodes can then choose the best slots to participate. The priority handler ensures that the energy is spread across the slots and not spent on the first few slots (as in the greedy approach).

A difficulty though is that individual feedback cannot be given to the nodes. We tweak the LWB protocol to make the sink include the information on which slots data was successfully received in the previous communication round. This information, or *ACK*, is piggybacked with the following communication round's schedule. With this ACK information, the node has four cases to deal with:

- The best case is if a node participated in a slot and the packet was received. The priority must be slightly increased in this case so that the node is more likely to participate in the slot again.

- Another case is when the node participated in forwarding data in a slot but it was not received at the sink due to either failure of CI or an energy outage at another intermediate node. Here, the node cannot do much but try to participate again.

- If a node sees that ACK is received in a slot it did not participate, then the node decrements the priority since its participation is not required for successful data delivery.

- The worst case is when a slot goes unserved i.e., the node did not participate and the data did not reach the sink as well. In this case, the node assumes responsibility by increasing its priority to a higher value.

One method to calculate the weight is to take (1 - PRR) per slot. We increment or decrement priority by 10% of its value. A source node's own slot will always have the highest priority.

Energy utilization. The optimal policy only allocates the energy but does not specify how to use it. With priorities defined to the slots, the problem becomes that of allocating the energy to as many high priority slots as possible. This can be proven as the classical 0/1 knapsack problem [126], which is *NP*-complete.

Instead of using the optimal dynamic programming solution, we adopt the low-complexity greedy approximation solution for the knapsack problem. The slot assignment algorithm is shown in Algorithm 11. In order to save energy, we lower the transmission power when the transmissions happen successfully. The advantages are two fold: (a) employing different transmission powers across nodes improves the performance of CI (see Chapter 4); and (b) If enough power is saved to serve more slots, then the next higher priority slots are chosen to participate in. Algorithm 12 shows the transmission power adaptation algorithm. This algorithm is loosely based on the DIPA algorithm (Chapter 4), but we do not include the feedback bytes. Instead, we assume that if the transmitted packet is received immediately in the next reception window, then the transmission is successful. While this algorithm is not as accurate as DIPA to capture the channel, it is however of much simpler as CRC need not be decoded by the application.

Algorithm 11 Slot Allocation Algorithm.

 1: //txPower indicates the current transmit power
 2: //txTime is the time required to complete one transmission
 3: //We assume the power required for transmission and reception are equal
 4: //slotEnergy indicates the energy required to participate in a slot
 5: At the beginning of the communication round k:
 6: slotEnergy ← txPower * txTime * η * 2;
 7: $A(k)$ ← min($E(k)$, average_harvested_energy(k - slotEnergy);
 8: n_{slots} ← $A(k)$/slotEnergy;
 9: Sort the slots in descending order of their priority;
10: Schedule the first n_{slots} for participation;

6.6. EVALUATION

In order to evaluate GLEAM module, we implemented it in Contiki OS [81] for WSNs and evaluated it on the Indriya testbed [83], where the nodes are spread over three floors. The experiments were conducted on 30 Tmote Sky nodes on the first floor of the testbed.

We implemented the energy-harvesting battery model in software as in Chapter 3. We consider that each node stores the harvested energy in a supercapacitor of size E_{max} =20 mJ. We perform extensive experiments with nodes harvesting energy with

Algorithm 12 Transmit Power Adaptation Algorithm.

```
 1: Function OnReceive (Packet p)
 2: //txPower indicates the current transmit power
 3: if p.IsCRCValid () == TRUE then
 4:     Call decreaseTransmitPower ();
 5: else
 6:     if txPower == MAX_TRANSMIT_POWER then
 7:         Call randomizeTransmitPower ();
 8:     else
 9:         Call increaseTransmitPower ();
10:     end if
11: end if
```
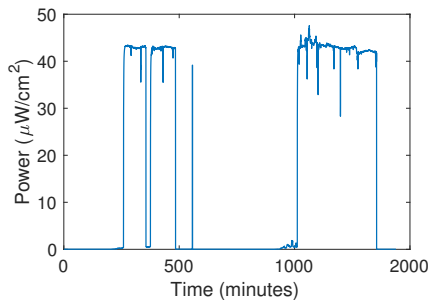

Figure 6.9: Power trace from a PV harvester powered by indoor lighting [125].

a uniform arrival process having a mean rate of $50\mu J/s$. This is the amount of energy that can be harvested from indoor lighting [125], which is shown in Figure 6.9. The dataset used in the figure is from a node kept in a bookshelf of an office. The harvested power is more or less constant except when the lights are switched off or someone walks past the harvester, in which case the harvested power drops a bit. The harvested energy is significantly less than the amount of energy spent in a communication round. For example, a 100 B packet to be sent in a LWB slot with $\eta=2$ consumes almost $900\mu J$. Furthermore, the nodes need to report their sensed data periodically; and the periodicity is application dependent. To evaluate GLEAM, we experimented with two communication round intervals of 30 s and 60 s. For each interval, packets of different length (50 B and 100 B) and different number of source nodes (10 and 20) are also experimented with. We chose these scenarios to test GLEAM for potential worst case scenarios.

While the uniform distribution may correspond to the indoor lighting source, we also consider Moser's model (described in Chapter 3) to evaluate under an outdoor solar model. The evaluation with this model is done in the FlockLab testbed with 30 Tmote Sky nodes [84]. In this testbed, we only conducted evaluation for 60 s interval with different packet lengths (50 B and 100 B) and different number of source nodes (10 and 20).

In order to compare GLEAM, we implemented LWB with greedy (simply referred

(a)

(b)
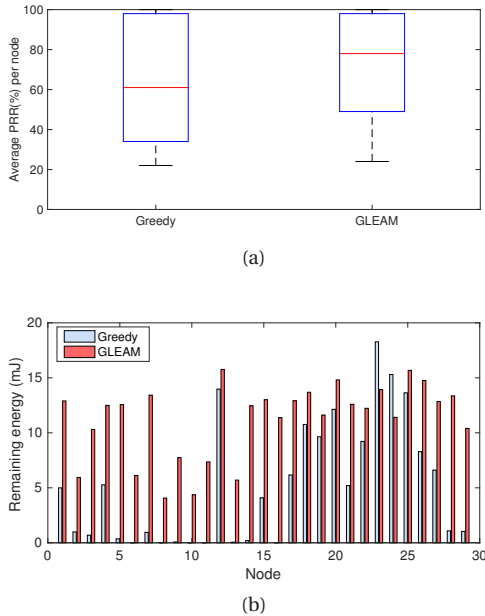
Figure 6.10: Scenario 30s, 20n and 50B: (a) Average PRR. (c) Remaining energy per node after 60 rounds.

to as *greedy*) energy allocation policy for comparison. Note that the greedy policy here also employs forwarder selection [101] and therefore participates *intelligently* in only the necessary slots. Thus the improvements we get from GLEAM are significant. Two metrics are used here: PRR and average remaining energy in the nodes to infer the lifetime indirectly.

A word on notation: In the figures, 30s and 60s indicate the corresponding period of communication rounds, 30 seconds and 60 seconds, respectively; 10n and 20n indicate 10 and 20 source nodes that periodically send data, respectively. The data size is either 50B or 100B (bytes).

At the outset, we set that all the nodes have a fully charged capacitor. If energy expenditure per round is higher than the harvested energy, the remaining energy in the capacitor starts decreasing over time. As a result, nodes cannot participate in all the slots. This impacts the PRR at the sink in the long run. Figure 6.10(a) shows the average PRR of a 20 source node network, with 30s interval. Even though it is impossible to deliver all the packets with low harvesting rate, it is clear that GLEAM improves the average PRR as opposed to the greedy LWB; in this case by at least 19%. The improvement stems from the fact that GLEAM does not start participating in all the slots from the beginning. Rather, it identifies the high priority data slots where there is scope for improving the PRR. Furthermore, as the greedy approach starts operating from the beginning of a round until the energy lasts, only the nodes transmitting data in the first few slots get delivered. This is evident in the box plot with the quartiles spanning a long range.

Figure 6.10(b) shows that the greedy approach drains almost all energy to maxi-
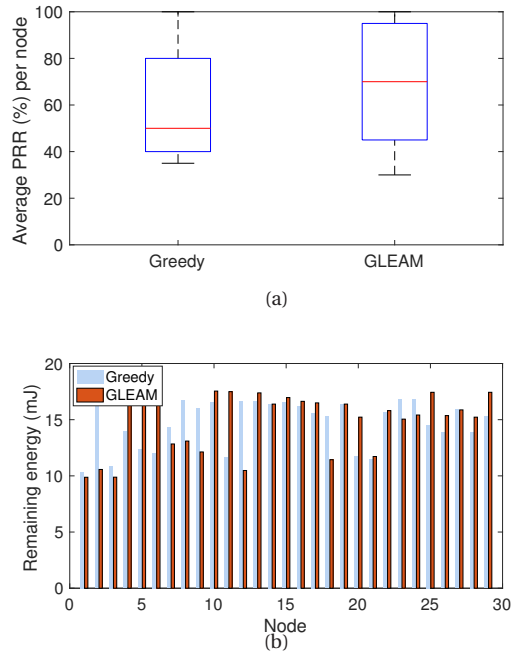
Figure 6.11: Scenario 60s, 20n and 50B with Moser's model: (a) Average PRR. (c) Remaining energy per node after 30 rounds.

mize participation in slots whereas, GLEAM is more energy-aware. Thus, even if the harvesting rate drops in the next rounds, the network can sustain for a longer time. However, this does not affect (reduce) the PRR of the network as evident from Figure 6.10(a).

Figure 6.11 shows the results from FlockLab testbed with Moser's energy arrival model. In Figure 6.11(a), we see that the average PRR from GLEAM is higher than that of the greedy LWB protocol. The median of GLEAM is around 20% higher than that of greedy LWB. Similar to uniform distribution based energy arrival model, the average residual energy in every node is slightly higher with GLEAM than with greedy LWB as shown in Figure 6.11(b).

Heavy vs. Light traffic. We compare the performance of the greedy and GLEAM for different traffic intensities with the same energy arrival profile. Figure 6.12(a) shows the PRR for data collection over 30s and 60s intervals sending 100 B of data. Evidently, with more time to harvest and lower the traffic, the performance of both algorithms improve[2]. Furthermore, the difference between the two schemes reduces with more energy in the buffer. However, a noteworthy aspect is that in the worst case, i.e., data collection period being 30 s and 20 source nodes, GLEAM shows that it can outperform greedy approach significantly. In this case, it achieves *2.5* times better than the greedy approach. This performance is due to the multifold components of

---

[2]Indeed we want to design GLEAM to deliver in hard circumstances; with more energy LWB delivers anyway.

GLEAM, particularly dynamic node activation and power adaptation. Figure 6.12(b) shows the light traffic scenario wherein 10 nodes transmit data and both the methods perform extremely well. Figure 6.12(c) shows the average amount of energy remaining on the nodes for a payload length of 100 B. We see that GLEAM keeps a buffer of more energy on the average. A big part of this is due to dynamic node activation.

Figure 6.13(a) shows the average PRR for 60 s periodic data collection for different number of source nodes and payload lengths, with Moser's enegy arrival model. Similar to the results with the uniformly distributed energy arrival model, GLEAM has higher PRR as compared to greedy LWB in all cases. Figure 6.13(b) shows results with GLEAM achieving only slightly higher energy on the average than greedy LWB in the scenario with 20 source nodes.

Payload length. The payload length also significantly influences the performance, as larger the payload, more is the required energy to transmit. Figure 6.12(a), Figure 6.12(b) and Figure 6.13(a) show the results when 50B and 100 B were sent by the source nodes for 60 s periodicity. It is again evident that more payload length has an influence on the performance. Again, GLEAM outperforms the greedy approach.

Density. Figure 6.12(a) clearly shows that higher the density of redundant nodes, better is the performance. Furthermore, due to the dynamic activation of redundant nodes, GLEAM performs better than greedy approach. This is because, not all nodes exhaust energy in all participatable slots and due to this, there is a higher chance for GLEAM to find at least one forwarder to send its packets. This needs further investigation as to how much this helps. Therefore, we conduct more experiments.

6.6.1. Importance of Redundant Nodes

GLEAM outperforms greedy due to several factors described previously. However, it still does not achieve a highly reliable data collection scheme. High energy arrivals, light traffic or a high number of redundant nodes helps in achieving reliable data collection. The first two parameters are not in our control while the last one can be controlled.

In GLEAM, the nodes with energy more than 75% of its maximum capacity, will participate in all its slots in a communication round. However, when it is below this number, the node chooses with a probability, $p = 0.5$, to participate or not. This reduces the number of redundant nodes wasting their energy unnecessarily. To evaluate the benefits, we implemented a dynamic node activation (DNA) for the greedy LWB scheme and compare them. Figure 6.14(a) shows the average PRR for different scenarios with 30 s communication round interval. We see that DNA is not helpful when there is light traffic, however, when the traffic intensity increases, the importance of redundant nodes also increases. There are more forwarders available for every transmitted packet for the DNA than the greedy approach. In fact, DNA helps the 2.5 times gain obtained in Figure 6.12(a), and further improved significantly by the other components.

An important observation can be made in Figure 6.14(c) that with increasing traffic intensity, while the average remaining energy decreases for the greedy approach, the remaining energy for DNA decreases only slightly. This indicates that many nodes were not activated always. Therefore, GLEAM outperforms the greedy approach significantly.
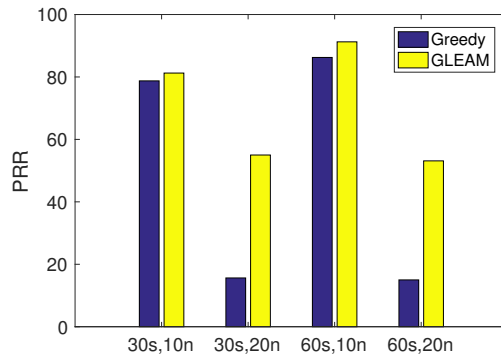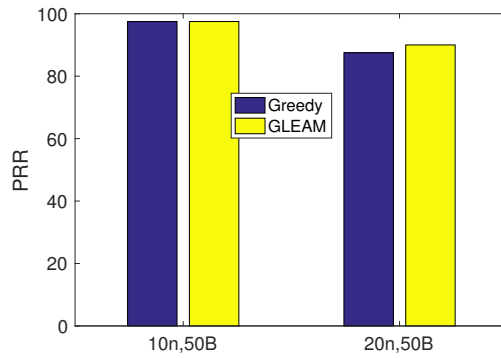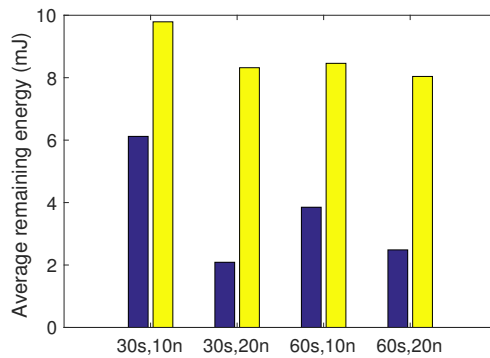
Figure 6.12: (a) Average PRR for different traffic intensities and source nodes. (b) Average PRR for payload length 50 B at 60 s periodicity. (c) Average remaining energy for different number of sources, and payload length of 100 B.
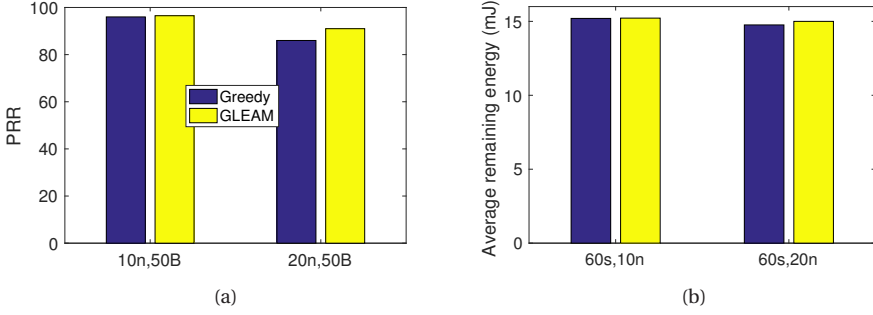
Figure 6.13: Results with Moser's model: (a) Average PRR for different traffic intensities and source nodes. (b) Average remaining energy for different number of sources, and payload length of 100 B.

6.6.2. ESTIMATING THE CRITICAL NODE DENSITY

We have seen that the redundant nodes help GLEAM in achieving a higher PRR. CND is the minimum number of nodes required to ensure a 100% PRR. An obvious question is what the required Critical Node Density (CND) is for a highly reliable data collection in energy-harvesting WSNs. In this case, we seek to calculate CND for the energy-harvesting nodes. We provide an outline of an analytical method to achieve this below.

We consider a random geometric graph (RGG) model, which has been used extensively in the analysis of wireless sensor networks [127, 128]. Let $G = (N, r)$ represent the RGG, deployed in a unit area, where r is the radius of communication. We assume that the graph is connected when all its nodes are *active*. A node is said to be active if it has energy greater than E_{min}, which is the minimum amount of energy required for participating in one slot of a communication round. Let $f_i(e)$ denote the probability density function (p.d.f.) of the energy harvested by node i. With this representation, we proceed to estimate the required density for the case with nodes having no energy buffer, i.e., nodes are active if they are harvesting energy in the current slot.

We assume that the p.d.f. of all the nodes are *i.i.d.* Therefore, the availability of node i is,

$$Pr[L_i] = Pr[E(k) \geq E_{min}] \tag{6.7}$$

$$= 1 - \int_0^{E_{min}} f_i(e)\,de.$$

With N nodes in the network, the joint p.d.f. is the sum of independent random variables. Therefore, the average number of nodes available out of N nodes is given by,

$$\mathbb{E}_N = N Pr[L_i], \tag{6.8}$$

for any node i.

The degree of a RGG [127] is given by $\mathbb{E}[\Delta] = \pi r^2 N$, which can be extended here to compute the expected degree as,

$$\mathbb{E}[\Delta_G] = \pi r^2 \mathbb{E}_N. \tag{6.9}$$
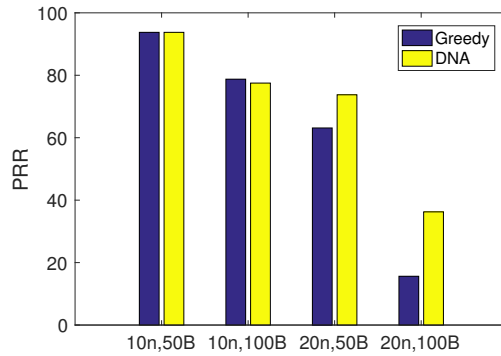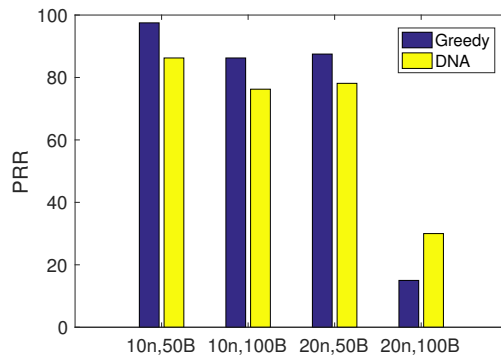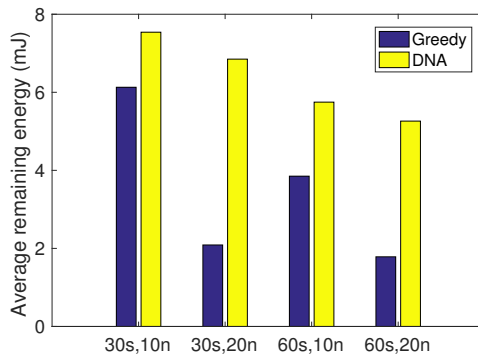
Figure 6.14: Comparison between greedy and dynamic node activation (DNA) scheme. (a) Average PRR for source nodes for 30 s interval (100 B). (b) Average PRR for source nodes for 60 s interval (100 B). (c) Average remaining energy for different number of sources, and payload length of 100 B.

Furthermore, we know the probability of the graph being connected [127] is

$$Pr[C] = exp(-exp(-\alpha)),$$

where

$$\alpha = \mathbb{E}[\Delta_G] - ln\mathbb{E}_N. \tag{6.10}$$

We can compute the critical density for the network to be connected by back-calculating from this equation. We know that $\lim_{\alpha \to \infty} Pr[C] \to 1$. When $\alpha \to 5.2$, the network is connected a.s [82]. By employing a root finding algorithm [129], such as Newton-Raphson's method, we can compute the required average number of nodes necessary for connectivity $\mathbb{E}_N$.

6.7. RELATED WORK

The work on routing in energy-harvesting WSNs has attracted less attention compared to their battery-powered counterparts. Table 6.2 summarizes the most significant networking protocols in WSNs and energy-harvesting WSNs. Of these limited works, most of them such as ORiNoCo [118] (opportunistic receiver initiated no-overhead collection protocol) and SP-BCP [117] (solar-powered backpressure collection protocol) target reliably delivering packets to the sink through higher energy nodes. The reasons for not targeting low latency in energy-harvesting WSNs: (a) energy variations make it difficult to get the nodes globally synchronized as traditional synchronization protocols are energy demanding, (b) schemes such as Low Power Listening still have considerable amount of overheads before successfully transmitting data, and (c) packet losses on the wireless channel consume significant amount of energy for retransmission.

A common strategy employed to make WSN protocol energy-harvesting aware is by using power management techniques such as adaptive duty-cycling, scheduling tasks and transmission policies. However, directly using them on LWB will not render the desired features. Adaptive duty-cycling techniques [8, 75] determine how long a node should be awake based on residual energy and energy harvesting rates. While these algorithms can be tweaked to determine how much energy to spend, they do not schedule the operation of tasks. Task scheduling [85, 131] algorithms, on the other hand, maximize the number of tasks executed within specified deadlines by considering the energy remaining in the storage element. Task schedulers for energy-harvesting WSNs employ *clairvoyance* or prediction of energy in order to minimize deadline violations. However, these algorithms are myopic in their approach i.e., the node being alive in the next slot is not considered.

Markov models representing energy availability have been proposed to determine optimal transmission policies [121, 120]. Each packet to be transmitted is considered to have a certain value, and the node gets a reward if the packet is transmitted. On similar lines, transmission power policies have also been constructed [132]. Higher the energy state, more reward can be accrued. These models target to maximize the average reward over an infinite horizon, which implies that the node will optimize its energy usage and packet transmissions. These works also cannot be used since they either schedule packet transmission in a future time when the energy is higher or do not consider transmission power to improve the performance of CI.

Name	Storage	Working Principle	Basic Idea	Node Wakeup	Reliability	Latency Guarantees
CTP [49]	Battery	Tree-based	Nodes select parents with lower routing cost and ETX	Asynchronous	High	Yes, with increased duty cycle
ORW [130]	Battery	Opportunistic	Nodes select parents with lower expected duty cycles	Asynchronous	High	Yes, with increased duty cycle
Dozer [119]	Battery	Time-slotted	Nodes select parents with lower hop-count and load	Scheduled	High	No, collisions cause delays
LWB [99]	Battery	CI based	Every packet is flooded	Scheduled	High	High
ORiNoCo [118]	Super-capacitor	Opportunistic with receiver initiated MAC	Nodes send packets to parents with low routing cost. High energy nodes wakeup more often	Asynchronous	High	No
EHOR [116]	Super-capacitor	Opportunistic	Routing metric is a function of residual energy and hop-count	Asynchronous	High	No
SP-BCP [117]	Rechargeable battery	Back-pressure	Backpressure calculation is made harvesting energy aware	Asynchronous	Medium to high	No

Table 6.2: Summary of available routing protocols for WSNs and energy-harvesting WSNs.

6

6.8. Conclusions

End-to-end latency and reliability are the critical parameters that determine the usability and success of an energy-harvesting IoT deployment. The current state-of-the-art for energy-harvesting WSNs does not attempt to provide guarantees on these metrics. To this end, we considered to use the recent data collection protocol LWB based on Glossy, which can provide the best possible performance on battery-powered WSNs. However, in energy-harvesting WSNs setting LWB does not perform well because of the stochastic nature of energy harvesting. To this end, we proposed a distributed, energy-management module called GLEAM. In GLEAM, the energy allocation problem is modeled as a Markov Decision Process. We proposed a policy and also proved that it is indeed an optimal policy. We also proposed protocol optimization to make good use of the allocated energy. We used Indriya and FlockLab testbeds, varying number of nodes from 10 to 20 with a maximum of 5 hops. Under the worst case conditions with just 50μJ/s energy, we showed that we even get an improvement of 2.5 times higher PRR with respect to the greedy policy using the efficient LWB protocol. Through this evaluation, we showed that GLEAM is more than sum of its individual components. Lastly, we provided an outline of a random geometric graph based method to calculate the critical density, which is a vital factor to achieve higher PRR in energy-harvesting WSNs.

GLEAM is just the beginning with several questions left to be answered in making energy variations transparent to the higher layers.

1. The first of these is to determine the theoretical critical density required for a finite energy buffer case.

2. Next is to design an optimal dynamic node activation policy in order to maximize the benefits.

3. Make low-power wireless bus consume much lower power so as to make every node participate in more slots, and reduce dependency on redundant node deployment.

6

7

CONTEXT-EVENT TRIGGERING SYSTEMS

7.1. INTRODUCTION

With rapid advancements in embedded systems and wireless technologies, the vision of Mark Weiser is becoming a reality. In 1991, he envisioned *ubiquitous computing* [4], where he stated that "personal" computers will integrate seamlessly into a person's environment and enrich his/her everyday life by automating many routine tasks and providing information relevant to the *context*. Context is any information that can characterize the situation of a user or an entity in general [133]. Employing contextual information in applications to enrich user experience has led to powerful ideas such as *smart spaces* [134, 135, 136].

The smart space paradigm is based on ubiquitous computing, where environments are embedded with devices to capture the context and adapt the ambiance around the user accordingly to improve his experience. While Internet of Things (IoT) enable connecting with 'things' (physical objects) and controlling them [3], the smart space concept takes it a step forward in order to realize 'smart IoT spaces'. Smart IoT spaces are envisioned to integrate smartness across various domains such as cities, utility grids (e.g., electricity), transportation, and logistics.

The core idea of smart IoT spaces is to gather contextual information and then act appropriately based on the derived context. One of the most common approaches to gather data is by using Wireless Sensor Networks (WSNs) [137]. Nodes in WSNs are low-power, battery operated, tiny embedded devices that have a sensor(s) and a radio transceiver. Typical WSNs are ad hoc networks where a multi-hop approach is used for communication between the nodes and a sink to conserve energy. The nodes report sensor data periodically to the sink. This is called periodic sampling. The sink then processes the data to determine the context and/or change in the situation. In this work, we limit ourselves to smart spaces in indoor environments such as a home or an office. In these spaces, events occur randomly and sporadically.

The approach of periodic sampling has two problems.

1. The sink needs to process a huge amount of sensor data generated by the nodes, particularly in large spaces, and

2. The approach is not energy-efficient with respect to the sensor nodes as data is sent periodically even when there is no change in the context. This drains their batteries quickly.

A large number of sensors are envisioned to be deployed in indoor spaces. The data generated from these nodes can, therefore, be huge. However, only part of the data may be significant for representing the context. Several techniques are proposed to reduce the data sent by each node, for example predicting the measured values both at the source and the sink node, thus only requiring nodes to send the reading that deviate from the prediction [138, 139]. In these techniques, the nodes sense periodically but send data only when an 'event' (or deviation) occurs.

While many research efforts have targeted energy efficiency and lifetime extension of the sensor networks, these techniques merely prolong the lifetime of the nodes and do not eliminate battery replacement. As we have seen in Chapter 1, there has recently been tremendous growth in energy-harvesting technologies targeting perennial lifetime for the WSNs recently [7]. In energy-harvesting WSNs, the nodes scavenge energy from ambient sources, for example, light, heat, water flow, vibrations, etc. While harvesting alleviates the second problem of the periodic sampling approach, it does not solve the first one. To address the first problem, the sink should be notified only if there is a change in context. This requires a context-event triggering mechanism. In this chapter, we propose a context-event triggering technique driven by energy-harvesting to address both problems together. This mechanism also eliminates periodic sensing as a means to detect events.

In many cases, the energy-harvesting source for a node will be related to the physical parameter that the sensor is measuring. For instance, a light sensor should have a photovoltaic (PV) harvester that harvests energy, which is directly proportional to the intensity of light. Therefore, in this chapter, we propose to exploit this property of energy harvesters to detect the change in the context: if a node begins (or stops) to harvest energy, this indicates that there is a change in context and hence, the sensor should send the data. We, further, adapt the context-event triggering framework in order to exploit the proposed mechanism. This chapter demonstrates the above concepts and the framework with a real-world use-case.

The contributions of the chapter are as follows.

1. We propose to exploit the energy harvesters as transducers and to detect a change in context. We give examples thereof.

2. We then propose an adaptation of the context-aware framework to utilize the proposed mechanism. Furthermore, we show the benefits of this approach for a practical use-case.

3. We then present open questions that need to be solved in order realize this in practice. We also discuss the cases wherein the context-event triggering systems using energy harvesters may not be appropriate.

There is one drawback in our proposed approach. Not every physical parameter change can be context triggered through a harvester. For example, there is no harvester that can trigger an event due to a change in CO_2 concentration levels. Another

example is that an accelerometer sensor can be used to get the orientation of the device. Unfortunately, this change cannot be used to harvest energy, hence this event cannot be captured through a harvester.

The remainder of this chapter is organized as follows: Section 7.2, briefly describes context-aware systems. In Section 7.3, we describe our context-event triggering mechanism using energy-harvesting. In the same section, we propose an adaptation to the framework. We demonstrate our proposal and its benefits with a use-case in Section 7.4 along with energy savings compared to other approaches. In Section 7.5 we describe the challenges and open questions to be addressed in order to realize a reliable system. We present the conclusions in Section 7.6.

7.2. CONTEXT AND CONTEXT-AWARENESS IN SMART SPACES

Many authors have defined context from their own viewpoint leading to different definitions. Generally, context identifies aspects of a smart space that can influence action of users in the smart space. Schilit et al. [140] define context as "information addressing where you are, who you are with, and what resources are nearby". Dey and Abowd [133] define context as "any information that can be used to characterize the situation of an entity. An entity can be a person, place or an object that is considered relevant to the interaction between the user and the application". Bolchini et al. [141] define context as "the set of variables that may be of interest to an agent and influence its actions". Dey's definition is the most generic of them all and is therefore the most widely accepted one. We too adopt this definition in this work.

Context-awareness is defined as the ability to provide services with awareness of the user's context. A context-aware system [142] determines *why* the situation is occurring based on the contextual information. The system can then either adapt the environment or react to the situation. For example, in an indoor smart environment, the temperature of a room where the user is present can be adapted according to his preference. If he moves to another room, the context-aware system reacts to this action by adjusting the temperature in the new location. Context and context-awareness form the basis for creating smart IoT spaces.

A context source is any source that captures information about a user and can provide this information to the sink for deriving context. Since any sensor information in the smart space can be contextually relevant, it is a huge task to collect and process all the data in real-time. Hence, to reduce this complexity, context sources are grouped into dimensions [143], which are then weighted to pick the most relevant sources. The major dimensions of context are listed below.

- **Ambient dimension**: The set of contextual sources that are in the proximity of the user. This includes real-time raw sensor data about the user and his/her ambiance. Examples include room temperature, and user location.

- **Time dimension**: The time of occurrence of an event.

- **User and social dimensions**: The set of sources that characterize the user's preferences (such as choice of color or music). The social dimension captures the awareness of being an actor part of a bigger system (such as people around a person and the current social situation around the person).
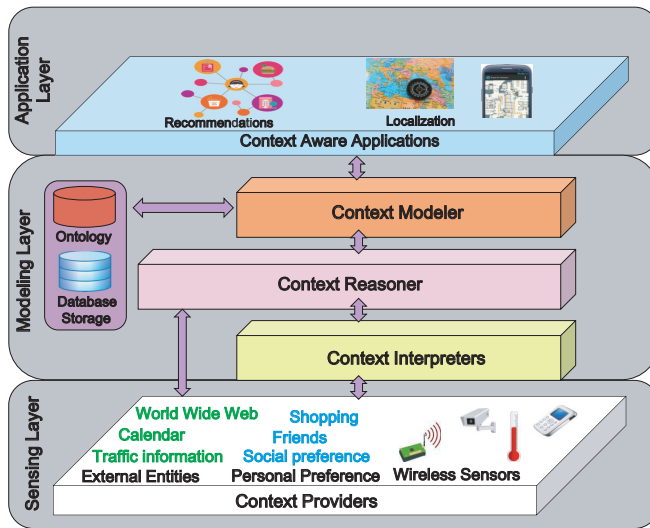
Figure 7.1: A generalized framework for context-aware systems.

- **Derived dimension**: The information is obtained from external sources such as the world wide web (WWW), calendars, weather, social networks, traffic information, and so on. This information may play a role in identifying the current situation of the user. Here the user's social network graph members and their preferences are also considered in determining the context, e.g., user's shopping information and recommendations.

Of the different dimensions, the ambient dimension plays the most significant role since it is close to the user and can capture the action of a user and his environment in indoor smart spaces. In these smart spaces, a large number of sensors are deployed to capture the user and ambiance information.

A generalized framework for context-aware systems [144] in smart spaces is shown in Figure 7.1. The framework consists of three layers namely sensing, modeling and application layers. Each module in the framework is briefly explained below.

Context providers furnish data about the contextual parameters. These can be sensors, user preferences or external entities which provide data such as temperature, humidity, light, RFID, location, shopping preferences, social preferences, calendars, weather and traffic information.

A context interpreter harmonizes the format of the data given by heterogeneous context providers. This module is required since the data will be of diverse data types, formats and values.

A context reasoner infers the big picture from the contextual information. The context reasoner considers relevance and quality of the contextual information gathered. A reasoner employs inference and rule-based mechanisms to derive new high-level contextual information. The reasoner may use additional resources (e.g., location, time, and user information) for deriving new high-level contextual information.

A context modeler and storage is used to represent contextual information in a machine understandable format. The contextual information can be modeled using a
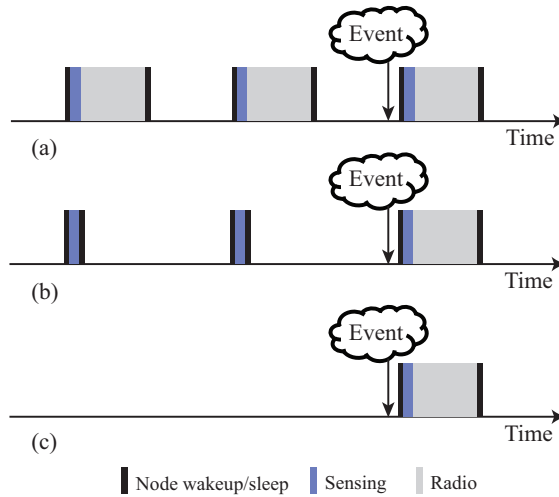
Figure 7.2: Different context-event data gathering schemes. (a) Periodic data gathering; (b) Event data gathering; (c) Context-event triggered data gathering.

variety of approaches such as key-value models, object-oriented models, logic-based models and ontology-based models [145]. Finally, the context model is used by the applications to adapt and/or respond to the user's situation.

In the following section, we propose a method that triggers an event of context change to aid in spotting the moments only when data gathering should be done.

7.3. CONTEXT-EVENT TRIGGERED SENSING

Before we proceed to describe the working of our context-event triggering mechanism, we first look at the state of the art.

7.3.1. RELATED WORK

Context data gathering has attracted a lot of attention over the years [137]. The work can be broadly classified into: context oblivious and context aware gathering methods [146]. Figure 7.2 shows different data gathering methods.

Context oblivious data gathering schemes require the sensor nodes to send data periodically. This method has two main advantages: the sink has complete knowledge of all sensor values, and low or no computation is required on the sensor nodes. The disadvantage of this method is that the energy requirements and network overhead are high. This method is shown in Figure 7.2(a).

On the other hand, context-aware gathering methods reduce the energy requirements and network overhead by sending data only when an event occurs. Typically in these methods, the nodes are given an event definition that can be used to classify sensor data as to whether an event has occurred or not. In other words, a reasoner is implemented with temporal logic and sometimes with spatial logic [147, 148, 86]. Another method for event detection is by a creating model of the data at both the sink and the nodes [149]. The sink and a node of interest both predict data periodically.

Table 7.1: Examples of energy-harvesting in indoor smart spaces.

Energy Source	Harvesting Technology	Example usage
Sun light	Photovoltaics	Sensors near the windows
Ambient light	Photovoltaics	Sensors in the rooms
Wind	Aeroelastic flutter	In air-conditioner ducts
Water	Micro-hydro turbines	In kitchens and showers
Thermo-electric	Seebeck effect	In heaters and on human bodies
Vibrations	Piezoelectric	In wheelchairs, appliances like washing machines, refrigerators
Push buttons	Magnetic coils	Wireless switches, remote controls
Shoe inserts	Microgenerators	In shoes

The node matches its prediction with actual sensor data. If the data from the sensor differs by more than the value estimated from the model, then the data is sent to the sink [138, 139]. Figure 7.2(b) depicts such a context-aware gathering method.

In contrast to these methods wherein a node has to wakeup periodically and perform certain tasks, we propose a method that allows a node to wakeup only when an event begins to occur. This is depicted in Figure 7.2(c).

7.3.2. CONTEXT-EVENT TRIGGERING THROUGH HARVESTERS

The sensors powered from the ambient sources, such as light, radio frequency, thermal, wind, water, and motion/mechanical movements can operate for long periods of time. Furthermore, since the energy harvesting source for a sensor will most often be related to the physical parameters that the sensor measures, we can use these harvesters as context-event triggering transducers. We shall describe this method with examples.

Activity Detection through Shoe-inserts:　Sensors in shoes track the activities of a user who wears them. If the sensors are powered through shoe-insert harvesters, then the sensors get triggered only when there is a user movement. Therefore, instead of periodically sensing user activity even when he is stationary, the sensor now is only activated when the harvester generates energy. At this point, the context-event is triggered and notified to the sink. Furthermore, the amount of energy harvested can be used to estimate the user's activity and the calories burnt.

We can model a shoe-insert harvester using a second-order spring-mass model [9]. With this model, we can estimate the power that can be harvested with data from an accelerometer. Figure 7.3 shows an example of accelerometer data and corresponding power generated by the motion. It is evident that not only the harvester can works as a transducer but also that the rate of harvesting can be used to classify data.

The data for Figure 7.3 was taken from a public dataset [150] for a certain user, user M5. The details on the method of data collection and the user activities can be found in [9].

(a) Accelerometer data
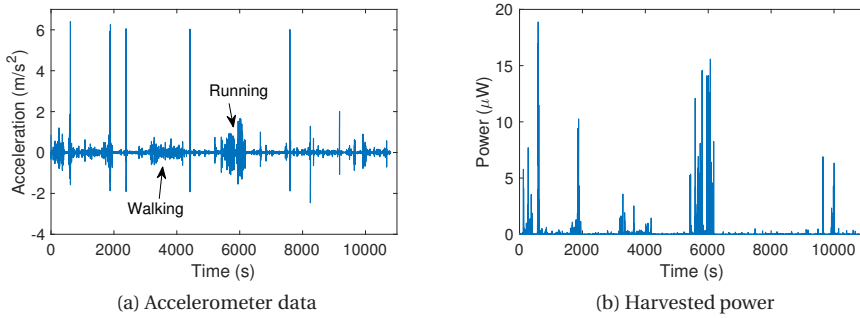
(b) Harvested power

Figure 7.3: An example of acceleration data from a user's activities and corresponding harvested power in a random period of 3 hours.

(a) Irradiance

(b) Energy harvested
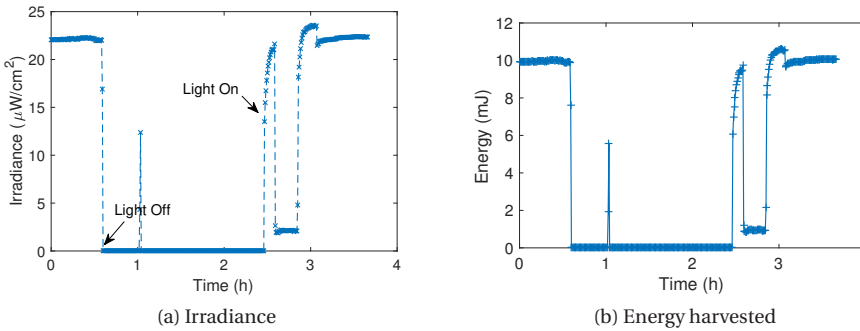
Figure 7.4: An example of light data from a sensor placed in an office room with artificial lights.

Presence detection through PV harvester: Another example is when a PV harvester can act as a transducer. When there is change in light intensity, the energy generated by the PV harvester changes proportionally. This change can be used to trigger the context-event notification and to initiate other sensors for further monitoring. Figure 7.4 shows an example of a few hours of irradiance as observed by a sensor in an office room with artificial light. A person walks in and out of the room randomly. When the user enters the room, he/she switches on the light and turns it off when leaving. The light is on as long as the person is in the room. It is evident from the figure when the light was switched on and off. The corresponding energy generated is shown in Figure 7.4(b). Therefore, with the rate of harvesting, it is possible to get the context of a person's presence (or absence) in the room.

The data for Figure 7.4 was taken from another public dataset [125]. The chosen data trace is SetupA for October 1, 2009. To convert from irradiance to energy, we considered a 10 cm × 10 cm solar panel that has an efficiency of 15 %. Furthermore, we considered the average irradiance value between consecutive measurements for computing the energy.

7

Table 7.2: Examples of events and contextual information from harvesters.

Energy Harvester	Events detected	Contextual information derived
Photovoltaics (indoor)	Lights turned on/off	Occupancy in the room; life sign
Hydro turbine	User presence; usage of water	User location (in kitchen, shower etc.,); water usage patterns and activities, advanced metering
Thermo-electric (on body sensor)	Change in body parameters;	Indicates probable change in other body parameters, advanced metering
Piezoelectric	Appliance usage; Movement on wheelchairs	Indicates life sign for elderly using wheelchairs; Also appliances with this harvesters detect usage patterns
Wireless switches	Lights on/off	User location (range)
Shoe inserts	Movement	Life sign; Indicates energy spent and change in body parameters;

Many such examples can be envisioned in smart spaces including smart homes, smart transportation, smart cities, advanced energy metering infrastructure [151] etc. Table 7.1 summarizes the sources and power that can be harvested from ambient sources in indoor smart IoT spaces. Table 7.2 shows the examples of possible contexts generated by different harvesters in indoor smart spaces.

The harvester, therefore, can be used to derive initial high-level contextual information. Unlike the classical method of periodic sensing to detect context changes, now we can rely on harvesters to detect context changes and use sensors to precisely monitor all the changes occurring from then on. If need be, the sensors can operate on a low sensing frequency until a context change is detected. Consequently, all the deployed sensor nodes can be more energy efficient. Thus, energy-harvesting sensor nodes can not only be made to support perpetual operation of nodes but can also be made to assist in deriving contextual information.

7.3.3. ADAPTED FRAMEWORK FOR CONTEXT-EVENT TRIGGERED SYSTEMS

With some intelligence in the nodes along with our proposed technique of using harvesters as transducers, the nodes can infer *what* may be happening in the smart space. This needs to be incorporated into the general context-aware framework that was discussed in Section 7.2 (Figure 7.1).

At a basic level, the energy harvesters replace the batteries in WSNs. Therefore, they act as any other sensor node in collecting contextual data. Context Reasoner has the responsibility of inferring high-level context from the sensor data. For example, consider the case of a user walking into his/her bedroom and turning on the light.
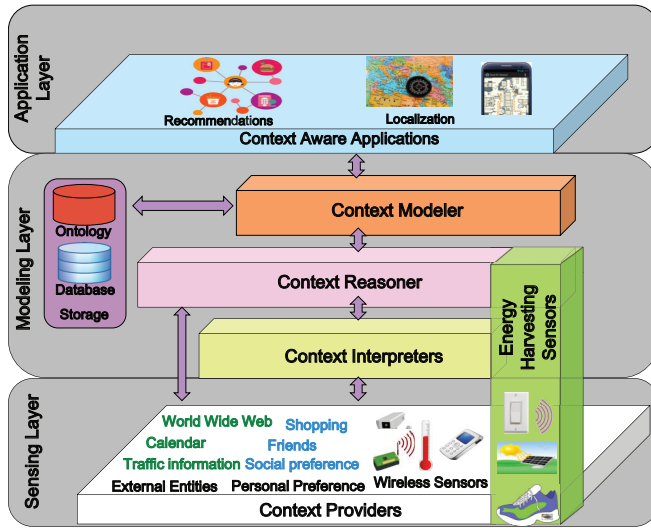
Figure 7.5: Proposed framework for context-event triggered systems.

In the context oblivious approach, WSNs periodically send all the luminosity values to the sink. At the point where luminosity values jump, the reasoner determines the high-level context: the user walked into the bedroom. In our proposed method, when the PV harvester generates more energy, the sensor node concludes that a light is on in the bedroom. The sensor can then directly report the reasoned context to the sink. Furthermore, shoe-inserts can detect gait of the person wearing them, and also identify the person if configured [152]. This can also be reported to the sink. Thus, the reasoner is not required to collect and process huge amounts of data to infer which user has performed what action.

The context information generated by the harvester can then directly be sent to the Context Reasoner. This calls for a cross layer design as compared to the traditional framework. Figure 7.5 shows the framework with this adaptation for context-event triggered systems.

7.4. USE-CASE: A SMART FITNESS ROOM

In this section, we describe a simple use-case where we demonstrate how our proposed method and framework can be employed in real-life scenarios. We then show the benefits of our proposal in terms of energy savings and data processing.

Alice is an early adopter of indoor smart IoT spaces. In her house, she has a fitness room for physical exercise activities. She has converted her fitness room into a smart IoT space. This room is equipped with wireless switches, motion detection, temperature, humidity, and light sensors and an Internet access point that also acts as a sink to the wireless sensors. She bought a wireless pulse rate monitoring device that can be worn on her wrist. All the wireless devices, except the pulse rate monitoring device, are equipped with suitable energy harvesters. The pulse rate monitor is battery operated. The shoe has a shoe-insert energy harvester and the wireless switches have
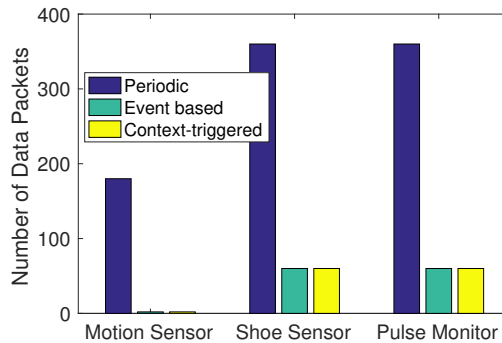
Figure 7.6: Number of data packets generated during Alice's activities.

linear motion harvesters. The temperature, humidity, light and motion sensors have PV harvesters to power the nodes.

We consider the following scenario: Alice enters her fitness room and switches on the light. She then wears her pulse rate monitor. She begins her routine exercise of running on a treadmill for 30 minutes. Then she turns off the light and goes out of the room.

With our proposed technique in place, the scenario will unfold as follows: Alice enters her fitness room and presses the wireless light switch. Immediately, the switch harvests energy and sends a notification to the sink, which then turns the light on. The sink also notes that Alice is in the room (from the shoe-inserts' input). The change in light conditions triggers the temperature, humidity and light sensors' PV harvester. They conclude a person's presence in the ambiance and start recording values. Alice then wears her pulse rate monitor. She begins her routine exercise of running. The moment she starts running, the shoe-insert detects a significant change in the harvested energy. It immediately notes that Alice is performing a physical activity and sends this contextual information to the sink. The shoe needs to trigger body sensors to monitor the changes. Thus, it broadcasts a notification to the wearable sensors indicating that they should start monitoring at a higher sensing frequency. In this case, the pulse rate monitor picks up this message and it begins monitoring her heart-beats. At the end of the exercise, the shoe again detects the change in Alice's activity and thus notifies the sink. It also notifies the body sensors, the pulse rate monitor, to switch off.

We classify Alice's activities into three parts:

- detecting presence of Alice in the fitness room,

- her pulse rate monitoring, and

- her activity monitoring.

We compare our method to the periodic and event-based sensing approaches for this scenario. We assume the following: the motion detection sensor sends data every 60 s in the periodic sensing approach, but sends data only when Alice enters and leaves the room in the other two approaches. Secondly, the shoe monitors for Alice's
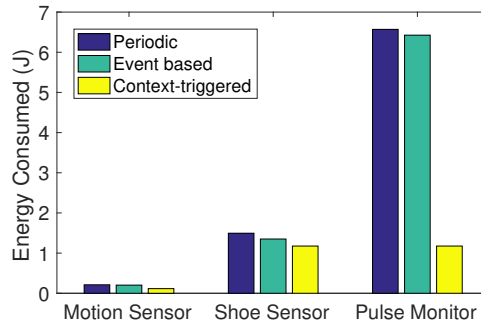
Figure 7.7: Energy consumed by the nodes for Alice's activities.

activity every 30 s, and once the activity is detected it begins sampling every 1 s but the data is sent every 30 s. While the data is sent every 30 s in the periodic case, the data is sent every 30 s only when Alice is training in the event band context-triggered based approaches. Similarly, the pulse rate monitor senses at the rate of 1 s for all the considered approaches whenever it is switched on. Furthermore, we are interested in the pulse rate only during the period when Alice performs her exercises. Thirdly, all the nodes are considered to be in radio range of the sink. Lastly, we assume 32 B packets are to be sent and the nodes use maximum transmission power of +4.5 dBm. We performed calculations for this use-case by considering the power requirements of TI CC2530 sensor node [43] (see Chapter 1). For this purpose, we consider a 3 hour period during which Alice trains for 30 minutes. These calculations give an idea of energy-efficiency and reduction in data processing that can be achieved in ideal conditions.

Figure 7.6 shows the number of data packets generated in all the approaches for the three different sensors. The number of data packets generated is lower than the periodic case in the event and context-triggered based approaches since only the important data is transmitted.

Figure 7.7 presents the energy consumed for the different sensors in all the approaches. As evident from the figure, our proposed method consumes lower energy for detecting the contexts. Our approach saves 43.07 %, 12.95 % and 81.7 % as compared to the event-based approach for motion sensor, shoe sensor and pulse monitoring respectively.

This usecase shows the benefits of the context-triggered approach in which the events are sporadic as compared to the event-based method. While the energy consumption of low power nodes are 'considered' negligible in sleeping and sensing modes, in case of sporadic event sensing deployments, the sleep and sense operations consume a significant amount of energy. The savings are non-negligible for a three hour period of this usecase, and therefore, can have significant impact when the network is deployed for a long period.

7.5. Challenges in Realizing Context-event Triggering Systems

As demonstrated in the previous section, our proposed method can detect and notify the context instead of just sending raw sensor data periodically. This saves significant amount of energy and data processing. While we outlined the benefits, there are a few challenges that need to be addressed in order to realize a reliable context-aware system that exploits context-event triggering systems. The challenges are mainly due to the limited availability of energy on the energy-harvesting sensor nodes. We describe them below.

- **Reliable detection of events with harvesters in real-time**: The detection of events in our approach is highly dependent on the sensitivity of harvesters to the energy sources. In current harvesting systems, the sensitivity is quite low. For example, solar panels cannot detect minor changes in illumination, especially when the panel is exposed to a bright light source. Similarly, other harvesters also have a tipping point before which no energy is harvested. Making the harvesters to detect the events robustly is an important challenge. Furthermore, detecting the events in real-time is more challenging. With the new developments in harvesting technology, this problem can be addressed. For instance, dye-sensitized solar cells are known to operate well even in low-light conditions [153] and are being awaited to be used.

- **Quality of contextual data**: The notion of quality of context (QoC) is typically used to determine the performance of context-aware systems [146, 154]. QoC is characterized by several parameters such as freshness of the data (or data age), data precision, resolution and significance [155]. While QoC is concerned only with the information quality, context-event triggers sometimes may not be enough. In applications where fine-grained activity is required, context-event triggered sensing needs to be adapted. For example in ambient-assisted living for the elderly, if a shoe-insert detects a 'fall' activity, then the other sensors need to start collecting fine-grained data in order to understand the situation. Therefore, our approach needs to consider designing smart applications [21] that try to match the requirements.

- **Distributed architecture**: A distributed architecture, especially with our proposed method, facilitates the nodes to take distributed actions for context-aware adaptation of the environment. This is needed to make the system scalable.

  One method to achieve a distributed architecture is to have better context reasoning capabilities on the nodes. This implies the nodes need to have better contextual models and also learn over time. Making the nodes learn over time is challenging by itself since the nodes have limited resources.

- **Networking energy-harvesting WSNs**: If the nodes are to report data periodically, then we can make use of the protocol described in Chapter 6. However, when the events occur sporadically, it becomes more challenging to gather data in a multi-hop network with all nodes powered by energy-harvesting. A commonly used class of energy-efficient routing protocols for asynchronous traffic

7

is opportunistic routing [130]. Such protocols need to be adapted for energy-harvesting scenarios.

7.6. CONCLUSIONS

Context-awareness is one of the most sought-after technologies with the growth of Internet of Things applications. The current technology for context-event detection that occur sporadically drains the battery as the nodes need to sense periodically. With ambient energy-harvesting mechanisms, this can be addressed. We proposed to exploit harvesters to detect contextual changes in smart spaces, and act as context-event triggers. Therefore, energy consumption is reduced on the nodes. Furthermore, data can be processed on the nodes to detect the contextual information. We also proposed an adaptation to the commonly used context-aware framework to incorporate our method. We demonstrated the usefulness of our system with a use-case and compared our proposal with the currently used approaches. We outlined several practical challenges that need to be addressed in order to realize the proposed system.

7

8

CONCLUSIONS

Advances in low-power circuit design and networking techniques have reduced the overall power consumption of wireless sensor nodes drastically. This enables a wide range of avenues that may be explored to provide this low power for their operation. A promising approach for perpetual network operations is to harvest energy from ambient sources, such as light, radio frequency transmissions, temperature differences, vibrations, motion, salinity gradients, wind and water flows. In order to make the nodes operate perpetually and in a sustainable manner, we adopted to power the IoT sensor nodes using ambient energy-harvesting techniques.

Due to the challenges introduced by harvesting energy from the ambiance, it is not straight-forward to replace the batteries on IoT nodes with the harvesters. Ambient energy sources do not provide constant power, and the harvested energy from the sources varies drastically over location and time. The harvested energy, sometimes, is very low and sometimes in excess of the storage capacity of the nodes. One of the challenges is that the devices die and re-enter networks due to fluctuations in the harvested energy. This dissertation began with the goal of making wireless sensor networks battery-less by tapping into the harvesting opportunities in the ambiance and making the nodes gain autonomy with respect to energy. Let us take a holistic view in order to assess the contributions of this work.

8.1. RECAPITULATION

Discovering neighbors. We began with the first step to networking, i.e., the nodes discovering their neighbors. However, in an energy-harvesting WSN, this is non-trivial since the nodes may die and be reborn depending on the amount of energy they harvest. Even when the nodes are alive, while it is easy to discover the neighbors when a node has excess energy, it becomes highly challenging when the energy is limited. We adapted two most commonly used ND protocols to use for initial deployment and for keeping up-to-date with the dynamics of the network. We performed a parametric analysis of these protocols through analytical models to understand the performance of neighbor discovery. With the help of the analytical models, the important parameters that would influence the ND process were identified, e.g., transmitter beamwidth, node density, node duty cycle and the rate of energy arrival. A thorough simulation study established the trade-offs among these parameters, and several design recommendations were presented.

Constructing reliable topologies. In order to guarantee reliable routing of packets on an unreliable network, one approach is to choose multiple routes. This in turn requires a well-connected topology, where a certain k-connectivity may be required. However, a connected topology with many interfering links leads to wastage of energy due to collisions, retransmissions and idle-listening on these low-power nodes. Therefore, it is of prime importance to develop topology control (TC) algorithms that guarantee connectivity with a configurable amount of redundancy in wireless links and that do not add to the overhead significantly. As constructing a new topology every time energy-levels change is expensive in terms of energy consumption, localized TC algorithms are required. Our contribution through the chapter on topology control caters to these requirement through two localized topology construction, E-ACT-s and E-ACT-d, and a topology maintenance algorithm. E-ACT-s and E-ACT-d are designed for convergecast and a generic ad hoc network respectively. Both the algorithms select neighbors based on their energy-levels and distance. This is an important implication since it unburdens the lower energy nodes while also guaranteeing reliability and stability of the topology itself. The E-ACT-* algorithms do not target k-connected topologies, but by tuning the parameters, the generated topologies were not only well-connected but with a high value of k. Algorithms can make use of the constructed topology to choose reliable routing paths. We evaluated the proposed algorithms based on simulations and in real-world conditions using the Indriya testbed.

Understanding constructive interference. Constructive Interference (CI), due to its simplicity, has redefined services and applications, and opened up new avenues in wireless sensor networks. We found that constructive interference (CI) based protocols were shown to guarantee latency and reliability while being highly energy-efficient. In the process of building one such CI-based protocol, we found that the performance of CI was not consistent across scenarios. This lead us to first study and understand the phenomenon of CI. We extensively studied CI from the point of view of receivers both analytically and experimentally. We established how these parameters influence performance of CI and validated our arguments with results from exhaustive experiments. We drew inferences based on our experiments. In order improve its performance, we proposed *destructive* interference to gain feedback, and created an algorithm called DIPA to exploit it. We evaluated our algorithm on testbeds against Glossy, and showed significant energy savings and better packet reception due to the feedback.

Understanding synchronous transmissions. Capture effect (CE) and constructive interference (CI) are the two phenomena that enable successful transmissions when two or more nodes transmit simultaneously. While CI has been shown to be very effective, it has also drawn speculations if it really is CE happening in the background. We answered this question with rigorous experimentation in real-world settings and ideal wireless conditions. We conclude that CI and CE are two different phenomena albeit closely related. With the experiments, we have shown every symbol is decoded independently. Through these experiments we have extended the understanding of capture effect.

Reliable networking with latency guarantees in energy-harvesting WSN. In many IoT applications, latency and data yield guarantees are highly sought after in realizing many smart applications, such as smart buildings, smart offices, smart homes.

Energy-harvesting WSNs will be widely used in practice if they can provide reliable networking with latency guarantees. We addressed this tough problem in the chapter on latency and reliability guarantees as variations in the amount of energy harvested makes the network dynamic. With the understanding of CI, we proposed to use the recent data collection protocol LWB based on Glossy, which can provide the best possible performance. However, in energy-harvesting WSNs setting LWB does not perform well because of the stochastic nature of energy harvesting. To this end, we proposed a distributed, energy-management module called GLEAM. GLEAM implements an optimal energy allocation module based on Markov Decision Process, combined with dynamic node activation to make the best use of the redundant nodes deployed in the network. Furthermore, priority handler and transmit power adaptation algorithms are proposed to utilize the allocated energy efficiently. Under low-energy conditions, we showed that we even get an improvement of 2.5 times higher packet reception ratio with respect to the greedy policy using the efficient LWB protocol. Lastly, we provided an outline of a random geometric graph based method to calculate the critical density, which is a vital factor to achieve higher packet reception ratio in energy-harvesting WSNs.

Context-event triggering with energy-harvesters. One of the main drivers of IoT applications is to capture the context of the user. WSNs are used to gather contextual data, however, even event-based data collection can lead to lower energy efficiencies due to periodic wakeup and sensing. Ambient energy-harvesting mechanisms can be exploited to solve this problem. We proposed to use energy-harvesters as transducers to trigger when there is a change in user's context. We also proposed an adaptation to context-aware framework to utilize our proposed method. We demonstrated the usefulness of our system with a use-case and compared our proposal with the currently used approaches.

8.2. FUTURE WORK

This dissertation took a few steps forward in the domain of ambient-energy powered WSNs. However, to realize the vision of completely replacing batteries, there are some problems that need to be solved in short-term and in long-term.

SHORT-TERM GOALS

In neighbor discovery, based on the insights obtained in this work, a practical, lightweight ND protocol must be developed for energy-harvesting WSNs. Such a protocol must be naturally integrated into the MAC or networking layers. Of particular importance is that the protocol must be able to estimate the neighborhood density in a dense deployment in order to design energy-efficient topologies.

For topology control, it is important to determine the value of the energy threshold, and understand its implications. The next would be then to incorporate this into or design a routing protocol that can exploit the well-connected topologies.

Constructive interference is an interesting and useful phenomenon. While we proposed a mechanism that can improve Glossy's performance and energy-efficiency over one-hop, there are several possibilities to increase it further. These must be investigated. Furthermore, it will be interesting in the context of security to investigate the possibility of recovering data from two or more "destructively" interfering signals.

8

Estimating the critical density required in an energy-harvesting WSN to provide a data collection performance that is comparable to battery-powered WSN is an important step. While GLEAM provided one dynamic node activation method, an optimal policy for node activation also needs to be designed. Other methods to increase energy-efficiency with GLEAM also need to be investigated.

For context-event triggering mechanism through energy-harvesters, we need to address two main issues. First is to reliably detect events with harvesters in real-time even in low energy harvesting conditions. The second one is to provide guarantees on the quality of contextual data collected. This problem consists not only of collecting fine-grained data when required, but also to route it in real-time to the sink.

LONG-TERM GOALS

Several ideas and investigations in this work show the direction for making the IoT nodes battery-less. This work can pave the way to realize this vision in the future when the following goals are combined with improving harvesting and battery technologies.

The first goal that must be targeted is to provide performance that is comparable to the battery-powered IoT nodes for a variety of applications. In other words, make the energy-layer transparent to the higher layers of the network stack. As mentioned in Chapter 6, the performance of an IoT deployment is measured in terms of end-to-end latency, reliability and lifetime of the deployment. While we investigated one method for a multihop energy-harvesting WSN, similar or more sophisticated methods must be developed for other IoT technologies, such as LoRaWAN, to guarantee the performance. Several challenges need to be addressed in order to achieve this goal: (a) adapt to the energy variations better; (b) use no or less number of redundant nodes; and (c) make the protocol more energy-efficient.

The second goal is to make energy-harvesting a 'plug-and-play' type of technology. Furthermore, such a technology must be made inexpensive. Such a modular technology that makes the energy-layer transparent to the application will only increase the usability of energy-harvesting technology. In this work, we mainly considered indoor or outdoor lights as the harvesting source, however, for the future we need to design the module that may also have to work transient harvesting sources. Again, several hurdles lie that needs to be crossed: (a) each hardware (microcontroller) is different making it difficult to design a universal harvesting module; and (b) achieving energy-layer transparency by such a module without the knowledge of the harvesting-energy profile and the application layer is quite difficult.

Energy-harvesting is the way forward for a sustainable life. While creating and destroying batteries is harmful to the environment, creating harvesters, such as solar cells, is also not completely environment friendly. However, it is a much better technology for making our planet greener. As the success of the Paris climate accord looms, the only way forward to convince policy makers is by creating sustainable technology that works. This work adds a few steps in this effort. The ideas and solutions presented in this work can be adapted with the ever-improving technology for harvesting and low-power embedded systems in order to make our world breath longer.

8

BIBLIOGRAPHY

[1] Popular internet of things forecast of 50 billion devices by 2020 is outdated. [Online]. Available: http://spectrum.ieee.org/tech-talk/telecom/internet/popular-internet-of-things-forecast-of-50-billion-devices-by-2020-is-outdated

[2] K. Romer and F. Mattern, "The design space of wireless sensor networks," *IEEE wireless communications*, vol. 11, no. 6, pp. 54–61, 2004.

[3] K.-D. Kim and P. R. Kumar, "Cyber–physical systems: A perspective at the centennial," *Proceedings of the IEEE*, vol. 100, no. Special Centennial Issue, pp. 1287–1308, 2012.

[4] M. Weiser, "The computer for the 21st century," in *Scientific American*, editor, Ed., 1991, pp. pp.94 –104.

[5] G. Tolle, J. Polastre, R. Szewczyk, D. Culler, N. Turner, K. Tu, S. Burgess, T. Dawson, P. Buonadonna, D. Gay *et al.*, "A macroscope in the redwoods," in *Proceedings of the 3rd international conference on Embedded networked sensor systems.* ACM, 2005, pp. 51–63.

[6] M. C. McManus, "Environmental consequences of the use of batteries in low carbon systems: The impact of battery production," *Applied Energy*, vol. 93, pp. 288–295, 2012.

[7] R. V. Prasad, S. Devasenapathy, V. S. Rao, and J. Vazifehdan, "Reincarnation in the Ambiance: Devices and Networks with Energy Harvesting," *IEEE Communications Surveys & Tutorials*, vol. 16, no. 1, pp. 195–213, 2014.

[8] A. Kansal, J. Hsu, S. Zahedi, and M. B. Srivastava, "Power management in energy harvesting sensor networks," *ACM Transactions on Embedded Computing Systems (TECS)*, vol. 6, no. 4, p. 32, 2007.

[9] M. Gorlatova, J. Sarik, G. Grebla, M. Cong, I. Kymissis, and G. Zussman, "Movers and shakers: Kinetic energy harvesting for the internet of things," in *ACM SIGMETRICS Performance Evaluation Review*, vol. 42, no. 1.   ACM, 2014, pp. 407–419.

[10] S. Sudevalayam and P. Kulkarni, "Energy Harvesting Sensor Nodes : Survey and Implications," *IEEE Communications Surveys & Tutorials*, vol. 13, no. 3, pp. 443–461, 2011.

[11] M. Feldmeier and J. A. Paradiso, "Personalized HVAC control system," in *2010 Internet of Things (IOT)*.   IEEE, Nov. 2010, pp. 1–8. [Online]. Available: http://ieeexplore.ieee.org/xpls/abs_all.jsp?arnumber=5678444

[12] Flexous b.v. [Online]. Available: http://flexous.com/en/

[13] Nowi energy b.v. [Online]. Available: http://www.nowi-energy.com/

[14] Enocean gmbh. [Online]. Available: https://www.enocean.com/en/

[15] Green teg ag. [Online]. Available: https://www.greenteg.com/

[16] Sole power tech. [Online]. Available: http://www.solepowertech.com

[17] The permasense consortium. [Online]. Available: http://www.permasense.ch/

[18] W. Li, D. Torres, T. Wang, C. Wang, and N. Sepúlveda, "Flexible and biocompatible polypropylene ferroelectret nanogenerator (feng): On the path toward wearable devices powered by human motion," *Nano Energy*, vol. 30, pp. 649 – 657, 2016.

[19] D. Mascareñas, E. Flynn, C. Farrar, G. Park, and M. Todd, "A mobile host approach for wireless powering and interrogation of structural health monitoring sensor networks," *IEEE Sensors Journal*, vol. 9, no. 12, pp. 1719–1726, 2009.

[20] Turtlenet project at umass. [Online]. Available: http://prisms.cs.umass.edu/dome/turtlenet

[21] T. V. Prabhakar, "An Empirical Approach Towards Zero Energy Networks (ZEN)," Ph.D. dissertation, Delft University of Technology, 2012.

[22] Wiring harness in bmw. [Online]. Available: http://www.bmw.com/com/en/insights/technology/technology_guide/articles/wiring_harness.html

[23] H. Bai, M. Atiquzzaman, and D. Lilja, "Wireless sensor network for aircraft health monitoring," in *Broadband Networks, 2004. BroadNets 2004. Proceedings. First International Conference on.* IEEE, 2004, pp. 748–750.

[24] Energy harvesting materials for smart fabrics and interactive textiles. [Online]. Available: http://www.ecs.soton.ac.uk/research/projects/799

[25] E. Zarepour, N. Hassan, M. Hassan, C. T. Chou, and M. E. Warkiani, "Design and analysis of a wireless nanosensor network for monitoring human lung cells," in *Proceedings of the 10th EAI International Conference on Body Area Networks.* ICST (Institute for Computer Sciences, Social-Informatics and Telecommunications Engineering), 2015, pp. 139–145.

[26] S. Bush, J. Paluh, G. Piro, V. S. Rao, V. Prasad, and A. Eckford, "Defining communication at the bottom," *IEEE Transactions on Molecular, Biological and Multiscale Communications*, 2015.

[27] F. Yildiz, "Potential Ambient Energy-Harvesting Sources and Techniques." *Journal of Technology Studies*, vol. 35, no. 1, pp. 40–48, 2009. [Online]. Available: http://eric.ed.gov/ERICWebPortal/search/detailmini.jsp?_nfpb=true&_&ERICExtSearch_SearchValue_0=EJ888131&ERICExtSearch_SearchType_0=no&accno=EJ888131

[28] P. Poggi, G. Notton, M. Muselli, and A. Louche, "Stochastic Study of Hourly Total Solar Radiation in Corsica Using a Markov Model," *International Journal of Climatology*, vol. 20, no. 14, pp. 1843–1860, 2000.

[29] C. Bergonzini, D. Brunelli, and L. Benini, "Algorithms for harvested energy prediction in batteryless wireless sensor networks," in *3rd International Workshop on Advances in sensors and Interfaces*. Ieee, jun 2009, pp. 144–149.

[30] L. Martín, L. F. Zarzalejo, J. Polo, A. Navarro, R. Marchante, and M. Cony, "Prediction of global solar irradiance based on time series analysis: Application to solar thermal power plants energy production planning," *Solar Energy*, vol. 84, no. 10, pp. 1772–1781, oct 2010.

[31] J. Hsu, S. Zahedi, A. Kansal, M. B. Srivastava, and V. Raghunathan, "Adaptive Duty Cycling for Energy Harvesting Systems," in *International symposium on Low power electronics and design*. ACM, 2006, pp. 180–185.

[32] Mide Volture. [Online]. Available: https://www.mide.com/collections/vibration-energy-harvesting-with-protected-piezos

[33] Green teg ag. [Online]. Available: https://www.tellurex.com/

[34] Humdinger wind energy llc. [Online]. Available: http://www.humdingerwind.com/press.html

[35] D. V. Ragone, "Review of battery systems for electrically powered vehicles," SAE Technical Paper, Tech. Rep., 1968.

[36] D. Pech, M. Brunet, H. Durou, P. Huang, V. Mochalin, Y. Gogotsi, P.-L. Taberna, and P. Simon, "Ultrahigh-power micrometre-sized supercapacitors based on onion-like carbon," *Nature nanotechnology*, vol. 5, no. 9, pp. 651–654, 2010.

[37] F. Simjee and P. H. Chou, "Everlast: long-life, supercapacitor-operated wireless sensor node," in *Low Power Electronics and Design, 2006. ISLPED'06. Proceedings of the 2006 International Symposium on*. IEEE, 2006, pp. 197–202.

[38] T. Zhu, Z. Zhong, Y. Gu, T. He, and Z.-L. Zhang, "Leakage-aware energy synchronization for wireless sensor networks," in *Proceedings of the 7th international conference on Mobile systems, applications, and services*. ACM, 2009, pp. 319–332.

[39] S. Butt and S. Erickson, "Battery lifetime analysis for energy harvesting networks," *UCLA EE202A Project Report*, 2003.

[40] C. Alippi and C. Galperti, "Energy storage mechanisms in low power embedded systems: Twin batteries and supercapacitors," in *Wireless Communication, Vehicular Technology, Information Theory and Aerospace & Electronic Systems Technology, 2009. Wireless VITAE 2009. 1st International Conference on*. IEEE, 2009, pp. 31–35.

[41] P. Rong and M. Pedram, "An analytical model for predicting the remaining battery capacity of lithium-ion batteries," *IEEE Transactions on Very Large Scale Integration (VLSI) Systems*, vol. 14, no. 5, pp. 441–451, 2006.

[42] Moteiv, "Telos B Datasheet," p. 28, 2004. [Online]. Available: http://moss.csc. ncsu.edu/~mueller/rt/rt11/readings/projects/g4/datasheet.pdf

[43] "Texas Instruments CC2530," http://www.ti.com/product/cc2530.

[44] "CONFRRM - Cooperative Networks For Renewable Resource Measurements." [Online]. Available: http://rredc.nrel.gov/solar/new_data/confrrm/

[45] M. Rahimi, H. Shah, G. Sukhatme, J. Heideman, and D. Estrin, "Studying the feasibility of energy harvesting in a mobile sensor network," in *2003 IEEE International Conference on Robotics and Automation*, vol. 1. IEEE, 2003, pp. 19–24.

[46] T. Voigt, A. Dunkels, J. Alonso, H. Ritter, and J. Schiller, "Solar-aware clustering in wireless sensor networks," in *Proceedings. ISCC 2004. Ninth International Symposium on Computers And Communications*. IEEE, 2004, pp. 238–243.

[47] A. Shamshad, M. Bawadi, W. Wanhussin, T. Majid, and S. Sanusi, "First and second order Markov chain models for synthetic generation of wind speed time series," *Energy*, vol. 30, no. 5, pp. 693–708, Apr. 2005.

[48] F. Cottone, H. Vocca, and L. Gammaitoni, "Nonlinear energy harvesting," *Physical Review Letters*, vol. 102, no. 8, p. 080601, 2009.

[49] O. Gnawali, R. Fonseca, K. Jamieson, D. Moss, and P. Levis, "Collection tree protocol," in *Proceedings of the 7th ACM Conference on Embedded Networked Sensor Systems - SenSys '09*. New York, New York, USA: ACM Press, Nov. 2009, p. 1.

[50] P. Dutta and D. Culler, "Practical asynchronous neighbor discovery and rendezvous for mobile sensing applications," in *Proceedings of the 6th ACM conference on Embedded network sensor systems*. ACM, 2008, pp. 71–84.

[51] S. A. Borbash, A. Ephremides, and M. J. McGlynn, "An asynchronous neighbor discovery algorithm for wireless sensor networks," *Ad Hoc Networks*, vol. 5, no. 7, pp. 998–1016, 2007.

[52] V. Iyer, A. Pruteanu, and S. Dulman, "Netdetect: Neighborhood discovery in wireless networks using adaptive beacons," in *Self-Adaptive and Self-Organizing Systems (SASO), 2011 Fifth IEEE International Conference on*. IEEE, 2011, pp. 31–40.

[53] R. Cohen and B. Kapchits, "Continuous neighbor discovery in asynchronous sensor networks," *IEEE/ACM Transactions on Networking (ToN)*, vol. 19, no. 1, pp. 69–79, 2011.

[54] S. Vasudevan, D. Towsley, D. Goeckel, and R. Khalili, "Neighbor discovery in wireless networks and the coupon collector's problem," in *Proceedings of the 15th annual international conference on Mobile computing and networking*. ACM, 2009, pp. 181–192.

[55] X. An and R. Hekmat, "Self-adaptive neighbor discovery in ad hoc networks with directional antennas," in *2007 16th IST Mobile and Wireless Communications Summit*. IEEE, 2007, pp. 1–5.

[56] X. An, R. V. Prasad, and I. Niemegeers, "Impact of antenna pattern and link model on directional neighbor discovery in 60 ghz networks," *IEEE Transactions on Wireless Communications*, vol. 10, no. 5, pp. 1435–1447, 2011.

[57] R. Margolies, G. Grebla, T. Chen, D. Rubenstein, and G. Zussman, "Panda: Neighbor discovery on a power harvesting budget," *IEEE Journal on Selected Areas in Communications*, vol. PP, no. 99, pp. 1–1, 2016.

[58] X. An, R. V. Prasad, and I. Niemegeers, "Neighbor discovery in 60 ghz wireless personal area networks," in *World of Wireless Mobile and Multimedia Networks (WoWMoM), 2010 IEEE International Symposium on a*.   IEEE, 2010, pp. 1–8.

[59] M. Nilsson, "Spida: A direction-finding antenna for wireless sensor networks," in *Real-World Wireless Sensor Networks*.   Springer, 2010, pp. 138–145.

[60] A. S. Weddell, G. V. Merrett, T. J. Kazmierski, and B. M. Al-Hashimi, "Accurate supercapacitor modeling for energy harvesting wireless sensor nodes," *IEEE Transactions on Circuits and Systems II: Express Briefs*, vol. 58, no. 12, pp. 911–915, 2011.

[61] I. Crossbow, "Datasheet, crossbow technology, inc., san jose, ca, 2010."

[62] K. Kar, A. Krishnamurthy, and N. Jaggi, "Dynamic node activation in networks of rechargeable sensors," *IEEE/ACM Transactions on Networking*, vol. 14, no. 1, pp. 15–26, feb 2006.

[63] P. Santi, "Topology control in wireless ad hoc and sensor networks," *ACM computing surveys (CSUR)*, vol. 37, no. 2, pp. 164–194, 2005.

[64] S. Narayanaswamy, V. Kawadia, R. S. Sreenivas, and P. Kumar, "Power control in ad-hoc networks: Theory, architecture, algorithm and implementation of the compow protocol," in *European wireless conference*, vol. 2002.   Florence, Italy, 2002, pp. 156–162.

[65] N. Li, J. C. Hou, and L. Sha, "Design and analysis of an mst-based topology control algorithm," *Wireless Communications, IEEE Transactions on*, vol. 4, no. 3, pp. 1195–1206, 2005.

[66] X. Wang, M. Sheng, M. Liu, D. Zhai, and Y. Zhang, "Resp: A k-connected residual energy-aware topology control algorithm for ad hoc networks," in *Wireless Communications and Networking Conference (WCNC), 2013 IEEE*.   IEEE, 2013, pp. 1009–1014.

[67] Q. Tan, Y. Liu, Y. Han, W. An, S. Ci, and H. Tang, "Energy harvesting aware topology control with power adaptation in wireless sensor networks," in *Wireless Communications and Networking Conference (WCNC), 2014 IEEE*, April 2014, pp. 2722–2727.

[68] S. Khuller, "Approximation algorithms for finding highly connected subgraphs," *Vertex*, vol. 2, p. 2, 1997.

[69] M. Bahramgiri, M. Hajiaghayi, and V. S. Mirrokni, "Fault-tolerant and 3-dimensional distributed topology control algorithms in wireless multi-hop networks," *Wireless Networks*, vol. 12, no. 2, pp. 179–188, 2006.

[70] N. Li and J. Hou, "Localized fault-tolerant topology control in wireless ad hoc networks," *Parallel and Distributed Systems, IEEE Transactions on*, vol. 17, no. 4, pp. 307–320, April 2006.

[71] L. Li, J. Y. Halpern, P. Bahl, Y.-M. Wang, and R. Wattenhofer, "Analysis of a cone-based distributed topology control algorithm for wireless multi-hop networks," in *Proceedings of the twentieth annual ACM symposium on Principles of distributed computing*.   ACM, 2001, pp. 264–273.

[72] D. Blough, M. Leoncini, G. Resta, and P. Santi, "The k-neighbors approach to interference bounded and symmetric topology control in ad hoc networks," *Mobile Computing, IEEE Transactions on*, vol. 5, no. 9, pp. 1267–1282, Sept 2006.

[73] H. Bagci, I. Korpeoglu, and A. Yazıcı, "A distributed fault-tolerant topology control algorithm for heterogeneous wireless sensor networks," *Parallel and Distributed Systems, IEEE Transactions on*, vol. 26, no. 4, pp. 914–923, 2015.

[74] T. Instruments, "Cc2420: 2.4 ghz ieee 802.15. 4/zigbee-ready rf transceiver," *Available at Available at http://www. ti. com/lit/gpn/cc2420*, p. 53, 2006.

[75] C. M. Vigorito, D. Ganesan, and A. G. Barto, "Adaptive Control of Duty Cycling in Energy-Harvesting Wireless Sensor Networks," in *2007 4th Annual IEEE Communications Society Conference on Sensor, Mesh and Ad Hoc Communications and Networks*.   IEEE, jun 2007, pp. 21–30.

[76] P. Kumar, L. Reddy, and S. Varma, "Distance measurement and error estimation scheme for rssi based localization in wireless sensor networks," in *Wireless Communication and Sensor Networks (WCSN), 2009 Fifth IEEE Conference on*. IEEE, 2009, pp. 1–4.

[77] W. Ye, J. Heidemann, and D. Estrin, "An energy-efficient mac protocol for wireless sensor networks," in *INFOCOM 2002. Twenty-First Annual Joint Conference of the IEEE Computer and Communications Societies. Proceedings. IEEE*, vol. 3. IEEE, 2002, pp. 1567–1576.

[78] M. Jorgic, N. Goel, K. Kalaichevan, A. Nayak, and I. Stojmenovic, "Localized detection of k-connectivity in wireless ad hoc, actuator and sensor networks," in *Computer Communications and Networks, 2007. ICCCN 2007. Proceedings of 16th International Conference on*.   IEEE, 2007, pp. 33–38.

[79] B. Medepally, N. Mehta, and C. Murthy, "Implications of Energy Profile and Storage on Energy Harvesting Sensor Link Performance," in *IEEE Global Telecommunications Conference*, Electr. Commun. Eng. Dept., Indian Inst. of Sci. (IISc), Bangalore, India.   IEEE, Nov. 2009, Conference proceedings (article), pp. 1–6. [Online]. Available: http://ieeexplore.ieee.org/xpls/abs_all.jsp?arnumber=5425655

[80] F. Osterlind, A. Dunkels, J. Eriksson, N. Finne, and T. Voigt, "Cross-level sensor network simulation with cooja," in *Local Computer Networks, Proceedings 2006 31st IEEE Conference on.* IEEE, 2006, pp. 641–648.

[81] A. Dunkels, B. Grönvall, and T. Voigt, "Contiki-a lightweight and flexible operating system for tiny networked sensors," in *Local Computer Networks, 2004. 29th Annual IEEE International Conference on.* IEEE, 2004, pp. 455–462.

[82] F. Xue and P. R. Kumar, "The number of neighbors needed for connectivity of wireless networks," *Wireless networks*, vol. 10, no. 2, pp. 169–181, 2004.

[83] M. Doddavenkatappa, M. C. Chan, and A. L. Ananda, "Indriya: A low-cost, 3d wireless sensor network testbed," in *International Conference on Testbeds and Research Infrastructures.* Springer, 2011, pp. 302–316.

[84] R. Lim, F. Ferrari, M. Zimmerling, C. Walser, P. Sommer, and J. Beutel, "Flocklab: A testbed for distributed, synchronized tracing and profiling of wireless embedded systems," in *Proceedings of the 12th international conference on Information processing in sensor networks.* ACM, 2013, pp. 153–166.

[85] C. Moser, D. Brunelli, L. Thiele, and L. Benini, "Real-time scheduling for energy harvesting sensor nodes," *Real-Time Systems*, vol. 37, no. 3, pp. 233–260, jul 2007.

[86] G. Werner-Allen, K. Lorincz, J. Johnson, J. Lees, and M. Welsh, "Fidelity and yield in a volcano monitoring sensor network," in *Proceedings of the 7th symposium on Operating systems design and implementation.* USENIX Association, 2006, pp. 381–396.

[87] M. Maróti, B. Kusy, G. Simon, and Á. Lédeczi, "The flooding time synchronization protocol," in *Proceedings of the 2nd international conference on Embedded networked sensor systems.* ACM, 2004, pp. 39–49.

[88] P. Levis, N. Patel, D. Culler, and S. Shenker, "Trickle: A self-regulating algorithm for code propagation and maintenance in wireless sensor networks," in *Proceedings of the 1st Conference on Symposium on Networked Systems Design and Implementation - Volume 1*, ser. NSDI'04. Berkeley, CA, USA: USENIX Association, 2004, pp. 2–2. [Online]. Available: http://dl.acm.org/citation.cfm?id=1251175.1251177

[89] J. Lu and K. Whitehouse, "Flash flooding: Exploiting the capture effect for rapid flooding in wireless sensor networks," in *INFOCOM 2009, IEEE*, April 2009, pp. 2491–2499.

[90] F. Ferrari, M. Zimmerling, L. Thiele, and O. Saukh, "Efficient network flooding and time synchronization with glossy," in *Information Processing in Sensor Networks (IPSN), 2011 10th International Conference on.* IEEE, 2011, pp. 73–84.

[91] C. Noda, C. Pérez-Penichet, B. Seeber, M. Zennaro, M. Alves, and A. Moreira, "On the scalability of constructive interference in low-power wireless networks," in *12th European Conference on Wireless Sensor Networks*, 2015.

[92] Y. Wang, Y. He, D. Cheng, Y. Liu, and X.-Y. Li, "Triggercast: Enabling wireless constructive collisions," in *INFOCOM, 2013 Proceedings IEEE*, April 2013, pp. 480–484.

[93] IEEE Standard, *IEEE 802.15.4 specification.* IEEE, 2011.

[94] Y. Wang, Y. He, X. Mao, Y. Liu, and X.-Y. Li, "Exploiting constructive interference for scalable flooding in wireless networks," *IEEE/ACM Transactions on Networking (TON)*, vol. 21, no. 6, pp. 1880–1889, 2013.

[95] D. Yuan and M. Hollick, "Let's talk together: Understanding concurrent transmission in wireless sensor networks," in *Local Computer Networks (LCN), 2013 IEEE 38th Conference on.* IEEE, 2013, pp. 219–227.

[96] J. Park, J. Jeong, H. Jeong, C.-J. Liang, and J. Ko, "Improving the packet delivery performance for concurrent packet transmissions in wsns," *Communications Letters, IEEE*, vol. 18, no. 1, pp. 58–61, 2014.

[97] D. Wu, C. Dong, S. Tang, H. Dai, and G. Chen, "Fast and fine-grained counting and identification via constructive interference in wsns," in *Proceedings of the 13th international symposium on Information processing in sensor networks.* IEEE Press, 2014, pp. 191–202.

[98] M. Doddavenkatappa, M. C. Chan, and B. Leong, "Splash: Fast data dissemination with constructive interference in wireless sensor networks." in *NSDI*, 2013, pp. 269–282.

[99] F. Ferrari, M. Zimmerling, L. Mottola, and L. Thiele, "Low-power wireless bus," in *Proceedings of the 10th ACM Conference on Embedded Network Sensor Systems.* ACM, 2012, pp. 1–14.

[100] M. Suzuki, Y. Yamashita, and H. Morikawa, "Low-power, end-to-end reliable collection using glossy for wireless sensor networks," in *Vehicular Technology Conference (VTC Spring), 2013 IEEE 77th.* IEEE, 2013, pp. 1–5.

[101] D. Carlson, M. Chang, A. Terzis, Y. Chen, and O. Gnawali, "Forwarder selection in multi-transmitter networks," in *Distributed Computing in Sensor Systems (DCOSS), 2013 IEEE International Conference on.* IEEE, 2013, pp. 1–10.

[102] B. Bloessl, C. Leitner, F. Dressler, and C. Sommer, "A GNU Radio-based IEEE 802.15.4 Testbed," in *12. GI/ITG KuVS Fachgespräch Drahtlose Sensornetze (FGSN 2013)*, Cottbus, Germany, September 2013, pp. 37–40.

[103] F. Hermans, H. Wennerström, L. McNamara, C. Rohner, and P. Gunningberg, "All is not lost: Understanding and exploiting packet corruption in outdoor sensor networks," in *European Conference on Wireless Sensor Networks.* Springer, 2014, pp. 116–132.

[104] C. Sarkar, "LWB and FS-LWB implementation for sky platform using contiki," *ArXiV*, vol. abs/1607.06622, 2016. [Online]. Available: http://arxiv.org/abs/1607.06622

[105] "iMinds technical testing: iLab.t," http://ilabt.iminds.be/.

[106] F. Ferrari, M. Zimmerling, L. Mottola, and L. Thiele, "Virtual synchrony guarantees for cyber-physical systems," in *2013 IEEE 32nd International Symposium on Reliable Distributed Systems.* IEEE, 2013, pp. 20–30.

[107] O. Landsiedel, F. Ferrari, and M. Zimmerling, "Chaos: Versatile and efficient all-to-all data sharing and in-network processing at scale," in *Proceedings of the 11th ACM SenSys.* ACM, 2013, p. 1.

[108] Y. Wang, Y. Liu, Y. He, X.-Y. Li, and D. Cheng, "Disco: Improving packet delivery via deliberate synchronized constructive interference," *IEEE Transactions on Parallel and Distributed Systems*, vol. 26, no. 3, pp. 713–723, 2015.

[109] M. Doddavenkatappa and M. C. Chan, "P3: a practical packet pipeline using synchronous transmissions for wireless sensor networks," in *Proceedings of the 13th international symposium on Information processing in sensor networks.* IEEE Press, 2014, pp. 203–214.

[110] M. Wilhelm, V. Lenders, and J. B. Schmitt, "On the Reception of Concurrent Transmissions in Wireless Sensor Networks," *IEEE Transactions on Wireless Communications*, vol. 13, no. 12, pp. 6756–6767, dec 2014. [Online]. Available: http://ieeexplore.ieee.org/lpdocs/epic03/wrapper.htm?arnumber=6880859

[111] M. König and R. Wattenhofer, "Sharing a medium between concurrent protocols without overhead using the capture effect." in *EWSN*, 2016, pp. 113–124.

[112] ——, "Maintaining constructive interference using well-synchronized sensor nodes," in *Distributed Computing in Sensor Systems (DCOSS), 2016 International Conference on.* IEEE, 2016, pp. 206–215.

[113] K. Leentvaar and J. Flint, "The capture effect in fm receivers," *Communications, IEEE Transactions on*, vol. 24, no. 5, pp. 531–539, 1976.

[114] "Mini Circuits Combiner ZN4PD1-63-S," http://194.75.38.69/MCLStore/ModelInfoDisplay?14580505727450.28181547937167317.

[115] M. Ceriotti, M. Corrà, L. D. Orazio, R. Doriguzzi, D. Facchin, G. P. Jesi, R. L. Cigno, L. Mottola, A. L. Murphy, M. Pescalli *et al.*, "Is there light at the ends of the tunnel? wireless sensor networks for adaptive lighting in road tunnels," in *Information Processing in Sensor Networks (IPSN), 2011 10th International Conference on.* IEEE, 2011, pp. 187–198.

[116] Z. A. Eu, H.-P. Tan, and W. K. Seah, "Opportunistic routing in wireless sensor networks powered by ambient energy harvesting," *Computer Networks*, vol. 54, no. 17, pp. 2943–2966, Dec. 2010. [Online]. Available: http://dx.doi.org/10.1016/j.comnet.2010.05.012

[117] S. Yang, X. Yang, J. A. McCann, T. Zhang, G. Liu, and Z. Liu, "Distributed networking in autonomic solar powered wireless sensor networks," *Selected Areas in Communications, IEEE Journal on*, vol. 31, no. 12, pp. 750–761, 2013.

[118] C. Renner, S. Unterschütz, V. Turau, and K. Römer, "Perpetual Data Collection with Energy-Harvesting Sensor Networks," *ACM Transactions on Sensor Networks*, vol. 11, no. 1, pp. 1–45, Sep. 2014.

[119] N. Burri, P. Von Rickenbach, and R. Wattenhofer, "Dozer: ultra-low power data gathering in sensor networks," in *2007 6th International Symposium on Information Processing in Sensor Networks*. IEEE, 2007, pp. 450–459.

[120] J. Lei, R. Yates, and L. Greenstein, "A generic model for optimizing single-hop transmission policy of replenishable sensors," *Wireless Communications, IEEE Transactions on*, vol. 8, no. 2, pp. 547–551, feb 2009.

[121] N. Michelusi, K. Stamatiou, and M. Zorzi, "Transmission Policies for Energy Harvesting Sensors with Time-Correlated Energy Supply," *IEEE Transactions on Communications*, vol. 61, no. 7, pp. 2988–3001, jul 2013.

[122] L. Lei, Y. Kuang, Xuemin, Shen, K. Yang, J. Qiao, and Z. Zhong, "Optimal Reliability in Energy Harvesting Industrial Wireless Sensor Networks," may 2016.

[123] M. Puterman, *Markov Decision Processes: Discrete Stochastic Dynamic Programming*, 2nd ed. John Wiley & Sons, 2005.

[124] A. A. Borovkov, *Stochastic processes in queueing theory*. Springer Science & Business Media, 2012, vol. 4.

[125] M. Gorlatova, M. Zapas, E. Xu, M. Bahlke, I. J. Kymissis, and G. Zussman, "CRAWDAD dataset columbia/enhants (v. 2011-04-07)," Downloaded from http://crawdad.org/columbia/enhants/20110407/energy, Apr. 2011, traceset: energy.

[126] M. R. Garey and D. S. Johnson, *Computers and intractability*. wh freeman New York, 2002, vol. 29.

[127] M. Penrose, *Random geometric graphs*. Oxford University Press Oxford, 2003, vol. 5.

[128] S. Boyd, A. Ghosh, B. Prabhakar, and D. Shah, "Gossip algorithms: Design, analysis and applications," in *INFOCOM 2005. 24th Annual Joint Conference of the IEEE Computer and Communications Societies. Proceedings IEEE*, vol. 3. IEEE, 2005, pp. 1653–1664.

[129] W. H. Press, *Numerical recipes 3rd edition: The art of scientific computing*. Cambridge university press, 2007.

[130] O. Landsiedel, E. Ghadimi, S. Duquennoy, and M. Johansson, "Low power, low delay: opportunistic routing meets duty cycling," in *Information Processing in Sensor Networks (IPSN), 2012 ACM/IEEE 11th International Conference on*. IEEE, 2012, pp. 185–196.

[131] T. Zhu, A. Mohaisen, and D. Towsley, "DEOS: Dynamic energy-oriented scheduling for sustainable wireless sensor networks," in *2012 Proceedings IEEE INFOCOM*. IEEE, mar 2012, pp. 2363–2371.

[132] A. Sinha, "Optimal power allocation for a renewable energy source," in *2012 National Conference on Communications (NCC)*. IEEE, feb 2012, pp. 1–5.

[133] A. K. Dey, "Understanding and using context," *Personal Ubiquitous Comput.*, vol. 5, no. 1, pp. 4–7, Jan. 2001. [Online]. Available: http://dx.doi.org/10.1007/s007790170019

[134] C. Ramos, "Ambient intelligence environments," *Ubiquitous and Pervasive Computing: Concepts, Methodologies, Tools, and Applications: Concepts, Methodologies, Tools, and Applications*, p. 137, 2009.

[135] A. D. Wood, J. A. Stankovic, G. Virone, L. Selavo, Z. He, Q. Cao, T. Doan, Y. Wu, L. Fang, and R. Stoleru, "Context-aware wireless sensor networks for assisted living and residential monitoring," *IEEE network*, vol. 22, no. 4, pp. 26–33, 2008.

[136] X. Wang, J. Dong, C. Chin, S. Hettiarachchi, and D. Zhang, "Semantic space: an infrastructure for smart spaces," *Pervasive Computing, IEEE*, vol. 3, no. 3, pp. 32–39, 2004.

[137] C. Perera, A. Zaslavsky, P. Christen, and D. Georgakopoulos, "Context aware computing for the internet of things: A survey," *IEEE Communications Surveys & Tutorials*, vol. 16, no. 1, pp. 414–454, 2014.

[138] S. Santini and K. Romer, "An adaptive strategy for quality-based data reduction in wireless sensor networks," in *Proceedings of the 3rd international conference on networked sensing systems (INSS 2006)*, 2006, pp. 29–36.

[139] C. Sarkar, V. S. Rao, and R. V. Prasad, "No-sense: Sense with dormant sensors," in *Communications (NCC), 2014 Twentieth National Conference on*. IEEE, 2014, pp. 1–6.

[140] B. Schilit, N. Adams, and R. Want, "Context-aware computing applications," in *Mobile Computing Systems and Applications, 1994. WMCSA 1994. First Workshop on*. IEEE, 1994, pp. 85–90.

[141] C. Bolchini, C. Curino, G. Orsi, E. Quintarelli, R. Rossato, F. A. Schreiber, and L. Tanca, "And what can context do for data?" *Communications of the ACM*, vol. 52, no. 11, pp. 136–140, 2009.

[142] S. Pantsar-Syväniemi, K. Simula, and E. Ovaska, "Context-awareness in smart spaces," in *Computers and Communications (ISCC), 2010 IEEE Symposium on*. IEEE, 2010, pp. 1023–1028.

[143] V. Penela, C. Ruiz, and J. M. Gómez-Pérez, "What context matters? towards multidimensional context awareness," in *Ambient Intelligence and Future Trends-International Symposium on Ambient Intelligence (ISAmI 2010)*. Springer, 2010, pp. 113–120.

[144] M. M. Saleemi, N. D. Rodríguez, J. Lilius, and I. Porres, "A framework for context-aware applications for smart spaces," in *Smart Spaces and Next Generation Wired/Wireless Networking*. Springer, 2011, pp. 14–25.

[145] J. M. Fernández-de Alba, R. Fuentes-Fernández, and J. Pavón, "Architecture for management and fusion of context information," *Information Fusion*, vol. 21, pp. 100–113, 2015.

[146] P. Bellavista, A. Corradi, M. Fanelli, and L. Foschini, "A survey of context data distribution for mobile ubiquitous systems," *ACM Computing Surveys (CSUR)*, vol. 44, no. 4, p. 24, 2012.

[147] K. Kapitanova, S. H. Son, and K. Kang, "Event detection in wireless sensor networks," in *Second International Conference, ADHOCNETS*, 2010, pp. 18–20.

[148] B. Krishnamachari and S. Iyengar, "Distributed bayesian algorithms for fault-tolerant event region detection in wireless sensor networks," *IEEE Transactions on Computers*, vol. 53, no. 3, pp. 241–250, 2004.

[149] G. M. Dias, B. Bellalta, and S. Oechsner, "A survey about prediction-based data reduction in wireless sensor networks," *ACM Computing Surveys (CSUR)*, vol. 49, no. 3, p. 58, 2016.

[150] M. Cong, K. Kim, M. Gorlatova, J. Sarik, J. Kymissis, and G. Zussman, "CRAWDAD dataset columbia/kinetic (v. 2014-05-13)," Downloaded from http://crawdad.org/columbia/kinetic/20140513, May 2014.

[151] M. D. Vithanage, X. Fafoutis, C. B. Andersen, and N. Dragoni, "Medium access control for thermal energy harvesting in advanced metering infrastructures," in *EUROCON, 2013 IEEE*.   IEEE, 2013, pp. 291–299.

[152] W. Xu, G. Lan, Q. Lin, S. Khalifa, N. Bergmann, M. Hassan, and W. Hu, "Kehgait: Towards a mobile healthcare user authentication system by kinetic energy harvesting," in *Proceedings of NDSS*, 2017.

[153] Dye-sensitized solar cells by solarnix. [Online]. Available: https://www.solaronix.com/solarcells/

[154] T. Buchholz, A. Ku pper, and M. Schiffers, "Quality of context: What it is and why we need it." in *Proceedings of the 10th InternationalWorkshop of the HP OpenView University Association (HPOVUA)*, 2003.

[155] R. Neisse, M. Wegdam, and M. Van Sinderen, "Trustworthiness and quality of context information," in *Young Computer Scientists, 2008. ICYCS 2008. The 9th International Conference for*.   IEEE, 2008, pp. 1925–1931.

SUMMARY

The Internet of Things (IoT) is one of the disruptive technologies in today's connected world. The idea is to connect every *thing* to the Internet. IoT holds the key to many current and future technologies that will significantly influence the quality and sustainability of life. The vision of IoT is to enable large-scale monitoring and/or control in order to either observe a phenomenon or to automate tasks. Many novel IoT applications are fueling an exponential growth in the deployment of embedded devices. These devices equipped with sensors and/or actuators with wireless communication capabilities are central in realizing the IoT infrastructure. These devices must have a small form factor in order to be portable, deployable and economical. Therefore, these devices are resource constrained with respect to the available power, computing and memory. In order to reduce the usage of the power on communications involved, a multi-hop approach is adopted, leading to wireless sensor networks (WSNs).

Although IoT (or sensor) devices are required to last for a long time, batteries limit the lifetime of the devices, therefore that of the network and the applications. Powering all the IoT devices through batteries is neither scalable nor environmentally sustainable. Frequent battery replacement is labor intensive in most cases; in many other situations, battery replacement is impractical due to physical or deployment conditions. Therefore, we adopt ambient energy-harvesting techniques. By tapping into the harvesting opportunities in the ambiance, the nodes gain autonomy with respect to energy. While many existing works consider recharging batteries through the ambient energy-harvesting techniques, we look to eliminate batteries completely and replace them with sustainable energy storage buffers such as supercapacitors.

Unfortunately, merely replacing the batteries with energy harvesters does not provide the necessary alternative. Ambient energy sources do not provide constant power, and the harvested energy varies drastically over location and time. The harvested energy, sometimes, is very low and sometimes in excess of the storage capacity of the nodes. One of the challenges is that the devices die and re-enter networks due to fluctuations in harvested energy. Consequently, energy harvesting in these devices necessitates a redesign of algorithms, communication techniques, and network protocols to achieve perpetual operations while satisfying the application requirements.

In this dissertation, we analyze and propose methods for power management at various layers in the network stack. We begin with studying the neighbor discovery (ND) process in an energy-harvesting WSN. Due to the spatio-temporal variations in the available energy, the ND process becomes non-trivial. In order to identify the various parameters that affect ND, we describe a generic analytical model of an energy harvesting device. We analyze two ND protocols, one that the nodes can use to discover their neighbors during the initial deployment phase, and a second one that can be used for subsequent discovery.Based on exhaustive simulations, we present our insights and recommendations for ND in energy-harvesting WSNs.

One popular method in WSNs to increase energy-efficiency has been restriction of the number of communication links using topology control algorithms. Most of these algorithms are not effective when the nodes have different energy-levels and when the number of active nodes varies with location and time. To address this issue, we present two localized energy based topology control algorithms, namely E-ACT-s and E-ACT-d. A distinguishing feature of these localized algorithms is that they select neighbors based on energy while keeping the global topology well-connected.

Constructive Interference (CI) has generated huge interest since protocols employing it achieve significantly low latency in data dissemination with high reliability and high energy efficiency. Although few authors studied the workings of the CI phenomenon, there appears to be an inconsistent and contradicting picture. We provide comprehensive insights into the CI phenomenon. We derive the resultant signal obtained by the superposition of several concurrent transmissions in order to study CI from a receiver's perspective. Furthermore, we show the influence of various parameters from the expressions of the resultant signal. We validate the dependency on the factors through rigorous experimentation in different scenarios. Lastly, we leverage *destructive* interference on a designated byte to adapt transmission powers on the concurrent transmitters in order to make CI based protocols more reliable.

Packet capture, or simply capture effect (CE), has been well studied when there are concurrent transmissions. Due to the significant similarities between CE and CI, it is speculated that the underlying physical phenomenon of CI is just CE. Thus, we perform experiments in near ideal conditions to gain a deeper understanding. We enhance the state-of-the-art understanding of CI and CE; we explain what exactly *locking* to one of the many transmitted signals means in packet capture.

Many IoT applications require closed-loop control. End-to-end latency and reliability are the critical parameters that determine the success of the energy-harvesting IoT deployment. We propose a distributed, energy-management module called GLEAM to gain the benefits of CI based protocols, particularly low latency, and high reliability, in an energy-harvesting WSN. We propose a Markov decision model to maximize the energy utility in the infinite horizon by allocating energy optimally. To this end, we propose an optimal policy. We employ protocol optimization to achieve better node availability and CI performance. We find GLEAM to outperform LWB even when the harvested energy is low. We find that better usage of redundant nodes deployed in the network contributes significantly We outline a method to calculate the required node redundancy to achieve performance similar to battery-powered WSNs.

A large number of sensors are envisioned to be deployed in indoor smart spaces with IoT. The data generated from these nodes can be huge with only a part of the data being significant that represents the user's context. Although several techniques are proposed to reduce the data (event-based reporting), these techniques may not be energy efficient. We propose a technique driven by energy-harvesting to address both the problems together. We propose to exploit the energy harvesters as transducers and to detect a change in the context. Furthermore, we propose an adaptation of the context-aware framework to utilize the proposed mechanism.

The proposition of this thesis is to use ambient energy-harvesting techniques to completely replace the batteries in order to realize virtually immortal and sustainable IoT applications. We propose to achieve this by means of energy-aware power management across the communication stack in the energy-harvesting WSNs.

Propositions

accompanying the dissertation

AMBIENT-ENERGY POWERED

MULTI-HOP INTERNET OF THINGS

by

Vijay Sathyanarayana RAO

1. The dream of smart environments with battery-powered wireless sensors faces the nightmare of battery replacement for those sensors. (Chapter 1)

2. Traditional medium access control mechanisms for wireless sensor networks will become obsolete with the rise of concurrent transmission techniques. (Chapter 5)

3. There is no 'locking' to the phase of one of the carrier signals of the concurrently transmitted signals by a receiver for power capture to take place. (Chapter 6)

4. Ambient energy-harvesting solutions are not highly sustainable. (Chapter 8)

5. The irony of getting a Ph.D. degree is that not many doctoral candidates understand the 'philosophy' in their degree.

6. In the future, people will have eternal presence due to the digital models created during their lifetime.

7. A perfectionist cannot make a perfect mistake.

8. Intelligence can be artificial but stupidity cannot.

9. With the rise of the Internet, bullshit has found new avenues to become omnipresent.

These propositions are regarded as opposable and defendable, and have been approved as such by the promotor prof. dr. ir. I.G.M.M. Niemegeers.

ACKNOWLEDGMENTS

<div align="center">
योग नरसिंहाय नमः।
जगद्गुरु पादारविन्दयोः समर्पयामि।
</div>

This milestone in my life comes due to the blessings, guidance, support, and the efforts of many people. I wholeheartedly thank my promotor, Prof. Ignas Niemegeers, for his unwavering support and guidance. He kept believing in me throughout and pushed me through some of the rough patches during PhD. He has been a fatherly figure, and has always been there for me when it counted. I have hopefully added some of his methods of supervision and handling situations (probably the *Belgian* way) to my (small) repertoire. Sir, I thank you for everything.

Next, I would like to thank my copromotor, Dr. Venkatesha Prasad or VP, who has been my mentor, friend, family and philosopher for many years now already. VP, I am happy to have worked under your thoughtful guidance. I have learnt a great deal from you. One quality you did surprise me with was your patience as you showed me that I still have plenty of room to improve! Here I express my gratitude, though insufficient, through "*Thank you!*".

I would like to thank Dr. T. V. Prabhakar from Indian Institute of Science, Bangalore, with whom I have had the privilege to work with. Sir, I thank you for all the opportunities you have provided me with, most importantly, the internship during my Ph.D., which has played a critical role in shaping this thesis and my approach to research. I have always enjoyed working with you and the discussions we have had, and I hope to have many more in the years to come.

I would like to thank Prof. H. N. Shankar (CMRIT, Bangalore), who has been inspiring me and always has been there for me with the *right* questions. Sir, I feel blessed to even have the privilege to interact with you. Without your thoughtful guidance and support, I would not have been able to reach this milestone. My salutations to you!

I would also like to thank all my ZENLAB teammates - Madhusudan, Neha, Madhuri, Abhirami, Ujwal, Tejas and Sripad. You guys rock and it was absolute fun to have been there working with you all!

I would like to thank Prof. Koen Langendoen for his support. I would also like to thank all my colleagues of the Embedded Software group - Przemek, Ertan, Marco, Marco, Ioannis, Andreas, Yunus, Soumya, Amjad, Sinan, Paulo, Munire, Janneke and Paula for their kind support in various ways. I also thank my friends, Huaizhou Shi and Dyonisius Dony, and my master students.

In Delft, I was lucky enough to find awesome friends who made my life easy and equally happy outside home, taught me several things, and who were (and are) there for me. Sundeep (getting me down to Earth) and Kavya (the amazing cook), Kishor (the realist) and Sakshi (the other amazing cook), Chayan (the programmer), Akshay (Sir/the sounding board), Shruti (the perceptual) and Sujay (the geek), you guys have

practically been my family here. I specially thank Kishor, Sundeep, Chayan, Sujay and Akshay who have helped me get through some rough times. I would also like to thank another couple of my extended family, Akshay and Mukta, especially Mukta, for the care and warmth she has shown towards me for which I am thankful. My life in Delft has been memorable thanks to Jemima de Brauwere and Gert Middelkoop, who have provided me with a second home. Their graciousness and kind-heartedness is amazing, for which I will always be grateful. This extended family *extended* beyond the boundaries of the Netherlands up to Leuven: thanks to Hari (the confidant and the host), Marissa (the *actual* host), Ravi (Oogway of PJs), Susee, Gokul, Prashant, Padma and other members of the mokkai club. I will cherish all the moments I have had with this extended family.

The strongest support I received was from my family without who my life couldn't have been simpler - dad (Shri Sathyanarayana Rao), mom (Shrimati Pushpa), brother (Vinay), sister-in-law (Megha), and my niece (Dhruti). I received an equal amount of support also from my in-laws, father-in-law (Shri Balakrishna), mother-in-law (Shrimati Nagalakshmi), and my sisters-in-law (Jayanthi, Jyothi and Sindhu). You are all responsible for who I am! My heartfelt thanks to all for believing in me that I could go the distance and helping me reach there! Special thanks goes to my sister, Vasanthi, who provided me with motherly care every year during springs in Delft! I thank Atte (Shrimati Saraswathi) and Maava (Shri Ranga Rao) for their encouragement and best wishes. I would also like to thank my best pals, Vijay Olety, Vinay Gokula and Rishabh Mathur for their constant encouragement.

Saving the best for the last, my biggest gratitude goes out to my wife, Kruthika, for her unwavering love, care, support, and a zillion other things. Despite the many hurdles we faced, life wouldn't have been this simple and smooth without you!

Vijay
Delft, September 2017.

LIST OF PUBLICATIONS DURING PH.D.

1. Sujay Narayana, R Venkatesha Prasad, **Vijay S. Rao**, and Chris Verhoeven, *SWANS: Sensor Wireless Actuator Network in Space*, (Accepted), ACM SenSys 2017.

2. Paul Marcelis, **Vijay S. Rao**, and R. Venkatesha Prasad, *DaRe: Data Recovery through Application Layer Coding for LoRaWANs*, ACM/IEEE Transactions on Networking.

3. Paul Marcelis, **Vijay S. Rao**, and R. Venkatesha Prasad, *DaRe: Data Recovery through Application Layer Coding for LoRaWANs* (**best paper runner-up**), ACM/IEEE Internet of Things - Design and Implementation (IoTDI), 2017.

4. **Vijay S. Rao**, R Venkatesha Prasad, T Venkata Prabhakar, Chayan Sarkar, Madhusuhan Koppal and Ignas Niemegeers, *Understanding and Improving the Performance of Constructive Interference in WSNs*, ACM/IEEE Transactions on Networking.

5. **Vijay S. Rao**, Madhusuhan Koppal, R Venkatesha Prasad, T Venkata Prabhakar, Chayan Sarkar, and Ignas Niemegeers, *Murphy loves CI: Unfolding and Improving Constructive Interference in WSNs*, The 35th Annual IEEE International Conference on Computer Communications (INFOCOM 2016). San Francisco, USA, Apr. 2016

6. Xin Wang, **Vijay S. Rao**, Venkatesha Prasad, and Ignas Niemegeers, *Choose Wisely: Topology Control in Energy-Harvesting Wireless Sensor Networks*, 2016 13th Annual IEEE Consumer Communications and Networking Conference (CCNC 2016). Las Vegas, USA, Jan. 2016

7. Chayan Sarkar, **Vijay S. Rao**, R. Venkatesha Prasad, S N Das, Sudip Misra, and A Vasilakos, *VSF: An Energy-Efficient Sensing Framework using Virtual Sensors*, Sensors Journal, IEEE, 2016

8. Stephen Bush, Janet Paluh, Giuseppe Piro, **Vijay S Rao**, Venkatesha Prasad, and Andrew Eckford, *Defining Communication at the Bottom*, IEEE Transactions on Molecular, Biological and Multi-scale Communications, vol. 1, no. 1, pp. 90-96, March 2015

9. **Vijay S. Rao**, R Venkatesha Prasad, and I Niemegeers, *Optimal Task Scheduling Policy in Energy Harvesting Wireless Sensor Networks*, IEEE Wireless Communications and Networking Conference (WCNC), pp. 1-6, 2015

10. Sujay Narayana, R Venkatesha Prasad, **Vijay S. Rao**, TV Prabhakar, Sripad Kowshik, and Madhuri Iyer, *PIR sensors: characterization and novel localization technique*, Proceedings of the 14th International Conference on Information Processing in Sensor Networks (IPSN), pp. 142-153, ACM. 2015

11. **Vijay S. Rao**, SN Akshay Uttama Nambi, R Venkatesha Prasad, and I Niemegeers, *On Systems Generating Context Triggers Through Energy Harvesting*, IEEE Communications Magazine, vol. 52, no. 6, pp. 70-77, 2014

12. R Venkatesha Prasad, Shruti Devasenapathy, **Vijay S. Rao**, and Javad Vazifehdan, *Reincarnation in the Ambiance: Devices and Networks with Energy Harvesting*, IEEE Communications Surveys and Tutorials, vol. 16 no.1, pp. 195-213, 2014

13. Huaizhou Shi, R Venkatesha Prasad, **Vijay S. Rao**, IGMM Niemegeers and Ming Xu, *Spectrum- and energy-efficient D2DWRAN*, IEEE Communications Magazine, vol. 52, no. 7, pp. 38-45, 2014

14. Chayan Sarkar, **Vijay S. Rao**, and R Venkatesha Prasad, *No-sense: Sense with dormant sensors*, 2014 Twentieth IEEE National Conference on Communications (NCC), pp. 1-6, 2014

15. Chayan Sarkar, **Vijay S. Rao**, R Venkatesha Prasad, and Koen Langendoen, *SleepRoute: Assured Sensing with Aggressively Sleeping Nodes*, 11th IEEE Conf. on Mobile Ad hoc and Sensor Systems (MASS), pp. 31-36, 2014

16. Shruti Devasenapathy, **Vijay S. Rao**, R Venkatesha Prasad, Ignas Niemegeers, and Abdur Rahim, *Between Neighbors: Neighbor Discovery Analysis in EH-IoTs*, 10th International Conference on Autonomic Computing -Self-IoT Track - ICAC '13. pp. 193-200. Usenix. 2013

17. Shruti Devasenapathy, R Venkatesha Prasad, **Vijay S. Rao**, and Ignas Niemegeers, *Impact of antenna directionality and energy harvesting rate on Neighbor Discovery in EH-IoTs*, IEEE Consumer Communications and Networking Conference (CCNC), pp. 302-307, 2013

18. Huaizhou Shi, **Vijay S. Rao**, R Venkatesha Prasad, and IGMM Niemegeers, *Energy efficiency and channel allocation in P2PWRAN*, 2013 IEEE Wireless Communications and Networking Conference (WCNC), pp. 1808-1813, 2013

19. Huaizhou Shi, R Venkatesha Prasad, **Vijay S. Rao**, and IGMM Niemegeers, *Adapting IEEE 802.22 OFDMA system for P2PWRANs*, IEEE Global Communications Conference (GLOBECOM), pp. 974-979, 2013

20. Diptanil Debbarma, Qing Wang, Anthony Lo, Sonia Heemstra de Groot, Venkatesha Prasad, and **Vijay S. Rao**, *Multiuser - MIMO for Capacity Gain in Fi-Wi Hybrid Networks*, IEEE Eurocon 2013

21. Huaizhou Shi, R Venkatesha Prasad, **Vijay S. Rao**, and IGMM Niemegeers, *Fairness and network capacity trade-off in P2P IEEE 802.22 networks*, 2012 IEEE Global Communications Conference (GLOBECOM), pp. 1435-1440, 2012

22. Huaizhou Shi, R Venkatesha Prasad, **Vijay S. Rao**, and IGMM Niemegeers, *A fairness model for resource allocation in wireless networks*, IFIP NETWORKING, pp. 1-9, Springer 2012

23. R Venkatesha Prasad, **Vijay S. Rao**, Ignas Niemegeers and Sonia Heemstra de Groot, *Wireless Sensor Networks for a Zero-Energy Home*, Mobile Lightweight Wireless Systems, pp. 338-346, Springer, 2012

24. Huaizhou Shi, R Venkatesha Prasad, **Vijay S. Rao**, and IGMM Niemegeers, *Procedure to build interference map in peer to peer IEEE 802.22 networks*, 2012 IEEE Global Communications Conference (GLOBECOM), pp. 1103-1108, 2012

25. Chayan Sarkar, **Vijay S. Rao**, R Venkatesha Prasad, Abdur Rahim, and Ignas Niemegeers, *A distributed model for approximate service provisioning in Internet of Things*, Proceedings of the 2012 international workshop on Self-aware internet of things, pp. 31-36, ACM. 2012

26. **Vijay S. Rao**, Shruti Devasenapathy, R Venkatesha Prasad, TV Prabhakar, and Ignas Niemegeers, *Work in Progress: Prediction of Solar Energy for Infrastructure based Wireless Sensor Networks*, ExtremeCom. 2012

27. R Venkatesha Prasad, Chayan Sarkar, **Vijay S. Rao**, A Rahim Biswas, and Ignas Niemegeers, *Opportunistic Service Provisioning in the Future Internet using Cognitive Service Approximation*, 28th WWRF Meeting, Athens, Greece. 2012

28. Cheng Guo, R Venkatesha Prasad, Jing Wang, **Vijay S. Rao**, and Ignas Niemegeers, *Localizing Persons Using Body Area Sensor Network*, Developments in Wireless Network Prototyping, Design, and Deployment: Future Generations: Future Generations, p. 273, IGI Global, 2012